1-1-2018

Non-Invasive Mitochondrial Modulation With Near-Infrared Light Reduces Brain Injury After Stroke

Christos Dionisos Strubakos
Wayne State University,

NON-INVASIVE MITOCHONDRIAL MODULATION WITH NEAR-INFRARED LIGHT REDUCES BRAIN INJURY AFTER STROKE

by

CHRISTOS DIONISOS STRUBAKOS

DISSERTATION

Submitted to the Graduate School

of Wayne State University,

Detroit, Michigan

in partial fulfillment of the requirements

for the degree of

DOCTOR OF PHILOSOPHY

2018

MAJOR: PHYSIOLOGY

Approved By:

_____

Co-Advisor Date

_____

Co-Advisor Date

_____

_____

_____

_____

DEDICATION

I dedicate this work to my grandmother, Penelope Koufopantelis who passed away in 2013 and whom I consider to be one of the most influential people in my life. From her I learned everything from Greek Mythology to the scientific method as she allowed me to explore the world (and make messes of the kitchen) as a child. But most importantly, she taught me that life is meant to be lived: fully, passionately, and fearlessly and that I must always strive for personal excellence. ΑΙΩΝΙΑ Η ΜΝΗΜΗ.

ACKNOWLEDGEMENTS

I would like to acknowledge my advisor Dr. Thomas H. Sanderson and my co-advisor Dr. Maik Huttemann for their support in bringing this work to fruition. Ralph Waldo Emerson famously said, “the secret in education lies in respecting the student.” My advisors have embodied this principle, allowing me to explore my project and providing the support and guidance so that this work can feel like it is truly my own and for that I feel eternal gratitude. Moreover, I think all members of the Sanderson/Huttemann laboratories for their camaraderie and inspiration. I also thank all the members of my dissertation committee: Dr. Donald DeGracia, Dr. Joseph Dunbar, Dr. Kwaku Nantwi, and Dr. Karin Przyklenk. One could not ask for a more committed, intelligent group of people to guide a doctoral project.

I also thank Dr. Christian Reynolds and Dr. Zeljka Minic for their friendship. This work would not be possible without them and my life is forever richer because of their presence in it.

Dr. Panayiotis Mitsias has been a friend and father-figure for over a decade of my life and in many ways, I owe not only my approach to neurology to him, but also much of my worldview. I hope one day to become half the man he is.

Dr. Antonio Rossini, George Tzoganakis, Jess Falone, George Giavris and Carthic Rajagopalan have all enriched my life by their presence in it. Their contributions to this project and to my life in general are innumerable.

Ms. Christine Cupps has been a source of calm throughout my entire doctoral education. From our first meeting to discuss my potential joining the department, to helping me find a lab in which I could flourish, to navigating the paperwork, Chris is incomparable in both efficiency and humanity.

Fr. Nicholas Kyrtises and the Greek Community of St. John the Baptist in Sterling Heights Michigan have been a continuous presence during this educational journey and have provided support in all its forms.

Finally, I would like to acknowledge my parents, Theodore and Penelope Strubakos. This work exists at all only because they encouraged, above all else, my continuous pursuit of education. They worked hard to provide for me growing up and it is my hope that one day they will see how their many sacrifices have paid off.

TABLE OF CONTENTS

LIST OF FIGURES

LIST OF ABBREVIATIONS

Δpm proton gradient across inner mitochondrial membrane

Δψm mitochondrial membrane

ADP adenosine diphosphate

AIF apoptosis inducing factor

Apaf-1 apoptotic protease activating factor 1

ATP adenosine triphosphate

BAX Bcl-2 associated X protein

Bcl-2

Ca^{2+} calcium

CcO cytochrome c oxidase

DWI diffusion weighted imaging

FAD+ oxidized flavin adenine dinucleotide

FADH2 reduced flavin adenine dinucleotide

H^+ proton

H_2O water

H_2O_2 hydrogen peroxide

NIR infrared light

LED light-emitting diode

MCAO middle cerebral artery occlusion

MRI magnetic resonance imaging

NAD+ oxidized nicotinamide adenine dinucleotide

NADH reduced nicotinamide adenine dinucleotide

OxPhos oxidative phosphorylation

PWI perfusion weighted imaging

ROS reactive oxygen species

T2WI T2 weighted imaging

TMRM tetramethylrhodamine, methyl ester

CHAPTER 1 - STROKE INTRODUCTION AND MITOCHONDRIAL MECHANISMS OF ISCHEMIA/REPERFUSION INJURY

Stroke: Background, Anatomy and Gross Pathophysiology

Focal brain ischemia, i.e., stroke, is one of the leading causes of death and disability in the Western world.(Feigin, Norrving, and Mensah 2017) These cerebrovascular events are normally subdivided into hemorrhagic and ischemic strokes. Hemorrhagic strokes occur when an intracranial vessel ruptures, filling the subdural, subarachnoid or intracerebrum with blood and account for about 6.7% of stroke presentations to the Emergency Department. Ischemic strokes, on the other hand, occur when a blood vessel becomes occluded thus cutting off the adjacent brain tissue from critical blood supply. Most occlusions are cardioembolic, resulting from underlying cardiac arrhythmias such as atrial fibrillation, or congenital heart abnormalities such as a *patent foramen ovale* but these are not the only causes.(Chung J-W Fau - Chung et al. 2014) Large vessel atherosclerosis in the internal carotid artery, as well small vessel disease resulting from uncontrolled hypertension can all lead to focal brain lesions.(Chung J-W Fau - Chung et al. 2014)

Neurons rely almost entirely on oxidative phosphorylation to meet their high metabolic demands and so any disruption of blood supply to an area of the brain causes rapid, irreversible neuronal death.(Attwell and Laughlin 2001; Yellen 2018) For this reason, swift stroke intervention is needed in the clinic to restore blood supply to the affected tissue and thus save neurons – and by extension reduce stroke mortality and disability. To date, the only clinically approved therapies to reverse the ischemia and restore blood flow which carries crucial oxygen and metabolites to the starved neurons are either pharmacological, in the form of tissue plasminogen activator (tPA) or surgical

as seen in endovascular thrombectomy.('Tissue Plasminogen Activator for Acute Ischemic Stroke' 1995; Hacke 2015) Both of these interventions have been correlated with improvement in stroke outcomes though only a relatively small subset of the stroke patient population meets the stringent criteria to receive such treatments.

Affected ischemic brain tissue, however, cannot be considered homogenously. The anatomy and physiology of cerebral blood supply allows for tight regulation during vast physiological and pathophysiological fluctuations of cerebral blood flow. The brain receives its blood from four major vessels, two of which branch off the subclavian arteries and two directly from the aorta. The former, the carotid arteries, bifurcate in the neck into the external which courses into the face and the internal which inters at the base of the brain. The two vertebral arteries run parallel to the vertebral column and join together at the base of the brain to form the basilar artery. These arteries, along with adjoining “communicating arteries” form an anastomosis that was named after the famous physician Thomas Willis – forming the *Circle of Willis*. Of note, the internal carotid artery forms the origin of the middle cerebral artery (MCA) which supplies blood to the cortex through its cortical branches, as well as to the striatal subcortical structures through its lenticulostriate branches.(Liebeskind 2003) There are thus six arteries that supply blood to the brain: the right and left anterior, middle, and posterior cerebral arteries which are connected within the Circle of Willis by the communicating arteries at the origins, and by *Heubner’s leptomeningeal anastomoses* at their distal ends. Thus, any extra-cranial occlusion of one artery results in adequate perfusion throughout the brain through the other six arteries. This very elegant system ensures that the brain receives a constant supply of blood.(Hossmann 2009)

When an occlusion of one of these arteries within the brain takes place, neurons

directly proximal to the occluded vessel that receive their blood supply from it rapidly deplete their ATP stores and become at risk for dying in the absence of immediate intervention. Because neurons rely so heavily on mitochondrial ATP to maintain their ionic gradients, any disruption in oxidative phosphorylation leads to ionic equilibration, especially sodium, across the membrane resulting in rapid depolarization as well as an influx of water leading to cytotoxic edema.(Rungta et al. 2015) However, sodium is not the only ion to move down its concentration gradient into the cell, calcium also rapidly flows in, taxing the already dysfunctional mitochondria and initiating delayed neuronal death cascades – a crucial factor in disease progression.

In 1977 Astrups et al. published a seminal study in which they provided electrophysiological evidence that following focal brain ischemia in the primate brain, evoked cortical potentials could be transiently abolished in a manner directly related to the rate of blood flow.(Astrup J Fau - Symon et al. 1977) Simply put, as blood flow fell below critical thresholds, recovery of neuronal activity became more difficult. But, moving away from this core of inactivity directly proximal to the occlusion resulted in a zone of transient electrical quiescence that could be reversed upon restoration of flow to physiological levels. When collateral flow to these neurons was increased by increasing systemic blood pressure, these neurons could once gain reach action potential. Perhaps even more interestingly, it was noted that if ischemia were to persist beyond a critical window, even these neurons would undergo anoxic depolarization and subsequently die. Thus, it was found that regions of focal brain ischemia contained neurons that died in a flow-dependent and time-dependent manner. Astrups et al. called this area the *penumbra* and it came to be defined as a hypoperfused area of the parenchyma that was fed by collateral flow that was shunted to the area through changes in arterial pressure and local

factors.(Astrup, Siesjö, and Symon 1981) Because these neurons do not initially die they could be potentially salvaged by a therapeutic intervention.

This was a shocking discovery that is anatomically intuitive: moving away from the occlusion, neurons receive retrograde flow from Heubner's pial anastomoses and thus remain potentially viable. Much research has been conducted following Astrups' study to determine the viability of these neurons based on the rate of blood flow they receive.(Astrup, Siesjö, and Symon 1981; Mies et al. 1991; Hossmann 2009) Different neuronal functions break down across the ranges of flow reduction. It has been shown, for example, that protein synthesis is reduced by 50% when cerebral blood flow rates drop to 0.55 ml/g/min and stops below 0.35 ml/g/min. Anoxic depolarization takes place at much lower flow rates – at 0.06 - 0.15 ml/g/min extracellular ion changes, including but not limited to extracellular reductions in calcium due to the opening of calcium channels.(Hossmann 2009) Thus, rather than being a homogenous region, the ischemic parenchyma can be thought of as a shadowy zone in which neurons are undergoing multifaceted dysfunction depending on the extend of blood flow reduction.

Taken together, stroke therapy seeks to restore blood supply and save these penumbral neurons. However, re-oxygenation results in substantial tissue damage due to the production of Reactive Oxygen Species (ROS).(Granger and Kvietys 2015) Ischemia-reperfusion injury has proven to pose a perplexing clinical problem: while rapid restoration of blood is crucial in salvaging the penumbra, doing so can exacerbate brain injury due to the production of ROS.(Carden and Granger 2000; Raedschelders, Ansley Dm Fau - Chen, and Chen 2012)

Role of Mitochondria in Ischemia Reperfusion Injury

Studies have shown that the mitochondria play a pivotal role in the production of ROS

which goes on to further damage cells during reperfusion, but their role is not limited to this.(Murphy 2009) Mitochondria also initiate type II apoptosis through the release of apoptogenic proteins such as cytochrome *c*, APAF-1 and SMAC-DIABLO which lead to a cell death phenotype similar to apoptosis known as delayed neuronal death.(Green and Reed 1998) In what follows, we shall discuss mitochondrial mechanisms of cerebral ischemia reperfusion in greater detail, and outline unique findings in the Hüttemann-Sanderson laboratories that allow for the convergence of these mechanisms on the complex regulation of the mitochondrial membrane potential.

Oxidative Phosphorylation Summarized

A single molecule of glucose produces 38 ATP molecules: 2 from glycolysis, 2 from the Krebs cycle, and 34 from oxidative phosphorylation via the mitochondrial electron chain. Thus, oxidative phosphorylation plays a critical role in providing sufficient ATP to meet the cell's energy demands.(Krebs et al. 1953)

Glucose is fully oxidized during glycolysis and the TCA cycle, the latter of which takes place in the mitochondrial matrix.(Krebs et al. 1953) Energy is then stored in the reduced electron carriers NADH and $FADH_2$. These two carries donate their electrons to the complexes of the electron transport chain and are then passed from complex to complex which is coupled to proton pumping from the matrix to the intermembrane space. There are two primary sites through which electrons enter the electron transport chain: complex I (NADH dehydrogenase), and complex II (succinate dehydrogenase). Mammalian complex I is comprised of about 45 subunits, containing Flavin mononucleotide (FMN) that is not covalently bound and serves as the point of entry for electrons, and an iron-sulfur clusters.(Lenaz et al. 2006) When NADH is oxidized, two of its electrons are eventually transferred to ubiquinone (Coenzyme Q, CoQ).(Hirst et al.

2003; Sazanov 2007) Complex I is also a major site of ROS production.(Murphy 2009) Based on bacterial studies, there are seven iron sulfur clusters that pass electrons from FMN to CoQ.(Sazanov 2007) When O_2 reacts will the reduced FMN, superoxide can form, though this is not the primary mechanism of ROS production during reperfusion which likely occurs due to the semiquinone free radical which will be discussed below. It is also worth noting that the reduction state of FMN is determined by the $NADH/NAD^+$ ratio.(Kussmaul and Hirst 2006; Murphy 2009; Hirst, King Ms Fau - Pryde, and Pryde 2008) Thus, any changes in this ratio by, say, ischemia will increase the $NADH/NAD^+$ ratio and result in superoxide being formed. It must be noted that an additional mechanism of ROS formation by complex I occurs during reverse electron transport (RET).(Adam-Vizi and Chinopoulos 2006; Kudin et al. 2004; Votyakova 2001; Liu, Fiskum G Fau - Schubert, and Schubert 2002) This occurs when the CoQ supply is reduced by electrons and when the proton motive force is large enough to push electrons back from CoQH2 into complex, reducing NAD^+ to NADH.(Chance 1961) Moreover, when substrate succinate concentrations are high, RET can take place through complex I.(Liu, Fiskum G Fau - Schubert, and Schubert 2002) What is significant to this study about RET is the directly responsibility of Δp_m and thus even small reductions in Δp_m can halt the entire process by reducing the electrostatic forces that drive electrons to the sits where superoxide might be produced.(Lambert 2004; Votyakova 2001) Further noteworthy is that complex I produces ROS in proportion to the pH gradient rather than the membrane potential.(Lambert 2004; Liu 1997; Murphy 2009)

From complex I, electrons are transferred to complex III (bc1 complex) via the electron carrier ubiquinone.(Mitchell 1975b, 1975a; Crofts 1998, 2004; Trumpower 1976; Chobot 2008; Osyczka 2005) It is necessary to outline the Q cycle in some detail as

complex III is a site of ROS generation.(Cadenas E Fau - Boveris et al. 1977; Turrens, Alexandre, and Lehninger 1985) Briefly, ubiquinol (QH_2) binds to the Q_o site of complex III while ubiquinone binds to the Q_i sight. Ubiquinol then gives up its electron to the iron-sulfur cluster of the enzyme and to the bL heme group. This oxidation reaction results in the generation of a temporary radical, semiquinone which goes on to become completely oxidized forming ubiquinone, which leaves the Q_o binding site – and it is in fact center P of the Q_o site where superoxide is most formed by complex III. The iron-sulfur cluster which has received one electron from ubiquinol, loses the electron and then translocates to the cytochrome c_1 subunit where it donates its electron to cytochrome *c* which then dissociates from complex III. Furthermore, oxidation of the iron-sulfur cluster also releases a proton into the intermembrane space which comes from Q10. The additional electron reduces the b_H heme which then transfer it to the second ubiquinone molecule at the Q_i site. This electron must move against its electrical gradient because it must go to the negatively charged membrane. Ubiquinone then becomes reduced to the semiquinone radical which requires a second Q cycle to transfer an electron to reduce semiquinone to ubiquinol. Thus, in summary, the Q cycle pushes four protons into the intermembrane space. From here, cytochrome c carries its electrons which are bound to the heme group to complex IV. Cytochrome *c* also has a role in apoptosis, which shall be discussed in greater detail below.

The combination of moving electrons and pumping protons generates the proton-motive force which is the crux of the chemiosmosic hypothesis first formulated by Peter Mitchell which drives oxidative phosphorylation as it converts electro-chemical energy into mechanical energy.(Mitchell and Moyle 1967) This process produces the proton motive force, Δp_m which is comprised of the electrical component known as the

mitochondrial membrane potential ($\Delta\Psi_m$) and the chemical component which is the pH difference across the inner mitochondrial membrane. The proton motive force can be outlined according to the following equation: $\Delta p_m = \Delta\Psi_m - 59\Delta pH$ and in higher organisms, the electrical potential ($\Delta\Psi_m$) is the major driver of the proton motive force. In intact mitochondria, the protons that have accrued in the intermembrane space enter into the F_o complex of ATP-synthase and exit through the matrix. Their stored potential energy is converted to kinetic energy as they rush down their concentration gradient, clockwise rotating F_o and the stalk (around 6000 rpm). This rotation induces conformational changes in the head proteins that force ADP and P_i close enough together to bind thus forming ATP. ATP is then transported out of the matrix by a group of mitochondrial carrier proteins, specifically ATP/ADP translocase.

OxPhos Regulation

The electron transport chain has evolved in such a way as to allow the cell to meet its energy demands according to its needs. In order to achieve this goal, the functions of the ETC must be carefully regulated by a number of mechanisms. As we have seen, the proton motive force drives ATP production through a carefully orchestrated sequence of steps in which electrons are passed between ETC complexes and protons are shuttled into the intermembrane space thus generating an electrochemical gradient that powers complex V, ATP-synthase. Classically, the proton motive force and the mitochondrial membrane potential are regulated by the amount of substrate present and respiratory control.

At their core, the enzymes of the ETC are regulated by the presence or absence of substrate or product.(Arnold and Kadenbach 1999; Kadenbach et al. 2010) ATP and ADP can activate or inhibit cytochrome *c* oxidase (CcO), respectively, according to the

cell's energy needs. When ATP binds to cytochrome C, the reaction between cytochrome c and cytochrome c oxidase is curbed. CcO is modulated by the presence of ATP/ADP by means of its binding pocket located in the matrix domain and resulting in the inhibition of the enzyme when ATP is present and activation when there is more ADP.

In addition to the presence of substrate or product, the proton motive force itself regulates respiration by a process known as respiratory control. Originally demonstrated in the 1950s in isolated mitochondria, respiratory control occurs when the proton motive force itself inhibits the proton pumps of the ETC once the proton gradient passes a certain threshold thus not allowing for further protons to be pumped when Δp_m is high.(Chance B Fau - Williams and Williams 1955) In vivo, the reduction of the proton gradient because of ATD + P_i being converted to ATP by complex V allows the proton pumps to reinitiate electron transfer and proton pumping. In situations of excess of ATP, such as resting mitochondria, Δp_m increases to an inhibitory threshold and thus proton pumping ceases and so does respiration. This mechanism, which is connected to electron transport and thus $\Delta\Psi_m$ allows for tight regulation of mitochondrial membrane potential between 80 and 140 mV which optimizes energy production and minimizes ROS.(Sanderson et al. 2013)

While these basic mechanisms govern respiration in both prokaryotic and eukaryotic organisms, in recent years it has been demonstrated that higher eukaryotic organisms exhibit additional levels of respiratory control. Evidence for this can be found in increased complexity of eukaryotic ETC complexes – e.g., bacterial CcO contains 2-4 subunits whereas mammalian CcO is comprised of 13 subunits for each monomer and operates as a dimer.(Tsukihara et al. 1996; Huttemann et al. 2008)

As we have seen, Cyt c transfers electrons from the bc_1 complex to cytochrome c oxidase and in recent years has been shown to be subject to modulation by intracellular

signaling cascades. Specifically, studies on isolated enzyme have shown several phosphorylation sites. Lee et al. found that phosphorylation of cow heart Cyt c resulted in inhibition of the enzyme thus providing evidence for post-translational enzymatic control, and the inhibitory effect of phosphorylation.(Lee et al. 2006) Perhaps further solidifying this point were in vitro analyses performed by the Hüttemann lab with isolated enzyme from cow liver.(Yu et al. 2008) The group examined the Tyr-48 phosphorylation site and found that when phosphorylated, the maximal turnover of Cyt *c* was 3.7/sec; however, when the enzyme was dephosphorylated, activity increased drastically to 8.2/sec which amounted to a 2.2 fold increase. Thus, it can be concluded from these studies that the maximum number of chemical conversions of the substrate per second that a single catalytic site of Cyt c can complete decreases when the enzyme is phosphorylated and drastically increases upon dephosphorylation – a phenomenon which occurs during periods of cellular stress (brain ischemia, in particular).(Huttemann et al. 2008)

Having seen that Cyt c can be reversibly phosphorylated and deposphorylated and this activity can alter enzymatic reaction rates, the next question for us to ask is whether other ETC enzymes capitulate to the same principles. Of interest to this work in particular is how cytochrome c oxidase can be affected by phosphorylation/dephosphorylation. Early studies have shown in rat heart mitochondria that CcO can be phosphorylated by at residue Tyr304(Steenaart and Shore 1997); however, many of the early experiments failed to show the relevance of CcO phosphorylation because the enzymes had been removed from their native cellular environment. To address these shortcomings, the Hüttemann lab used liver issue to look at the cAMP signaling pathway and its effect on CcO activity. They found that high levels of cAMP resulted in the phosphorylation of the enzyme. Perhaps even more interestingly, once phosphorylated, enzymatic activity was

strongly inhibited even in the presence of high, non-physiological levels of substrate, 10 μM cytochrome *c*.(Lee et al. 2005) Furthermore, the cAMP pathway appears to be tissue-specific. Relevant to this study is the finding that under conditions of ischemia, CcO changes its phosphorylation state as was shown in rabbit heart.(Fang et al. 2007; Prabu et al. 2006) Guo et al (2007) showed that hypoxic stress induces increases in protein kinase C (PKC) signaling, specifically the PKCε isoform.(Guo et al. 2007) PKCε was found to co-localize with CcO during ischemia and its presence resulted in increased activity.(Ogbi and Johnson 2006; Ogbi et al. 2004) Furthermore, Ty304 on CcO was found to be reversibly phosphorylated where deposphorylation resulted in increased enzyme activity.(Huttemann et al. 2008)

The theory, then, is that cellular stress, like ischemia, causes changes in the phosphorylation states of the ETC complexes. In general, when the OxPhos enzymes are phosphorylated, they are inhibited thus reducing proton pumping and maintaining the membrane potential between 80 and 140 mV. However, during times of cellular stress, enzymes are dephosphorylated or change their phosphorylation state, which rapidly and drastically increases their activity, hyperpolarizing the membrane. Thus, ETC complexes can be found in multiple states of phosphorylation that directly regulates their activity. Hüttemann et al. argue that complexes I, III, and IV (which are the proton pumping complexes) undergo structural changes upon phosphorylation so that already intermediate (physiological) membrane potentials lead to inhibition of proton pumping.(Huttemann et al. 2008) When these complexes are dephosphorylated, however, they become maximally active and the membrane potential can only inhibit proton pumping once it has reached much higher pathological levels.

Membrane Potential and ROS

The mitochondrial membrane potential is tied to activation states of the OxPhos complexes and the production of ROS under conditions of cellular stress. The electrochemical gradient, or proton motive force, is comprised of the mitochondrial membrane potential, $\Delta\Psi_m$, and the pH difference across the membrane due to the proton pumping (the inner membrane being highly impermeable to protons). The electrical component, which is the greatest contributor to the proton motive force in mammals, can be measured using voltage-dependent fluorescent dyes such as tetramethylrhodamine methyl ester (TMRM).

While there are species and tissue specific differences in $\Delta\Psi_m$, generally the membrane potential during physiological conditions is kept between 80 and 140 mV. Moreover, Hüttemann et al. have argued that reversible phosphorylation, which was discussed in detail in the previous section, is the mechanism by which $\Delta\Psi_m$ is regulated.(Huttemann et al. 2008)

Under normal physiological conditions oxygen is fully reduced to H_2O by CcO with only a small number of electrons leaking and reacting with O_2 to form superoxide. Superoxide is produced at complexes I and III and is released mostly into the matrix by complex I and the intermembrane space by complex III. In both cases, superoxide generation has been shown to be dependent on membrane potential. When $\Delta\Psi_m$ is maintained within physiological range, ROS is minimized and ATP production can proceed as needed. Moreover, it must be noted that any ROS that is produced at low $\Delta\Psi_m$ takes place by mechanisms other than membrane potential.(Suski et al. 2012) Thus, ROS are formed by complexes I and III at higher membrane potential and, relevant to this study, are exponentially produced when the membrane is hyperpolarized (that is, greater than 140 mV).(Liu 1999; Starkov and Fiskum 2002; Liu 2010; Korshunov, Skulachev Vp

Fau - Starkov, and Starkov 1997) In complex III, once the half-life of semiquinone radical at the Q_o site is extended by $\Delta\Psi_m$, the radical is able to react with dioxygen to form superoxide.(Song and Buettner 2010)

Superoxide, once generated, reacts with water to generate H2O2 or protons to produce even more ROS such as peroxides and hydroxyl radicals. ROS destroy cells as they damage DNA, RNA, proteins, and lipids. Moreover, the half-life of most radicals is very short ranging from nanoseconds to seconds.

Role of Mitochondrial Metabolites in ROS Production

A compelling study was performed by Couchani et al. in which they investigated whether mitochondrial ROS during ischemia/reperfusion injury were produced by metabolites.(Chouchani et al. 2014) To interrogate their hypothesis, they utilized a metabolomics approach in which they quantified conserved metabolites in several tissues during ischemia/reperfusion injury. Using liquid-chromatography-mass spectrometry on tissues harvested from pig brain, kidney, liver, and heart that underwent in vivo ischemia, they found three primary metabolites elevated in all tissues: xanthine, hypoxanthine, and succinate. Of the three, succinate was increased the most.

Succinate that had accrued during ischemia returned to normal levels within 5 minutes in ex-vivo tissue and in in vivo hearts. Furthermore, succinate accumulations occurred in areas that had undergone ischemia and were marked by a striking absence of other Krebs Cycle metabolites. It was thus concluded that succinate accumulates rapidly during ischemia and is metabolized when flow is re-established which happens to correspond to the same time-frame as ROS production.

Succinate is produced in the mitochondria during the Krebs cycle and via the GABA shunt. Using radio-labeled carbon, Couchani et al. concluded that succinate

accumulation during ischemia does not take place from the usual carbon sources of metabolism. The group next examined whether in situations of anoxia leading to anaerobic metabolism, succinate dehydrogenase can reverse itself, reducing fumarate to succinate(Niatsetskaya et al. 2012; Taegtmeyer 1978) – a concept that has not yet been shown in ischemia. It was predicted that fumarate comes to SDH via the malate/aspartate shuttle in which the NADH/NAD ratio is high thus forming malate which is eventually converted to fumarate;(Hochachka Pw Fau - Storey and Storey 1975; Easlon et al. 2008; Barron, Gu L Fau - Parrillo, and Parrillo 1998) and, the activation of the purine-nucleotide cycle (PNC) that produces fumarate.(Van den Berghe, Vincent Mf Fau - Jaeken, and Jaeken 1997; Sridharan et al. 2008) When the group used the SDH competitive inhibitor dimethyl malonate, they saw a sharp decrease in succinate accretion in areas of ischemia thus supporting the hypothesis that ischemia drives SDH backwards.(Chouchani et al. 2014) Moreover, using radio-labelled aspartate, it was found that ischemic tissue activates both the malate/aspartate shuttle (MAS) and purine nucleotide cycle (PNC) pathways to increase the amount of fumarate that is produced, which in turn is converted to succinate by SDH working backwards.

It was hypothesized that during reperfusion, the accrued succinate becomes oxidized by SDH and because the complexes were already hyperactive, reverse electron transport becomes driven through complex I.(Hirst, King Ms Fau - Pryde, and Pryde 2008; Kussmaul and Hirst 2006; Pryde and Hirst 2011; Murphy 2009) This is compelling, because it has been previously shown that succinate can induce RET through complex I in cell culture models(Murphy 2009). Using the $\Delta\Psi_m$ fluorescent marker TMRM, the group discovered that when SDH was inhibited with dimethyl malonate, the membrane potential repolarization was significantly abated thus concluding that succinate accumulation in

combination with a higher than normal proton motive force leads to RET through complex I.(Chouchani et al. 2014)

Using these findings, Couchani et al. proposed the following model for the role of metabolites in IR injury:(Chouchani et al. 2014) When tissue becomes ischemic, fumarate increases because the MAS and PNC pathways become active. Fumarate is then reduced to succinate when SDH works backwards. When blood flow is restored, the excess succinate is quickly oxidized which generates a larger proton motive force due to electrons being shunted through complexes III and IV, while simultaneously RET is advanced through complex I thus producing ROS. In total these studies demonstrate the central role of succinate as a key energy source driving mitochondrial ROS following ischemia, with high $\Delta\Psi_m$ required to generate and release these deleterious radicals. Thus, dephorphorylation of ETC complexes leads to high membrane potential which when combined with reversed electron transport leads to the post-reperfusion ROS burst.

Model of Brain Ischemia/Reperfusion Injury

Quick restoration of blood flow during brain ischemia is of critical importance; however, doing so can exacerbate neuronal injury through the generation of ROS upon reperfusion. Having discussed above how the OxPhos complexes function and are regulated through reversible phosphorylation, and the role of the mitochondrial membrane potential in ROS generation, we are now able to describe a mitochondrial model for cerebral reperfusion injury. Because neurons rely nearly entirely on OxPhos, the mitochondria of ischemic neurons are starved of their substrate, oxygen; however, ischemia itself creates a double-edged sword in which oxygen-starved mitochondria become primed for hyperactivation.

One of the most energy expensive processes in neurons is the maintenance of

ionic gradients. Certainly, a high extracellular sodium and a high intracellular potassium concentration are critical for neuronal function in the generation of action potentials but these are not the only cations that must be carefully regulated by the cell – a difference achieved by the sodium/potassium ATPase. When the sodium/potassium pumps fail due to the cellular energy failure that occurs during ischemia, ions move down their concentration gradients: sodium rushes into the cell and potassium exits until they equilibrate across the membrane. This movement of sodium into the cell results in depolarization of the cell membrane which opens voltage gated calcium channels. Because the concentration of calcium is much higher extracellularly than intracellularly (10 mM vs. 0.0001 mM), calcium rushes into the cell. Under normal physiological conditions, transient depolarizations and intracellular calcium movement is critical for the docking of neurotransmitter-containing vesicles with the membrane and the release of their contents into the synaptic cleft; however, in ischemia, calcium accumulates in the cytosol, unable to be eliminated by ATP-dependent Ca^{2+} pumps. Furthermore, mitochondrial calcium sequestration through the mitochondrial calcium uniporter (MCU) takes place, but under physiological conditions, most calcium is eliminated through cytosolic rather than mitochondrial pathways.(Williams et al. 2013) This occurs because the MCU affinity for calcium is quite low and requires very high cytosolic calcium concentrations for transport of calcium into the mitochondria. In the case of ischemia, due to both the failure of the ATPases to remove calcium, as well as the unimpeded movement of calcium down its concentration gradient, cytosolic calcium increases.(Bourdillon Pd Fau - Poole-Wilson and Poole-Wilson 1981) As intracellular calcium increases, MCUs become active and sequester calcium into the mitochondria where it signals several deleterious pathways, one of which being programed cell death, which will be reviewed

in the following section.

The increased intermitochondrial calcium concentration activates phosphatases that dephosphorylate complexes and proteins, especially cytochrome *c* and CcO. This dephosphorylation leads to the OxPhos complexes being primed for hyperactivation even in the absence of the substrate oxygen and leads to a loss of allosteric inhibition by ATP.

As we have seen, hyperpolarization of the membrane results in exponential ROS production.(Liu 1999) Liu et al., and Starkov have clearly demonstrated that once membrane potential exceeds just 10 mV beyond the physiological 140 mV, 70 - 90 % increases in ROS follow.(Starkov and Fiskum 2002; Suski et al. 2012) Thus, the dephosphorylation of OxPhos proteins during ischemia results in enormous ROS bursts when reperfusion occurs due to a high membrane potential.

Once reperfusion is initiated, the deposphorylation of the complexes should serve to quickly restore membrane potential leading to the replenishment of ATP. This is sensible since deposphorylation causes them to work in overdrive thus reversing any depolarization that occurred due to lack of both electrons and the final substrate, oxygen. This was convincingly shown by Liu et al. who found that in brain ischemia, when blood flow was restored, the membrane potential returned to normal levels within 30 to 60 minutes.(Liu 1999) However, when allosteric regulation is lost, the membrane potential overshoots so to speak and dangerous hyperpolarization ensues. Moreover this has been confirmed by cell culture models of ischemia/reperfusion injury.(Iijima et al. 2006) Another interesting set of experiments conducted by Choi et al. (2009) found that blockade of complex I during reperfusion, halted membrane hyperpolarization and drastically reduced ROS formation.(Choi et al. 2009) These findings confirm what was discussed above regarding the exponential relationship between $\Delta\Psi_m$ and ROS production.

Studies looking at global brain ischemia have found that ROS bursts typically occur more intensely during the first 15 minutes of reperfusion(Kunimatsu et al. 2011) and these ROS have been shown to originate from the mitochondria(Piantadosi and Zhang 1996; Fabian, DeWitt Ds Fau - Kent, and Kent 1995; Kudin, Malinska D Fau - Kunz, and Kunz 2008)– specifically complex I in neurons.(Kudin, Malinska D Fau - Kunz, and Kunz 2008; Barja and Herrero 1998; Barja 1999; St-Pierre et al. 2002)

In conclusion, membrane hyperpolarization due to OxPhos complexes being primed for hyperactivation due to changes in their phosphorylation states leads to exponential production of ROS during the early stages of reperfusion in brain ischemia. Furthermore, as demonstrated by Choi et al, directly targeting the membrane potential during reperfusion can have dramatic effects on the amount of ROS produced. Thus, modulation of membrane potential can serve as a potential therapeutic strategy for brain ischemia/reperfusion injury.

Delayed Neuronal Death

Cell death has classically been characterized as either necrotic or apoptotic based on morphology. Necrosis, until very recently, was considered an unregulated pathway (Proskuryakov, Konoplyannikov Ag Fau - Gabai, and Gabai 2003) although it is now believed to arise from converging pathways. Morphologically cells dying by necrosis are identifiable by cell membrane rupture and spilling intracellular contents once they have been exposed to a stressor that pushes them beyond a threshold of recovery.

Apoptosis, in contrast, is a cell death paradigm that is executed and is classically subdivided into two pathways. Type I (extrinsic) apoptosis is activated either by death ligands (by the tumor necrosis factor (TNF) family proteins) that bind to extracellular receptors, or by disengagement of life ligands (such as netrin). Once death ligands bind,

they initiate a series of cell signaling pathways that ultimately result in programmed cell death that can either be mitochondrial dependent or not. Type II (intrinsic) apoptosis occurs when intracellular signals get transduced to the mitochondria and cause the release of apoptogenic factors that lead to apoptosis. Furthermore, the intrinsic pathway can be subdivided into caspase dependent and caspase independent mechanisms. Caspase dependent apoptosis requires cytochrome *c* to be released from the mitochondria which can involve the formation of the mitochondrial permeability transition pore (MPTP) or mitochondrial outer membrane permeabilization (MOMP). Under normal conditions a fraction of the cytochrome *c* pool remains bound to the inner mitochondrial membrane lipid cardiolipin. Due to peroxidation of cardiolipin during cell stress (often by ROS), cytochrome *c* dissociates and exits the mitochondria through the MPTP or MOMP. Moreover, once released, cytochrome *c* interacts with the IP3 receptor on the endoplasmic reticulum (ER) which causes the ER to discharge calcium into the cytosol. Calcium, as we have seen, leads to more cytochrome *c* release triggering a positive feedback loop. Once in the cytosol, Cyt *c* activates caspase 9 which in turn activates caspase 3 and caspase 7, which execute apoptosis. The caspase-independent pathway utilizes either the apoptosis inducing factor (AIF) which is released, or failure of the electron transport chain. The AIF ultimately induces chromatin condensation and DNA fragmentation.

In ischemia/reperfusion injury, there is evidence to support both pathways of programmed cell death playing important roles in death of neurons.(Puka-Sundvall et al. 2000; Northington et al. 2001) Furthermore, it is the release of apoptogenic factors from the mitochondria that seems to initiate the cell death paradigms.(Sanderson et al. 2008; Hetz et al. 2005; Cao et al. 2007; Sugawara et al. 1999) Cells that die because of ischemic

insults (specifically by delayed neuronal death pathways, not initial hypoxic insults) do so in an energy-dependent manner: it requires the expression of new genes; is mediated by the caspases; and employs the proteolytic mechanisms of apoptosis.(Dirnagl, Iadecola C Fau - Moskowitz, and Moskowitz 1999; Lee, Zipfel, and Choi 1999; Lipton 1999; MacManus and Linnik 1997; Schulz, Weller M Fau - Moskowitz, and Moskowitz 1999) Ischemic neuronal death is initiated in an programmed manner, beginning first in the mitochondria thus triggering cleavage of the caspases leading to destruction of key cellular structures and irreversible fraying of the genome, thus leading some investigators to term delayed neuronal death as regulated necrosis.

Fiskum et al. demonstrated that neuronal mitochondria are particularly sensitive to energy depletion and respond in turn according to the duration of ischemia.(Fiskum 2000; Fiskum, Murphy An Fau - Beal, and Beal 1999) Ouyang et al. found, by observing mitochondria in experimental stroke, MTP opening within 1 hour of ischemia;(Ouyang et al. 1999) furthermore, Friberg et al. showed that MPT opening corresponded to brain areas most sensitive to ischemia.(Friberg et al. 1999)

Because the mitochondrial membrane permeability to cell death mediators increase during ischemia, Fujimura et al. were able to demonstrate that parts of the mitochondria, such as cytochrome *c*, enter the cytosol 4 hours after MCA occlusion.(Fujimura et al. 1998) Because of these findings, it tempting to conclude that cell death following ischemia occurs according to an apoptotic paradigm, though this is not entirely accurate because similar phenotypes can be observed in necrosis as well.(Hirsch et al. 2005) At the same time, DNA damage that is observed in brain ischemia, while not necrotic, is different than what is seen in apoptosis.(MacManus and Buchan 2000; MacManus and Linnik 1997) These results were further corroborated by

Colbourne et al. who found no evidence of apoptosis in approximately 40,000 CA1 neurons that had undergone global ischemia.(Colbourne, Sutherland Gr Fau - Auer, and Auer 1999) Furthermore, ischemic neurons differ morphologically from classical apoptosis and thus their death cannot be explained by either classical necrosis, nor apoptosis paradigms. (Deshpande et al. 1992; van Lookeren Campagne and Gill 1996; Martin et al. 1998; Colbourne et al. 1999; Colbourne, Sutherland Gr Fau - Auer, and Auer 1999; Ishimaru et al. 1999)

A significant body of literature has looked at the Bcl-2 group of proteins that modulate permeability to cytochrome *c* and thus delayed neuronal death cascades. Bax and Bak seem to be the primary candidates that induce the release of cytochrome *c* but also other pro apopototic proteins like AIF, Smac/Diablo.(Cheng et al. 2001; Kuwana and Newmeyer 2003)

Thus, the question remains how neurons that are ischemic die. For MacManus et al. a combination of necrosis and apoptosis might be the answer with necrosis at one end of the spectrum and apoptosis on the other.(MacManus and Buchan 2000) These correspond to attractor states that Lipton (Lipton 1999) and DeGracia have convincingly argued is the most sensible way to approach neuronal death or survival.(DeGracia et al. 2017) McManus et al. argue that the attractor state, where an ischemic cell ends up is dependent upon the severity of the ischemic insult, ATP availability, and both the age and location of the neurons.(Dirnagl, Iadecola C Fau - Moskowitz, and Moskowitz 1999)

Therapies for Ischemia/Reperfusion Injury

Since free radicals have a deleterious effect on cells following reperfusion, eliminating them during early reflow is a critical concern of therapy. Studies have shown that following reflow, ROS production greatly surpasses any endogenous antioxidants.

To address this issue, a series of clinical trials was undertaken and funded by AstraZeneca in the early 2000s which looked at whether a known ROS trapping compound, NXY-059, given intravenously following the administration of tPA, would show the same neuroprotection in patients as it did in animal models. NXY-059 is a chemical derivative of phenylbutylnitrone (PBN). The original Stroke-Acute Ischemic NXY Treatment I (SAINTI) trial enrolled 1699 patients and administered either the compound or placebo within 6 hours of stroke onset for a 72-hour infusion. The outcome measures assigned were based on the modified Rankin scale which assesses the degree of stroke disability on a 6 point scale – 0 being no symptoms and 6 corresponding to death. The SAINT I trial found that administration of NXY-059 significantly reduced disability three months after stroke, but did not improve other outcome measures. The authors concluded that additional trials would need to be done.(Lees et al. 2006)

Soon thereafter the SAINT II trial was conducted which enrolled more patients (3306). Like the SAINT I trial, NXY-059 was infused for 72 hours within 6 hours following the beginning of stroke symptoms. The primary endpoints as before were disability scores on the modified Rankin scale 90 days later and secondary endpoints were scores on neurologic and activities of daily living scales. The SAINT II trial found no significant difference between NXY-059 and placebo groups for either their primary or secondary endpoints.(Shuaib et al. 2007) The authors of SAINT II argue that the false positive observed in SAINT I likely occurred by chance, potentially because the first trial included patients who went on to develop a poorer progression who were included in the placebo group. In any case, intravenous ROS scavenging was shown to be ineffective to treat reperfusion injury following acute ischemic stroke. It is likely that these studies failed for several reasons: first, rapid delivery of a compound to the tissue is difficult, not only

because of vascular occlusions, but also the ability to cross the blood brain barrier; secondly the half-life of ROS is extremely short and by the time the compound diffuses from the blood, across the plasma membrane, through the cytosol and into the mitochondria, the ROS burst is likely over and the damage has been done. Thus, systemic antioxidants have not been effective in targeting ROS mediated reperfusion injury. It is for this reason that this study has sought, based on the previous work of the Hüttemann/Sanderson labs, to limit ROS production rather than scavenge ROS. Here we propose that direct targeting of the main mechanism of ROS generation – $\Delta\Psi_m$ – can be a promising, novel therapeutic strategy and has been shown to be itself protective. (Iijima et al. 2006; Pandya, Pauly Jr Fau - Sullivan, and Sullivan 2009; Brennan et al. 2006)

Conclusions

This chapter has sought to present a working model for ischemia/reperfusion injury based on the role of the mitochondria in generating ROS during early reflow. Our group has demonstrated support for this model in previous works. We hypothesize that mitochondrial membrane potential hyperpolarization is directly responsible for ROS production, which in turn causes oxidative damage to the cell and initiates delayed neuronal death pathways. We argue that ischemia leads to post-translational modification of OxPhos complexes, primarily dephosphorylation, due to calcium-mediated activation of endogenous phosphatases. This leads to a loss of allosteric regulation and priming of ETC enzymes for hyperactivity and membrane hyperpolarization when the substrate, O_2, is restored during reperfusion. Because of the membrane potential hyperpolarization when oxygen does return, ROS is quickly and exponentially generated by complexes I and III which inundates any endogenous antioxidants, damages the cell, and activates delayed-neuronal death cascades. Furthermore, ROS scavenging has been shown to be

ineffective in targeting this ROS, likely due to the inability to deliver adequate doses to sub-cellular compartments, in particular the mitochondria, quickly enough. However, our model opens the door for the development of a novel therapeutic strategy that targets the membrane potential itself thus eliminating the need for ROS scavenging and stopping its production at its source.

CHAPTER 2 - MITOCHONDRIAL MODULATION BY NEAR-INFRARED LIGHT IN BRAIN ISCHEMIA

Introduction

Brain ischemia is a major cause of death and disability globally. As was outlined in detail in Chapter 1, because neurons are both metabolically demanding, and rely almost entirely on oxidative phosphorylation to meet these energy demands, any disruption in the delivery system of oxygen and metabolites to brain tissue has dire consequences. Blood flow can be disrupted to the brain in three primary pathologies. First, global brain ischemia occurs when systemic arterial pressure falls below the ability of the brain's autoregulatory system to maintain adequate cerebral perfusion. This occurs most commonly during cardiac arrest when cardiac output plummets and, since, it is systemic pressure that falls, neither the usual anatomic nor physiological mechanisms can ensure blood flow to the brain and thus the entire brain experiences ischemia. Brain regions that are most susceptible to death following global brain ischemia are the CA_1 region of the hippocampus as well as areas that lie between the distal ends of two collateral vessels. Known as watershed zones, these areas heavily rely on adequate perfusion pressure through the collateral vessels to receive blood. Furthermore, it has been noted that brain damage following cardiac arrest/resuscitation leading to global brain ischemia results in three processes: 1) most structural damage is seen during the reperfusion phase and not during the initial ischemia; 2) cortical pyramidal neurons in layers III and V and the CA_1 and CA_4 hippocampus are most sensitive and display what is known as "selective vulnerability"; 3) during reperfusion, these selectively vulnerable neurons demonstrate a sustained reduction to synthesize new proteins.(White et al. 1996) Like global brain ischemia, several pathologies taking place following birth can induce brain ischemia in

neonates resulting in neonatal hypoxic-ischemia encephalopathy. Finally, relevant to this study, focal brain ischemia occurs when a limited region of the brain becomes ischemic due to the occlusion of a blood vessel. In all three cases of brain ischemia, quickly restoring blood supply is crucial for saving neurons and preventing further brain damage. However, as was outlined in detail in Chapter 1, restoration of blood flow results in the generation of mitochondrial ROS due to mitochondrial membrane hyperpolarization that go on to further damage cells in a pathology known as reperfusion injury. Thus, to effectively treat reperfusion injury, ROS must be reduced as quickly as possible. As we described previously, pharmacological approaches have been unsuccessful in achieving this goal.

These approaches for reducing ROS have largely been ineffective likely due to a combination of factors including the inability of compounds to reach brain tissue via the blood stream when an artery is occluded; as well as the difficulty in getting compounds into sub cellular compartments fast enough following the initial ROS burst within the first seconds to minutes following reperfusion. It has thus been the goal of our laboratory to develop a non-invasive therapy that can be applied immediately upon reflow and reduce the amount of ROS produced rather than scavenging them. Our approach has been to use infrared light (NIR) which, unlike other wavelengths of the visible light spectrum can easily penetrate tissues within a range of 700-1000 nm and thus can target deep cellular structures.

Modulating Mitochondrial Activity Using Near Infrared Light

Near-infrared light has been shown to be beneficial and to influence the mitochondria(Yu 1997; Yeager 2005; Wong-Riley et al. 2005; Streeter 2004; Eells 2004, 2003; Wong-Riley 2001). Furthermore, it has shown promise in regenerating nerves,

stroke, peripheral neuropathy and wound healing.(Wong-Riley et al. 2005; Whelan 2003; Leonard 2004; Bae 2004; DeLellis 2005; Lim 2009; Lapchak 2007; Oron 2006; Detaboada 2006; Lapchak 2004) However, results have been inconsistent at best. The contradictory nature of the results is likely due to a limited understanding of how NIR exerts its action upon cell function.

Cytochrome *c* oxidase (CcO) is the terminal enzyme in the electron transport chain and the proposed rate limiting step of the entire reaction. The dimeric enzyme is comprised of 13 subunits per monomer and is regulated, as we previously described, by post translational phosphorylations, and the ATP/ADP ratio which in healthy cells adjusts energy production to energy demand. It is widely accepted that CcO is the primary photoreceptor of NIR. The enzyme is composed of chromophores that include two copper centers that are involved in enzymatic action and have been shown in previous studies to be the sites of photoreception of NIR.(Karu 1999; Karu and Afanas'eva 1995; Mason 2014) Copper broadly absorbs light in the near NIR range of wavelengths (700 to 1000 nM).(Hazeki O 1988; Griffiths DE 1961; Wharton DC 1964) The Hüttemann lab used N,N,N',N'-tetramethyl-p-phenylenediamine (TMPD) which is an electron transport catalyst that alters the phase of CcO kinetics from biphasic to monophasic in order to gain mechanistic knowledge of how NIR affects CcO. Unlike in vivo where cytochrome *c* associates and dissociates from CcO, in the presence of TMPD, cytochrome *c* stays bound to CcO while the compound itself shuttles electrons to cytochrome *c* from ascorbate which is a reductant thus eliminating the need for cytochrome *c* to bind and then dissociate from CcO. It was found that in the presence of TMPD, the inhibitory effect of NIR is significantly reduced and thus it is hypothesized that the inhibitory wavelengths affect the binding of CcO with cytochrome *c* at the Cu_A center of CcO next to the

cytochrome *c* binding site. Despite these insights, detailed understanding of the mechanism of how NIR can modulate the activity of CcO is not yet fully understood.

Many studies have shown that NIR can activate CcO.(Wong-Riley 2001; Wong-Riley et al. 2005; Yu 1997; Yeager 2005; Streeter 2004; Eells 2004, 2003) For example, applying wavelengths of 670 nm and 808 nm increased CcO activity and in turn overall mitochondrial respiration,(Wong-Riley et al. 2005; Pastore, Greco, and Passarella 2000) and the Hüttemann lab has shown that this holds true for one wavelength (810 nm). This was tested on isolated CcO enzyme from cow liver and pig brain (unpublished), in which four wavelengths were discovered that show CcO inhibition for the first time after scanning the near NIR range between 700-1000 nm: 750, 870, 910, 950 nm.(Sanderson et al. 2018) This range was chosen because it is classically considered the “therapeutic window of opportunity” because NIR absorbance by other biological compounds like blood and water are minimal. Using a light-protected oxygen electrode chamber that was combined with a double beam spectrophotometer, isolated and purified CcO was subjected to the wavelengths of NIR and its activity measured. It was later shown that CcO activity can also be optimally inhibited by two wavelengths of NIR, specifically 750 nm or 950 nm, and this effect is compounded when the wavelengths are combined.(Sanderson et al. 2018)

Next, the Hüttemann/Sanderson laboratories isolated mitochondria in order to measure the effect of NIR on mitochondrial respiration.(Sanderson et al. 2018) It was found that applying the inhibitory wavelengths reduced respiration by 24-25% while the excitatory 810 nm wavelength increased respiration and thus overall oxygen consumption. When the inhibitory wavelengths were combined (750 + 950 nm), respiration was reduced by 34 %.

NIR Proposed Mechanism in Reducing ROS

As was described in chapter 1, the ETC transfers electrons to oxygen, a reaction that is the rate limiting step(Villani 1997; Kunz 2000; Acin-Perez 2003; Piccoli 2006; Dalmonte 2009), catalyzed by cytochrome *c* and CcO. As electrons pass through complexes I, III, and IV, protons are simultaneously pumped across the inner mitochondrial membrane, into the intermembrane space. The action of transferring these protons generates the mitochondrial membrane potential ($\Delta\Psi_m$) which is a measure of the difference in electrical potential across the membrane. Moreover, as described in detail in Chapter 1, reperfusion hyperpolarizes the membrane, increasing $\Delta\Psi_m$, and inducing an exponential increase in ROS production. Therefore, it stands to reason that any action enacted on the rate limiting step, cytochrome *c*/CcO, can either speed up or slow down the entire reaction. Moreover, direct modulation of CcO with NIR, may allow for controlling $\Delta\Psi_m$ and thus ROS production.

To interrogate this hypothesis, the Sanderson laboratory used live-cell imaging with the $\Delta\Psi_m$ fluorescent probe, TMRM.(Sanderson et al. 2018) They found that irradiating the cells with NIR with the 950-nm wavelength, decreased the membrane potential which rapidly returned to basal levels when the light was no longer applied. Next, NIR was tested in an in vitro model of ischemia reperfusion injury. Using immortalized hippocampal cells (HT22 neurons), it was discovered that the mitochondrial membrane potential is indeed hyperpolarized during the first 30 minutes following reperfusion. Moreover, irradiation of the cells with the inhibitory NIR reduced the membrane potential.

Next, the group examined the survivability of neurons that were given NIR treatment following oxygen-glucose deprivation.(Sanderson et al. 2018) Cells received NIR treatment via fiber-optic light guides for an hour following reoxygenation and the

number of cells that died were quantified using a Live/Dead viability assay 24 hours later. Fewer cells died when treated with inhibitory NIR wavelengths (750 nm and 950 nm). In contrast the excitatory wavelength of (810 nm) did not save cells.

NIR Reduced ROS Production in CA1 Hippocampal Neurons Following Reperfusion

Next it was necessary to show that CcO is hyperactive following ischemia.(Sanderson et al. 2018) To interrogate this hypothesis, brains were harvested after 8 minutes of global ischemia followed by reperfusion. CcO specific activity was measured and a significant increase in activity was observed in brain tissue during ischemia and reperfusion compared to non-ischemic controls. It is hypothesized that these changes cause membrane hyperpolarization in vivo as shown previously.(Liu, Fiskum G Fau - Schubert, and Schubert 2002) In order to confirm this theory, ROS production was quantified using MitoSOX fluorescence, which detects mitochondrial superoxide production. Following 8 minutes of brain ischemia and 30 minutes of reflow, a seven-fold increase in MitoSOX fluorescence was observed in CA1 hippocampus, indicating an accretion of ROS in these neurons. Consistent with our hypothesis, irradiation with CcO-inhibitory NIR showed MitoSOX fluorescence similar to the sham-surgery control groups, suggesting that CcO-inhibitory NIR treatment can prevent ROS formation.

NIR Therapy Given at the Onset of Reperfusion Reduces CA1 Hippocampal Neuronal Death Following Global Brain Ischemia/Reperfusion

The first in vivo study of the neuroprotective efficacy of NIR was performed in the rat global ischemia model following bilateral carotid occlusion with hypotension.(Sanderson et al. 2013) As described above, neuronal death occurs predominantly in the CA1 hippocampus in this model. These neurons are particularly

sensitive to this insult and a near total loss of CA1 hippocampal neurons can be seen 3-7 days following reperfusion. In our study, untreated controls showed a significant loss of CA1 hippocampal neurons after 14 days (88%) as measured by cresyl violet staining and neuN fluorescent neuronal markers. Furthermore, gliosis was seen, characterized by immune responses; particularly inflammatory cells entering the area. Ischemia/reperfusion injury induced the translocation of microglia and macrophages as well as astrocytes, all seen in the CA1 hippocampus using confocal microscopy.

Animals treated with CcO-inhibitory wavelengths of 750nm and 950 nm, either alone or combined, showed significant reductions in hippocampal neuronal death. Animals treated with the NIR inhibitory wavelengths only had 11 to 35 % of their CA1 hippocampal neurons die. As predicted, the CcO-excitatory wavelength of 810 nm did not improve the survivability of these neuron populations.(Sanderson et al. 2018)

NIR Therapy Reduces Brain Injury in Neonates Following Simulated Hypoxia

Approximately 0.002-0.004% of at-term hospital births result in the neonatal brain becoming hypoxic which leads to a condition known as hypoxic-ischemic encephalopathy (HIE). This pathology can cause long-term health issues such as cerebral palsy or epilepsy.(Al-Macki 2009) A number of factors can contribute to HIE such as maternal hypotension; however, the most common cause is compression of the umbilical cord or prolapse and placental abruption. Moreover, neonatal brains are also susceptible to reperfusion injury. Unpublished work from our laboratory has shown that in the Vinucci-Rice model of HIE, the inhibitory NIR wavelength of 750 nm reduced brain injury due to hypoxia-ischemia in neonates – a finding that is consistent with the global ischemia model. Moreover, inhibitory NIR applied at the onset of reperfusion reduced caspace-3 cleavage thus stopping cells from undergoing programmed cell death.(Reynolds 2015)

Conclusion

Both the published and unpublished data from the Hüttemann/Sanderson laboratories provide evidence for our model of IR injury in which transient reductions in mitochondrial membrane potential during reperfusion can reduce ROS production, which is the number one cause of neuronal death in IR injury. (Mason 2014; Hazeki O 1988) As was described in chapter 1, the relationship between ROS and $\Delta\Psi_m$ is exponential – when the membrane potential exceeds 140 mV due to hyperactivation of the complexes, ROS increases exponentially. We thus argue that even moderate reductions in membrane potential can enact an exponential decreases in ROS production. This was first shown in HT22 cells in which we showed that inhibitory NIR reduces CcO activity. When the same wavelengths were applied immediately upon reperfusion in an in vivo rat model of global brain ischemia, we saw significant reductions in CA1 hippocampus neuronal death which was corroborated by behavioral improvements as measured by memory and spatial learning tasks. Moreover, similar results were seen in a neonatal model of brain ischemia/reperfusion. Thus, in two animal models, NIR has been shown to reduce ROS production in early reperfusion by directly targeting the rate limiting enzyme of the ETC, CcO, reducing its activity and thus reducing overall $\Delta\Psi_m$.

CHAPTER 3 - MAGNETIC RESONANCE IMAGING IN STROKE RESEARCH AND IAGNOSIS

MRI Fundamentals

A series of elegant experiments in 1938 by Isidor Rabi first performed in gas beams revealed a unique principle of matter: magnetic resonance.(Rabi et al. 1938) In 1973, Paul Lauterbur published the first magnetic resonance image in *Nature*.(Lauterbur 1973) He placed two 1-mm tubes of water in a 1.4 T magnet and when he applied magnetic field gradients rotating by 45 degrees, he was able to produce four, one-dimensional projections of the signal. When working backwards, these images were then able to produce a 2-dimmensional image.

Physiologically, water is the most abundant compound in the brain followed next by lipids, both of which are heavily comprised of protons which can generate an MRI signal and they have a mass, a charge (positive), and a spin. Spin, in the case of subatomic particles, is an intrinsic component of the proton, which means that it is independent of any external force, causing the particle to spin like a top along an axis with a wobble. Furthermore, spin on an individual proton is ½ Plank's constant. Thus, the combination of the charge and spin means that protons have a nuclear magnetic moment, which is defined as a nonzero magnetic dipole. Thus, protons rotating on an axis generate a small magnetic field. However, it must be noted that at room temperature they are randomly oriented with their spins being either -1/2 or +1/2 and as a result, there is no net magnetization – body tissues, for example, are not magnetic.

If a tangential force is applied along the z-axis the proton wobble increases. This force, in MRI, is generated by a radio-frequency (RF-pulse) which is time-dependent sinusoidal wave that matches the precessional, or Larmor frequency of the protons. It is

critical that the RF pulse matches the Larmor frequency because the key is to generate resonance strong enough to push the protons into the transverse rotational plane. Applying an RF pulse at a proton's Larmor frequency causes its net magnetization (M) to flip and rotate into the transverse magnetization. Due to Faraday's law of electromagnetic induction, any magnetic field can interact with an electric circuit to produce an electromotive force. Thus, as protons begin rotating in the transverse plane due to their spins being flipped 90 degrees by the RF pulse, they induce a current each time they spin through the copper receiving coil. Thus, the current signal that is produced encodes the Larmor frequency. Since the protons composing different tissues, fat, bone, muscle, etc. have different precessional frequencies due to the atomic composition of the tissue itself, frequency encoding can differentiate the tissues based on the RF pulse applied.

MRI in Stroke

Brain imaging in cases of acute stroke provides critical information to clinicians regarding stroke severity and location in a timely manner, thus allowing physicians to quickly determine whether the patient is a candidate for receiving fibrinolytic therapy. Prior to initiating this treatment, other pathologies such has cerebral hemorrhage must be ruled out. To date, computed tomography (CT) imaging is still the best approach for differentiating hemorrhagic from ischemic stroke. However, due to the requirement for systemic administration of a radioactive contrast agent, as well as low sensitivity in detecting ischemic lesions, it remains suboptimal. Many studies since the early 1990's have provided convincing evidence that MRI is a far superior imaging modality for use in diagnosis of acute ischemic stroke.(Baird and Warach 1988; Barber et al. 1998; Schellinger et al. 2001; Tong et al. 1998) In what follows we shall review in greater detail the most common and useful MRI modalities both in the clinic and in the utilization in this

study.

Diffusion Weighted Imaging (DWI)

In 1905, Albert Einstein published a paper in which he refined the theory of the Scottish-born botanist, Robert Brown to describe the apparent movement of molecules suspended in a liquid due to the molecular-kinetic theory of heat.(Einstein 1905) If a drop of ink were to be added to a beaker of water, the ink atoms would diffuse throughout the beaker seemingly, though, because the diffusion is unimpeded, the probability of finding any particle of ink, according to Einstein, can be predicted using a diffusion coefficient that is related to the mean square displacement of the Brownian particle, where, the mean square displacement reflects the derivation of the particle's position with respect to a certain position over a given period of time.(Michalet 2010) Thus, diffusion maps can be generated in Euclidean space comprised of a set of coordinates that were determined from the eigenvalues and eigenvectors of the diffusion constant.(Coifman and Lafon 2006; Coifman et al. 2005)

Within most fluids diffusion is even, as we saw in the example of the ink in the water, which results in equal diffusion of particles in all directions across time. This is called *isotropic* diffusion and defined with a single diffusion coefficient. Biological tissues, however, present a myriad of impediments to free diffusion and thus result in a number of diffusion coefficients in multiple directions. This behavior is known as anisotropy, where diffusion must be described by a 3 x 3 matrix known as the diffusion tensor. The nervous system in particular is highly anisotropic due to the presence of cell membranes and myelination, both of which are highly hydrophobic and thus impede the free diffusion of water.(Beaulieu 2002)

During brain ischemia, cessation of blood flow has a direct effect on the ionic

gradients. Hossmann et al. performed a key set of experiments in which they recorded the activity of extracellular sodium and subarachnoid sodium ions using ion-sensitive electrodes. During ischemia, they found extracellular [K^+] increases from 3.3 to 56 mEq per liter and [Na^+] decreases from 133 to 53 mEq per liter. Following reperfusion, ionic distribution gradually returned to physiological levels within an hour. Most notably, they found that the intracellular uptake of sodium was accompanied by a water shift into the intracellular compartment which resulted in shrinking of the extracellular space from 18.9 to 8.5 vol%.(Hossmann Ka Fau - Sakaki, Sakaki S Fau - Zimmerman, and Zimmerman 1977) Because acute stroke leads to rapid reductions in the OxPhos capabilities of the cell, ATP stores plummet and lactic acid accumulation increases which leads to failure of the Na^+/K^+-ATPase. As Hossmann found, pump failure causes ions to equilibrate across the neuronal membrane following their concentration gradients. This in turn leads to a shift of fluid into the cell. Furthermore, these processes occur in a matter of minutes following ischemia.(Hossmann Ka Fau - Sakaki, Sakaki S Fau - Zimmerman, and Zimmerman 1977; Moseley, Kucharczyk J Fau - Mintorovitch, et al. 1990) The reduction of the extracellular space by about 55% increases the anisotropy of ischemic brain tissue thus trapping water molecules between membranes that were previously free to diffuse along membranes. Using strong magnetic field gradient strengths (b values of 1413 s/mm^2), Moseley et al. found that, in MCA occluded cats, DWI signal strength showed a significant hyperintensity following 45 minutes of ischemia that was not seen in other imaging modalities such as T2 weighted imaging (T2WI).(Moseley, Cohen Y Fau - Mintorovitch, et al. 1990) Thus, as water becomes more impeded during ischemia, DWI signal intensity increases.

However, the question then arises, does DWI show actual cell death or just

edema? Sodium ion influx into the cell following ATP reduction also leads to chloride influx through the chloride channels leading to an increase in osmolality that favors water to shift inward through the aquaporin channels.(Badaut et al. 2001; Badaut et al. 2002; Kimelberg 2004; Moseley, Cohen Y Fau - Mintorovitch, et al. 1990) As the intracellular fluid volume increases and the extracellular space decreases, alterations form in membrane architecture resulting in blebbing. Thus, when the ionic pumps fail, the cell dies via a process known as *oncosis*,(Weerasinghe and Buja 2012) first coined by von Recklinghausen.(Szabo 2008) Furthermore, oncotic death can be morphologically characterized by damage to membrane phospholemma and organelle membranes, as well as loss of phospholipids and the eventual disappearance of nuclei.(Barros, Castro J Fau - Bittner, and Bittner 2002; Barros, Hermosilla T Fau - Castro, and Castro 2001; Majno and Joris 1995) Thus, cellular edema in brain is definitively cytotoxic and therefore a positive DWI signal indicates very early on the extent of neuronal infarction plus edema.(Liang et al. 2007) It is important to clarify that the early time point shows edema in addition to ischemic cell death because infarct sizes become smaller when measured by T2 weighted imaging during the chronic phase of stroke.

The quantification of impedance of water is known as the apparent diffusion coefficient (ADC), which is calculated by software and reflects the degree of diffusion of water within the tissue under examination.(Schlaug et al. 1997) The higher the ADC value, the more freely water diffuses and therefore the brighter the area on the image. An ischemic lesion that has restricted diffusion of water due to the death of cells will have a lower ADC and thus appear hypointense.(Baird and Warach 1998)

In addition to the ADC, another important variable in DWI is the b value. The b-value is a measure of the strength and duration of the field gradients: the higher the b

value, the more powerful the diffusion weighting and thus the more accurate the imaging of diffusion effects.(Stejskal and Tanner 1965; Kingsley and Monahan 2004; Burdette et al. 2001) In this modality, acute stroke appears hyperintense to surrounding tissue.

In conclusion, though initially shown in animal models that DWI can become positive as early as 5 minutes into ischemia, this occurs 2 to 6 hours after the onset of symptoms in humans. (Reith et al. 1995; Back et al. 1994; Sevick et al. 1992; Perez-Trepichio et al. 1995; Marks et al. 1996; Sorensen et al. 1996; Warach, Dashe Jf Fau - Edelman, and Edelman 1996) The ability to detect lesions is certainly an advantage of DWI but it is not the only one: other assets to the technique include low false negative rates (5%)(Singer et al. 1998) and it is also able to clearly delineate between ischemic and non-ischemic parenchyma(Lutsep et al. 2004; Marks et al. 1996; Koroshetz Wj Fau - Gonzalez and Gonzalez 1997), and the ability to differentiate acute and chronic ischemic zones.(Lutsep et al. 2004; Singer et al. 1998) Thus, it has been shown clinically that DWI is far superior to other imaging modalities in detecting early strokes and shows a high correlation between stroke lesion volume and clinical outcome. (van Everdingen et al. 1998)

T2-Weighted Imaging

T2 weighted imaging relies on the transverse relaxation, also known as “spin-spin” relaxation of the magnetization vector. Once the RF pulse inverts the proton spins, they begin to relax away from the transverse plane to the longitudinal one. While this is happening, the spins deteriorate from their position in the transverse plane and the amount of time of decay reflects the T2. The amount of time it takes for each proton to undergo T2 decay depends on inherent properties of the tissues but also its magnetic susceptibility.

The T2 sequence is comprised of the following imaging characteristics that equip the modality for imagining of the brain in both its physiological and pathological states. The T2 signal increases (appears brighter) when there is greater water content, such as in cases of edema, tumors, infarction, and infections. Blood also appears bright as does cerebral spinal fluid (CSF). The reason why these compounds appear brighter is because they have a longer transverse relaxation time, or a faster relaxation time. In pure water, the T2 is very long, on the order of 3-4 seconds because unimpeded water moves faster than the Larmor frequency. As protons become more constrained in larger molecules, the relaxation time shortens because the motion of the protons slows down. A shorter relaxation time means that the protons stay for a shorter amount of time in the transverse plane before returning to their net magnetization position and thus produce a darker image. As the amount of water in a tissue decreases, such as in cases of bone or soft tissue, the signal is lost more quickly and the image appears darker in those areas. (Allisy-Roberts and Williams 2008; Mitchell Dg Fau - Burk et al. 1987)

In stroke, T2 lesions appear as bright, hyperintense regions that become positive in humans within the first 3-8 hours after the onset of ischemia.(Mohr et al. 1995) N van Bruggen et al. found that, consistent with previous findings, cerebral edema is accurately identified by T2WI which they corroborated histologically by tracing the localization of a tracer protein. (van Bruggen et al. 1992) Interestingly, there is a lag time before T2 becomes positive, with T2 becoming positive more chronically and DWI more acutely.(van Bruggen et al. 1992) For this reason, both imaging modalities are commonly used clinically: DWI very early in the course of stroke to identify lesions quickly, and T2WI to track chronic lesions.(Powers et al. 2018)

Perfusion Weighted Imaging

Measuring cerebral perfusion both during ischemia and reperfusion provides important information on the extent of tissue that is at risk for infarction in the absence of intervention. Tracking the movement of blood through the brain's vasculature can be accomplished by several imaging modalities, most notably CT angiography (Knauth et al. 1997; Shrier et al. 1997) and gadolinium based MRI.(Merten et al. 1999) In what follows, arterial spin labeling (ASL) MRI will be discussed as a viable alternative to both these techniques.

Arterial Spin Labeling Perfusion MRI (ASL)

Arterial spin labeling is an MRI modality that uses arterial blood as an endogenous contrast to measure perfusion thus eliminating the need for injecting contrast agents or tracers.(Alsop and Detre 1995; Buxton et al. 1998; Rosen et al. 1990; Detre et al. 1994; Wolf and Detre 2007; Petersen et al. 2006; Alsop and Detre 1998; Williams et al. 1992; MacIntosh et al. 2010; Liu and Brown 2007; Wong et al. 2006; Golay, Hendrikse J Fau - Lim, and Lim 2004; Wu et al. 2007; Zhang et al. 1995; Barbier, Lamalle L Fau - Decorps, and Decorps 2001; Detre et al. 1992) The technique works as follows: first, the computer obtains control images of an area of interest. Following this, radio frequency pulses are applied to an area that is upstream from the region of interest that invert the magnetization of the protons composing water within this slab (usually in the neck). These inverted protons which are magnetically labeled can flow into the region of interest where they mix and displace their magnetization to the unlabeled water thus slightly reducing the equilibrium magnetization in the region of interest. The region of interest is imaged once more and the tagged images are subtracted from the control images. Because the labeled water molecules freely cross from capillaries into extracellular space and even enter cells,

perfusion rates can be calculated.

ASL can be further subdivided into continuous ASL (CASL) and pulsed ASL (PASL). CASL, first proposed by Williams et al. in 1992,(Williams et al. 1992) involves continuous radiofrequency labeling through a narrow slice of the neck. Magnetization is inverted by the dual application of a continuous pulsed RF for two to four seconds and a magnetic field gradient oriented in the direction of blood flow.(Ferré et al. 2013) An advantage of using CASL is that it has higher contrast.(Wang et al. 2002) However, notable disadvantages are the high magnetization transfer (MT) and the high level of energy that is applied to the tissue.(Ferré et al. 2013)

PASL, in contrast uses very short RF pulses over larger areas.(Ferré et al. 2013) Symmetrical PASL uses the flow alternating inversion recovery (FAIR) method in which a non-descript pulse that inverts the protons is applied during the control phase that eventually becomes selective when a slice-selection gradient is applied during the labeling phase.(Kim 1995) The asymmetrical methods, which are the ones employed in this study, involve what was described above: a labeling zone with a 10-15 mm thickness that is located away from the region of interest that is subtracted from a control image. (Edelman et al. 1994)

The goal of perfusion imaging in the context of acute stroke is to identify hypoperfused tissue (penumbra) and to differentiate it from the ischemic core.(Parsons et al. 2010; Bivard et al. 2011) The usefulness of perfusion weighted imaging lies in both its ability to track cerebral blood flow within a specific volume of tissue per unit time and thus an ischemic threshold can be set; but also, volumetric analysis can be performed on gross tissue to determine the ratio between at-risk and infarcted tissue – this is known as the perfusion/diffusion mismatch and will be outlined in greater detail below.

Perfusion/Diffusion Mismatch

Identifying tissue that has the potential to be salvaged by conventional stroke therapies is paramount in the clinical setting. Ischemic stroke zones, as we have previously seen, can be broadly defined as core and penumbra. The core is classically defined as the area of brain most proximal to the occluded vessel containing neurons that rapidly undergo energy depletion, anoxic depolarization and death following a necrosis morphology; unfortunately, nothing can be done to salvage these neurons. Surrounding the ischemic core is an area of brain that receives enough blood flow from collateral vessels that maintains neuronal viability even in the absence of their electrical activity. This area has been termed the penumbra and if left untreated eventually goes on to die via a delayed neuronal death program. Thus, restoration of blood flow through tPA or thrombectomy in a timely manner is of critical importance to save penumbral neurons. However, as we previously described, the very same intervention designed to save them can result in their downfall following reperfusion; though ROS is only one component of the injury mechanism.

Since the ischemic brain is not homogenous but is comprised of different zones of viability and activity according to collateral flow rates, it stands to reason that they can be imaged, in vivo, and conclusions drawn regarding the extent of the ischemia as well as the potential for saving the penumbra.

In any given area of ischemic brain, PWI hypointensities can be defined as an area that is at risk for infarction and DWI hyperintensity as already infarcted tissue. It was thus theorized that a volume for volume mismatch exists between at-risk and infarcted tissue or PWI and DWI on MRI modalities during the early phase of ischemia – a mismatch that eventually grows smaller as the infarcted area grows larger over time due to either lack

of intervention or reperfusion injury. Thus, the difference between PWI and DWI during ischemia reflects potentially salvageable brain tissue. Some of the most compelling data to the validity of the mismatch are that eventually diffusion abnormalities grow into the at-risk area. For example, in clinical studies that enrolled patients in neuroprotective therapies it was shown that lesions on average grow from 144% to 180% from their initial volume across time. Patients who were reperfused within clinically relevant time windows had diffusion abnormalities stop growing which may suggest that the mismatch area was salvaged. This was shown convincingly by Jansen et al.(Jansen O Fau - Schellinger et al. 1999) Further corroborating these results, Parsons found that tPA treated patients had higher mismatches than untreated controls – a finding which suggests that more at-risk tissue was salvaged due to reperfusion.(Parsons et al. 2002) Interestingly, the PWI/DWI mismatch may occur in patients as late as 24 hours and even later from the onset of symptoms. Darby et al showed that while mismatch decreased across time, around 60-70% of patients still had significant mismatches as late as 24 hours. (Darby et al. 1999)

It must be noted, however, that the PWI/DWI mismatch, at least according to Kidwell et al, is based on two fundamental assumptions. First, the boundary of PWI hypointensity that is seen delineates between the penumbra and healthy tissue. Second, the boundary between PWI and DWI regions reflects the core. In what follows, shortcomings of the PWI/DWI mismatch will be described in greater detail.

The primary criticism of this theory is that it is not easy to differentiate between true penumbra and benign oligemia. The initial Astrups study found that rather than two clearly defined regions of core and penumbra, there is an additional, third zone in which blood flow falls below physiological levels but the tissue is at no time at risk for infarction. Astrups defined these regions according to the amount of blood flow received per 100

grams of tissue per minute. Core flow rates fell between 6 and 10 ml/100g/min. Penumbra values fall between 10 and 20 ml/100g/min. While this criticism is valid, it still does not explain how infarction volumes eventually expand into the at-risk volume if left untreated.

Conclusions

Multi-modal MRI has developed into the gold standard for stroke diagnosis and treatment in the clinic. The ability to image the brain in real-time across a number of parameters can give clinicians up to date information on the extent of brain injury as well as the amount of tissue that can be salvaged by any therapeutic intervention. Perfusion-weighted MRI is a powerful tool that gives insight on both relative cerebral perfusion rates within a voxel of tissue or across slices, as well as the volume of hypoperfused tissue. Diffusion weighted imaging can give an early assessment of infarcted brain tissue as well as be a powerful predictor of final infarct size which can be computed in the chronic phase of stroke by T2 weighed imaging. This project has employed all of these MRI modalities in order to increase the translatability of our findings, as well as to track real-time, *in vivo* changes in infarct progression in individual animals.

CHAPTER 4 - INFRARED LIGHT THERAPY AS A NOVEL TREATMENT FOR STROKE: TWO TREATMENT WINDOWS

Introduction

Stroke is one of the leading causes of death and disability in the Western world and accounts for approximately 1 in 20 deaths in the United States.(Benjamin et al. 2017) Ischemic stroke occurs due to the occlusion of an intracranial artery resulting in rapid and cytotoxic reductions in blood flow to the brain parenchyma. Classically, neurons directly affected by the occlusion have been divided into two groups: the ischemic core and the penumbra. The core contains neurons that are closest to the occlusion which suffer rapid energy depletion, ionic equilibration, and irreversible necrosis. Surrounding the core is the penumbra which is a region that has increasing rates of perfusion moving outwards because it is fed by collateral vessels, and as such remains ischemic yet viable. Therefore, stroke therapies aim at reducing the size of the core and salvaging the penumbra. Moreover, MRI modalities are becoming the gold standard for identifying potentially salvageable brain tissue.

To date, the only approved treatment is rapid restoration of blood flow either pharmacologically with tPA or surgically with a thrombectomy. While patient outcomes have greatly improved due to these early interventions, a substantial amount of tissue damage occurs during the reperfusion phase. As the ischemic brain tissue is re-oxygenated, ROS are quickly generated, beginning at the early stages of reflow which goes on to cause further cell death by way of complex, interacting molecular pathways. It is important to note, however, that ROS are only part of the story. The inflammatory response must also be considered. Nonetheless ROS play a key role and to date, pharmacological treatment targeting ROS has thus far proven ineffective likely due to the

inability to deliver effective concentrations of the drug to sub-cellular targets at the critical stages of ROS generation during early reperfusion.

Mitochondria are the primary source of post-ischemic ROS generation. ETC hyper-activation due to changes (i.e., primarily loss) of post-translational modifications during ischemia promotes hyperpolarization of the mitochondrial membrane potential at the early phase of reoxygenation after ischemia and thus an exponential increase in mitochondrial ROS production. Thus a treatment needs to be found that targets mitochondria to limit reperfusion injury.

A series of studies looking at systemic hypothermia or mild hypothermia showed promise in reducing brain injury following cardiac arrest in the dog model. (Leonov, Sterz F Fau - Safar, Safar P Fau - Radovsky, and Radovsky 1990; Leonov, Sterz F Fau - Safar, Safar P Fau - Radovsky, Radovsky A Fau - Oku, et al. 1990; Sterz et al. 1991; Weinrauch et al. 1992; Kuboyama et al. 1993; Safar et al. 1996) In patients, therapeutic hypothermia was first shown to be effective in a seminal study in the late 1950's which reduced mortality following global brain ischemia in patients who had suffered from cardiac arrest.(Benson Dw Fau - Williams et al. 1959) Furthermore, two large clinical trials in recent years have shown the therapeutic benefit of hypothermia following cardiac arrest.(Bernard et al. 2002; 'Mild therapeutic hypothermia to improve the neurologic outcome after cardiac arrest' 2002) Several groups have reported that in MCA occluded rats hypothermia applied for as late as 3 hours following reperfusion could significantly reduce infarct volume up to 50%-90%.(Huh et al. 2009; Maier et al. 2001) The Cooling for Acute Ischemic Brain Damage (COOL AID) clinical trial showed some promise using endovascular cooling in acute ischemic stroke but concluded that more studies were needed.(De Georgia et al. 2004) Moreover, animal models of ischemia/reperfusion injury

have shown that hypothermia could reduce ROS production as well as improve mitochondrial function in the heart and the brain.(Gong et al. 2012; Tissier et al. 2013) Therapeutic hypothermia decreases cerebral metabolic rate by 6-7% for every 1 degree decrease in body temperature, which in turn reduces oxygen demand of the brain. (Polderman 2009; Erecinska, Thoresen M Fau - Silver, and Silver 2003) Results from groups studying energy metabolism found that in rats that had undergone a normothermic ischemic insult for 30 minutes and a 2 hour recovery (reperfusion) at 30° C had no decrease in the activity of mitochondrial complexes II-III and IV. On the other hand, decreases of 15-30% were seen in animals that had recovered at physiological temperature of 37° C.(Canevari et al. 1999) Taylor et al. (2002) conducted studies in which they looked at 6-hour whole body cooling to 30° C after three hours of normothermic brain hypoxia-ischemia in 7 day old rat pups.(Taylor et al. 2002) When the pups were sacrificed at 14 days, the PCr/Cr ratios were identical to control animals which indicated neural protection. Thus, mild, short-term hypothermia seems to normalize cerebral metabolic rate and reduce mitochondrial damage while increasing the duration of hypothermia can reduce secondary changes to energetics, including both mitochondria but also the immune response and thus salvage brain tissue.(Erecinska, Thoresen M Fau - Silver, and Silver 2003)

As discussed in Chapter 2, previous studies from our group and others have uncovered a novel property of the terminal enzyme in the mitochondrial ETC, cytochrome *c* oxidase (CcO). It was found that this enzyme has photoreceptive properties that allow CcO activity to be regulated by specific wavelengths of near infrared light (NIR). Previous studies demonstrated that CcO activity can be stimulated by applying NIR wavelengths of 670 nm and 808 nm, thus increasing mitochondrial respiration. The CcO multi-protein

complex has several chromophores involved in enzyme catalysis. It is well-accepted that the primary cellular photoreceptor for NIR are the catalytic copper centers of CcO, with a broad absorbance spectra covering the NIR range of 700-1000nm.

Based on our model, however, increasing CcO activity during reperfusion would be counterproductive since ETC complexes are already hyperactive due to changes in their post-translational modifications leading to exponential ROS production during early reperfusion. Our group has found that CcO activity can be reduced by applying inhibitory NIR wavelengths (750 nm and 950 nm and the combination). Reduction of CcO activity by inhibitory NIR leads to transient, reversible reductions in both mitochondrial respiration, and the mitochondrial membrane potential. This in turn would lead to a reduction in the amount of superoxide produced, thus salvaging neurons, a finding that our lab showed in cell culture following oxygen glucose deprivation. Moreover, in addition to cell culture models, we have shown profound neuroprotection of NIR in vivo in the rat model of global brain ischemia in which we saw up to 89% of CA1 hippocampal neurons salvaged due to NIR irradiation applied during reperfusion compared to 14% of surviving neurons in the controls. While these results have been promising, further questions remain regarding its applicability to a focal brain injury like acute ischemic stroke, which differs in the pathological evolution and severity from the global brain ischemia, the latter mimicking brain injury following cardiac arrest/resuscitation.

It was therefore our goal in this study to test the preclinical efficacy of this therapy in focal brain ischemia (stroke) using the rat middle cerebral artery occlusion (MCAO) model. We hypothesize that dual-wavelength NIR applied during reperfusion following stroke will provide profound neuroprotection as shown through significant reductions in infarct volume measured by multiple, clinically translatable MRI modalities. We also

hypothesized that NIR therapy would directly target salvageable penumbral tissue which would be measured by a significant perfusion/diffusion mismatch. Furthermore, we sought to uncover whether two treatment durations of NIR would influence infarct size at the acute, subacute and chronic time points. Building on our previous data, our first aim was to modulate mitochondrial activity for 120 minutes, initiated at reperfusion, to limit ROS bursts during early reperfusion. We next sought to extend treatment duration to 240 minutes, building on the results from the hypothermia literature.

Materials and Methods

Chemicals, reagents, and diodes

Chemicals and reagents were obtained from Sigma-Aldrich (St. Luis, Montana, USA) unless otherwise stated. Light emitting diodes (LEDs) were obtained from Roithner Lasertechnik (Vienna, Austria). For animal experiments LED array 60 chips were used (750 nm, LED750-66-60; 950 nm, LED950-66-60). Diodes were mounted on heat sinks (black aluminum, 47x20 for LED array 60 chips) together with a small fan (EC3010M05X; Evercool, New Taipei City, Taiwan) operated in reverse mode. Diodes were calibrated with an optical power and energy meter (842-PE; Newport, Irvine, California, USA) and operated with an energy density of 200 mW/cm^2.

Experimental Design

Animal use protocols were approved by the Wayne State University Institutional Animal Care and Use Committee and all experiments were performed in accordance with the IACUC protocol and relevant regulations. Animals were given free access to food and water prior to surgery and all surgical procedures were held around the same time of day to prevent confounding effects of daily humoral cycles. Animals underwent 90 minutes of transient right middle cerebral artery occlusion as described below. One hour into

ischemia, animals were placed in the MRI and arterial spin labeling (ASL) and diffusion weighted imaging (DWI) sequences were obtained. Animals were allowed to recover from the anesthesia until a few minutes before the 90-minute ischemic period was to end at which time they were re-anesthetized and the incision opened. After 90 minutes, the filament was withdrawn and treatment immediately initiated for 120 minutes. Following the treatment duration, animals were taken off the isoflurane and transported again to the MRI where ASL and DWI scans were obtained. Following these scans, the animals were given a subcutaneous injection of buprenorphine (0.015mg/kg) in 10 cc of saline and allowed to recover in a temperature/humidity controlled environment. Twenty-four hours following reperfusion the following MRI sequences were obtained: ASL, DWI, T2 weighted imaging (the transverse, spin-spin relaxation time). After these scans animals were given 15 cc of subcutaneous dextrose injections (5% in 0.95% NaCl) twice a day as we found a reduction in water intake because of stroke. On days 7 and 14 the animals were again imaged and the above-mentioned scans acquired. On day 14, following the MRI scans, animals were sacrificed by transcardial perfusion with phosphate buffered saline followed by 4% paraformaldehyde. Brains were removed and post-fixed in PFA for 24 hours and then cryoprotected in a sucrose gradient (20%, 30%) until they were sectioned on a cryostat at 50 micrometer coronal sections and stained with H&E for histological analysis.

Middle Cerebral Artery Occlusion/Reperfusion

Focal brain ischemia was induced in two randomly assigned groups of male spontaneously hypertensive rats (223-336 g purchased from Envigo) through the middle cerebral artery occlusion method as previously described (Uluç, 2011-Longa, 1989). Briefly, animals were anesthetized with isoflurane (5% induction, 2% maintenance in a mix of 70% nitrous oxide, 30% oxygen). The animals' temperature was closely monitored by a

homeothermic blanket (Harvard Apparatus) and kept at 37º C. A neck incision was made at the midline and underlying connective tissue was removed through blunt dissection until the common, external, and internal carotid arteries were visualized. The superior thyroid and occipital arteries, as well as the external carotid were permanently ligated with a 6-0 silk suture. Next, a commercially available silicon coated tip monofilament suture (Doccol corporation) was inserted through an incision made in the external carotid and advanced into the internal carotid artery until it sat at and occluded the origin of the MCA (18-20 mm from the carotid bifurcation). The suture was secured in place and the incision quickly sutured and the animal was given subcutaneous injections of lidocaine (20mg/mL diluted 1:4) around the incision, taken off the isoflurane and allowed to recover in a temperature- and humidity-controlled chamber for 90 minutes. We found in a pilot study that 90 minutes of ischemia was the optimal time for causing reproducible infarcts without increasing animal mortality. Following 90 minutes of ischemia animals were re-anesthetized with the above isoflurane protocol, the incision reopened, the filament withdrawn and NIR treatment immediately initiated (see below).

Administration of NIR Treatment

NIR was administered directly to the intact scalp as previously described (Sanderson, 2018). Briefly, LEDs were placed 1.5 cm from the scalp which had been shaved of fur to prevent light loss due to absorbance and reflection. LED intensity was 200 mW/cm^2 which converts to 2000 joules/second/meter squared as a dose of energy. Animals were treated with combined CcO-inhibitory wavelengths of 750nm and 950nm as it was shown to be most effective by our previous work. Irradiation began immediately when the filament was withdrawn and continued for 120 minutes (first group) and 240 minutes (second group). During treatment the animals were kept anesthetized on

isoflurane (1.5%) and on a homeothermic blanket (Harvard Apparatus) which kept core temperature at 37º C. Control animals underwent the same procedure (duration, anesthesia) but were not irradiated with NIR. Moreover, Sanderson et al. demonstrated in vivo that during irradiation with the combined wavelengths, brain temperature remained constant around 36º C.(Sanderson et al. 2018)

Imaging Procedures and Analysis

All MRI protocols were performed on a 7.0-Tesla, 20-cm bore superconducting magnet (ClinScan; Bruker, Karlsruhe, Germany) that was interfaced with a Siemens console. Prior to imaging, animals were anesthetized with isoflurane (4% induction in room air, 1.75% maintenance). Animals were first subjected to a series of localization scans. Next, pulsed arterial spin labeling was acquired according to the following sequence parameters: Relaxation time (TR) of 3500 ms; TE of 16 ms; FoV read 35.0 mm; FoV phase 81.3%; distance factor 25%; slice thickness 2.0 mm; 4 slices. Next diffusion weighted imaging (DWI) sequence was conducted according to the following parameters: TR 10000ms; TE 50 ms; FoV read 32.0mm; FoV phase 100.0%; distance factor 0%; slice thickness 0.5 mm; 32 slices. Following this a T2 weighted imaging scan was acquired according to the following parameters: TR 3530 ms; TE 38 ms; FoV read 32 mm; FoV phase 100.0%; distance factor 0%; slice thickness 1.0 mm; 24 slices. Relative cerebral blood flow in the MCA territory during ischemia and reperfusion was calculated as previously described and discussed in Chapter 3. Briefly, voxel intensity in ipsilateral and contralateral hemispheres was averaged across three coronal slices using ImageJ, giving the average relative cerebral blood flow (relCBF) voxel intensity value. Then, using the kinetic model equations, CBF was calculated for both hemispheres giving cerebral blood flow rates in mL/100g/min. In order to calculate at-risk volume, interspace gap had to be

considered along with slice thickness when multiplying the sum of hypoperfused areas. When this was done, it was seen that the volume generated was significantly smaller than the infarct volume that was calculated at 24 hours which is anatomically impossible. The slice thickness in ASL sequences is 2 mm apart and the software reports an interspace gap of 25% in order to account for slice cross talk – or interference between slices during image reconstruction. When incorporating the interspace gap with the slice thickness, volumes were still too small and thus a correction factor was derived. Whole brains were traced from ASL sequences of each animal in the two-hour treatment group using the relCBF images at 2 hours following reperfusion and areas were summed. Then, AnalyzePro software generated whole brain volumes from each brain (described below) using the 2-hour reperfusion DWI sequence. The DWI whole brain volume was divided by the ASL sum of areas to generate a correction factor for each animal. When the mean of the correction factors in the group was taken it gave 3.2. Thus, the sum of the ASL at-risk areas were multiplied by 3.2 to give at risk volume in mm^3.

Infarct volumes were computed using the semi-automated segmentation tool in Analyze 11.0 (Biomedical Imaging Resource, Mayo Clinic, Rochester, MN). Seed points were set in the hyperintense MCA territory and thresholds based on voxel intensity were set until the entire region was outlined. The software then automatically calculated the area within that voxel intensity on each slice of the MRI sequence and multiplied the sum of the areas by slice thickness to generate a volume which was reported as mm^3.

Statistical Analysis

Relative cerebral blood flow between groups were compared using an unpaired, two-tailed t-test with a critical level set to 0.05. Infarct volumes were computed using a two-way ANOVA with the Neuman-Keuls test for post-hoc analysis. Slopes and intercepts

of the PWI/DWI mismatch lines were compared by linear regression with significance set at 0.05. Slopes and intercepts of perfusion/diffusion mismatch lines were compared using Analysis of Co-variance (ANCOVA) and the Prism graph pad software.

Apomorphine Induced Rotation Test for Functional Recovery

Fourteen days following reperfusion animals that received four hours of NIR treatment were administered a rotameter test for functional recovery following stroke. The rotameter measures the number of clockwise turns an animal completes. Because of unilateral MCA occlusion damage to subcortical structures in the striatum, rats with a more severe injury will show increased clockwise turns in response to the dopamine agonist apomorphine. Animals were administered a subcutaneous injection of apmorphine (1 mg/mL, 0.1 mL per 100 g body weight) and the compound was allowed to reach peak activity which, according to Modo et al. was 30 minutes following the injection.(Modo et al. 2000) Then, the animals' rotations were recorded for 30 minutes and the number of clockwise rotations summed. We opted to sum the total number of clockwise rotations rather than do a ration of clockwise over counterclockwise because animals were not making counterclockwise turns.

Results

Measurements of Relative Cerebral Blood Flow During Ischemia and Reperfusion

Analysis of cerebral blood flow during ischemia and reperfusion were assessed using arterial spin labeling perfusion weighted MRI (ASL-PWI) in the ipsilateral and contralateral hemispheres (Figure 1) (Liebeskind 2003, Fau et al 1977, Turrens, et al. 1985, Mitchell and Moyle 1967, Kadenbach et al 2010). During ischemia, all animals

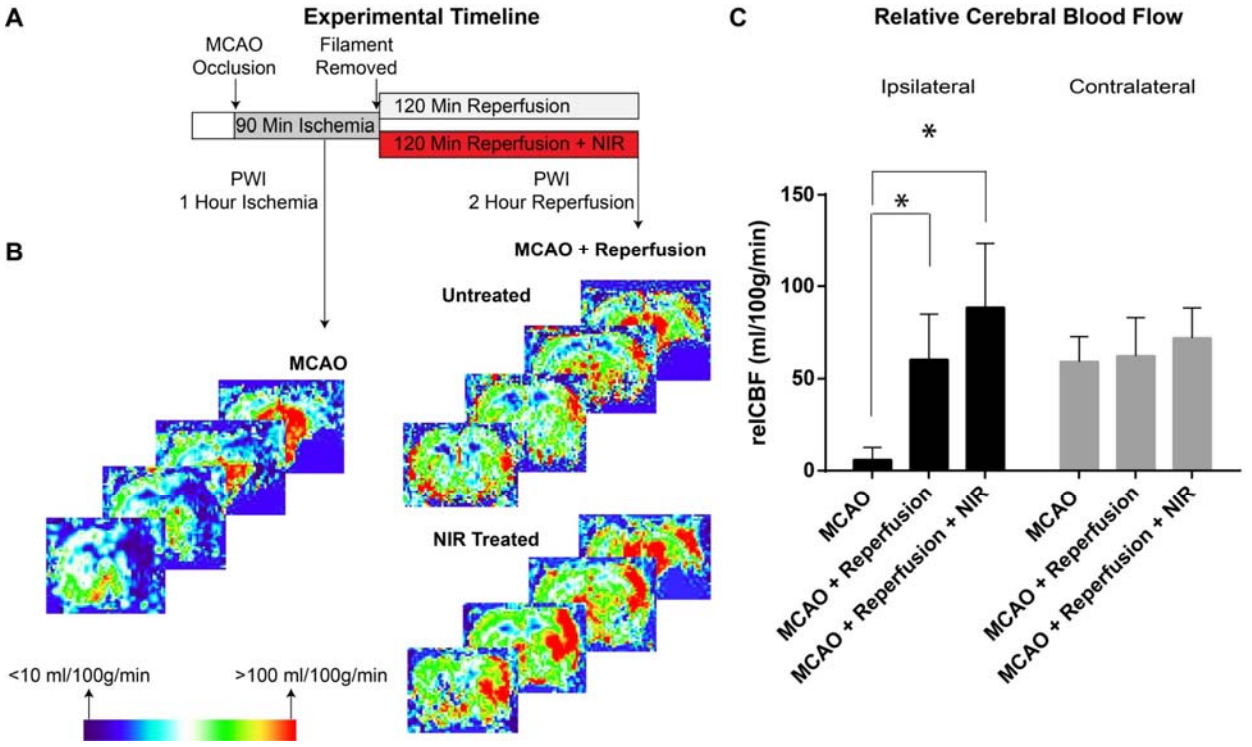

Figure 1. Relative blood flow during ischemia and following reperfusion. A. Experimental protocol: untreated control animals and NIR treated experimental animals both underwent MCAO with 90 minutes of ischemia. 60 minutes into ischemia a pulsed ASL sequence was obtained. Following 90 minutes of ischemia the filament was removed and treatment initiated for 120 minutes after which time ASL images were re-acquired. B. Representative ASL scans from both groups both during ischemia and following reperfusion. C. Averaged regional cerebral blood flow in the ipsilateral MCA territory and contralateral hemisphere both during ischemia and following reperfusion.

showed significant reductions in blood flow below established relCBF thresholds on the ipsilateral hemisphere without accompanying changes in flow on the contralateral hemisphere. Following treatment or no treatment, we repeated ASL scans and confirmed that the ipsilateral hemisphere was adequately perfused to levels comparable with the contralateral. Interestingly, there was no significant difference in relCBF between within the ipsilateral hemispheres of control and treated animals either during ischemia or reperfusion. Figure 4 shows the relative cerebral blood flow rates for animals treated for 4 hours. The untreated ischemic hemisphere had blood flow reduced to 10.94 mL/100 g/min on average while the contralateral hemisphere maintained physiological flow rates of 50.78 mL/100 g/min.

Infarct Volume in the Acute Phase of Stroke

We next looked at the effect of NIR on infarct volume in the acute phase of stroke, which we defined as 2 hours and 24 hours following MCAO/reperfusion (Figure 2A). Since DWI has been shown to be the most effective imaging modality both in quantification of early cytotoxic edema early on during brain ischemia, as well as predictive of final infarct size, we calculated DWI hypertensities during the acute phase (b=1000). Figure 2B shows that infarct sizes, which were acquired immediately post treatment (2 hours after reperfusion), did not significantly differ between NIR treated and control groups, although the infarct volumes of the treated animals were more spread than the untreated controls (control: 256.138 mm^3 ± 13.16; NIR treated: 210.377 mm^3 ± 29.09, $p>0.05$). At 24 hours following

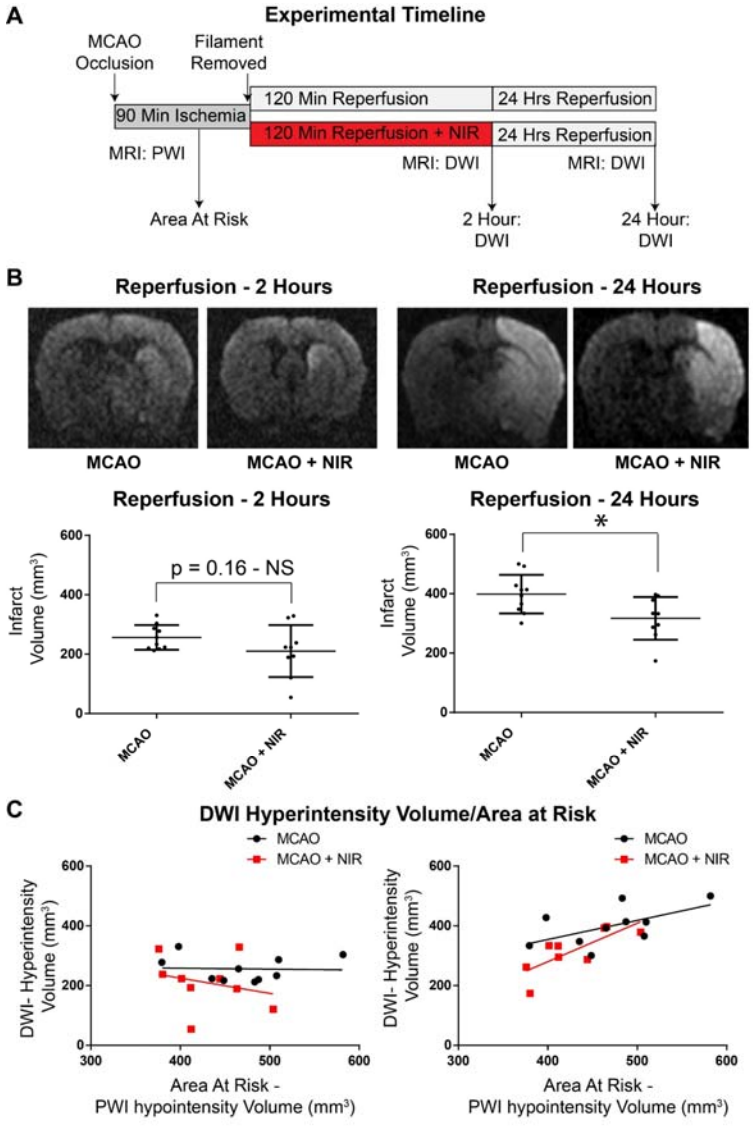

Figure 2. MRI analysis of cerebral injury in the acute reperfusion phase. A. Experimental design: with 2 hours of treatment. DWI images were obtained and (B) no significant difference in infarct volume was seen between NIR treated and control animals. B (continued): compared with untreated controls, NIR treated MCAO rats showed significant reduction of infarct volume at 24 hours as measured by DWI. C. Perfusion diffusion mismatch. Non-linear relationship was seen between at risk area analyzed by ASL at 1 hour ischemia (x-axis) and infarcted area (y-axis) 2 hours following reperfusion. At 24 hours linearity is seen where there is a positive correlation between the at-risk and ischemic areas. Statistical analysis was conducted by an unpaired, two-tailed t-test with significance set at $p<0.05$.

reperfusion, animals were re-imaged and based on infarct volumes that were calculated again using DWI (b=1000), NIR-treated animals showed a significant reduction of 20.5% in infarct size when compared to untreated controls: 398.86 mm^3 ± 20.54 vs. 317.03 mm^3 ± 23.96, $p<0.05$ (Figure 2B). The two-way ANOVA also indicated that infarct volumes were significantly different from 2 to 24 hours between both groups thus suggesting that the infarcts evolved over time. We next asked whether there was a mismatch between diffusion and perfusion weighted imaging. We theorized that a mismatch between at-risk volume calculated during ischemia and ischemic hyperintensities would mean that viable tissue in the penumbra was being salvaged by the therapy. Figure 2C shows the relationship between at risk volume, which was calculated using ASL images 1 hour into ischemia, and infarcted tissue taken from DWI images at both 2 and 24 hours post reperfusion. At 2 hours following reperfusion no relationship is seen between at-risk and ischemic tissue. At 24 hours, however, a positive linear relationship is seen in both treated and untreated animals suggesting that infarct size could be correlated to the size of at-risk tissue. Despite the linearity of the relationship, the means of infarct volume remained different even though at risk tissue remains the same between both groups.

Figure 5A shows infarct volumes (in mm^3) between NIR treated and untreated animals, treated with NIR for 4 hours following reperfusion. A significant difference was seen between two groups in the early reperfusion phase (control group: 228.4 mm^3, SD 39.79; NIR treated group: 138.4 mm^3, SD 82.623; $p=0.0229$). Next, DWI hyperintense lesion volumes were calculated from scans taken 24 hours following reperfusion. A highly significant 24% reduction in infarct volume was observed between control (351.3 mm^3, SD 51.25) and NIR-treated (266.3 mm^3, SD 50.62; $p=0.0088$) animals. Moreover, a significant difference was seen in infarct volumes from 4 to 24 hours in both groups as

calculated by two-way ANOVA indicating that the infarcts continued to evolve from 4 to 24 hours.

Figure 6A shows the perfusion/diffusion mismatch with at-risk area obtained from pulsed ASL perfusion weighted imaging 60 minutes into ischemia, and area of infarction obtained from DWI 4 hours following reperfusion. When analysis of covariance was performed, the slopes of the lines were not significantly different ($p=0.41$) but the intercepts were significantly different ($p=0.031$). 6B shows at-risk area plotted against area with the area of infarction obtained 24 hours post reperfusion. As at the 4 hour time point, ANCOVA results indicated that the slopes of the two lines are not significantly different ($p=0.23$) while the intercepts are highly significant ($p=0.0061$). What this means is that while the distribution of at-risk volumes remains the same between both groups, the treated animals displayed smaller MRI-measured infarcts. This indicates to us that tissue that was at risk to become infarcted following reperfusion was salvaged by the therapeutic intervention.

Infarct Volume in the Chronic Phase of Stroke

Early therapeutic efficacy in the context of stroke has shown promise acutely but diminished in chronic stroke.(Schellinger et al. 2012; Lees et al. 2012; Mergenthaler and Meisel 2012; Gladstone, Black Se Fau - Hakim, and Hakim 2002; Lapchak, Zhang Jh Fau - Noble-Haeusslein, and Noble-Haeusslein 2013) Thus, it was necessary to assess whether the therapeutic benefits of NIR in reducing infarct size were maintained during the chronic phase of stroke. To accomplish this, T2 weighted MRI images were acquired at 7 and 14 days following MCAO/reperfusion (Figure 3A). Seven days following MCAO NIR treated animals maintained a significant 25.4% reduction in infarct size when compared to untreated control animals: 363.3 mm^3 vs 270.7 mm^3, $p=0.015$ (Figure 3B).

Fourteen days after MCAO and prior to sacrificing the animals, T2WI images were acquired and a significant reduction of infarct size of 24.9% between control and treated animals was observed: 316.9 mm^3 vs. 240.8 mm^3, p=0.015 (Figure 3B). Furthermore, there was no significant difference in infarct volumes from 7 to 14 days. These data demonstrate significant reduction in infarct volumes, as measured by multiple MRI modalities, following NIR treatment both acutely and chronically following MCAO/reperfusion; however, as measured by the ANOVA, the infarcts remained fully evolved by 7 days even though the treatment effect remained to 14 days. We analyzed the relationship between at-risk tissue (PWI) and infarcted tissue (T2WI) during the chronic phase of stroke and found that despite an even spread of the data along the

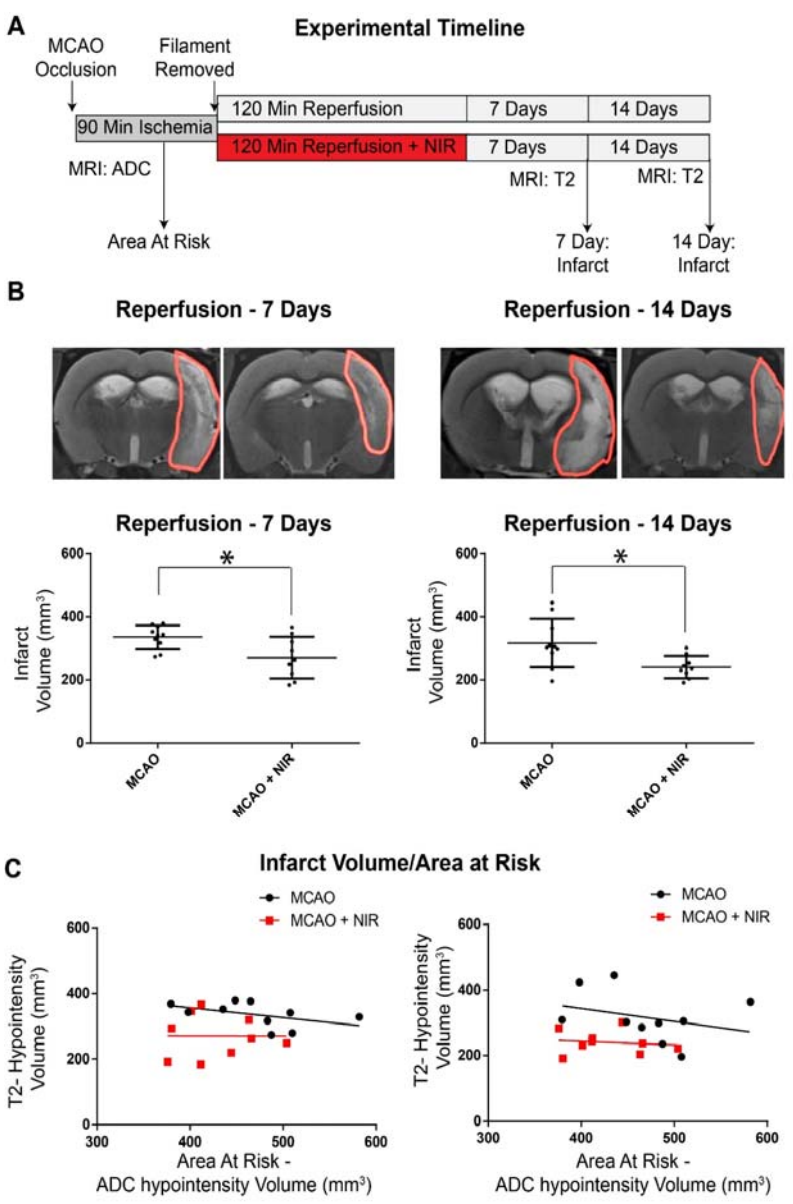

Figure 3. Cerebral infarct in chronic phase of post-stroke reperfusion injury. A. experimental design: 7 and 14 days following reperfusion T2WI images were acquired. B. 7 days. Compared with untreated controls, NIR treated MCAO rats showed a significant reduction in infarct volume. Significant reduction in infarct volume persisted to 14 days post stroke. Statistical analysis was conducted by an unpaired, two-tailed t-test with significance set at $p<0.05$. C. PWI/DWI mismatch.

x-axis (indicating a range of at-risk volumes during ischemia), there was reduced infarcted volume in the NIR treated group (Figure 3C) at both 7 and 14 days post reperfusion.

We next assessed whether a 4 hour treatment duration would improve the neuroprotective effect by targeting the acute and chronic phases of reperfusion injury. Using T2 weighted imaging, control and NIR treated animals were scanned 7 days following reperfusion (Figure 3A). T2 hyperintensities yielded a highly significant 48% difference in volume between control (449.3 mm^3, SD 16.4) and NIR-treated (234.8 mm^3, SD 111.2) animals (p=0.0056). We next asked whether this difference would persist to 14 days following reperfusion. As shown in Figure 3B, using T2 weighted imaging, infarct volumes showed a significant 48% reduction in stroke size between control and NIR treated animals (control: 339.9 mm^3, SD 73.92; NIR treated: 178.4 mm^3, SD 113.3; p=0.036) with no significant difference in infarct evolution from 7 to 14 days.

We next examined the PWI/DWI mismatch during the chronic phase of 4-hour treated animals. Figure 6C shows at risk area plotted with infarction area at 7 days. Slopes remain non-significant (p=0.34) while intercepts show significant difference (p=0.018). Figure 6D shows at-risk area plotted against area of infarction at 14 days.

Two-Hour Treatment Histology

At 14 days animals were sacrificed and transcardially perfused as described above. Due to the variability in tissue integrity following the staining protocol, we measured the volume of non-infarcted tissue on the ipsilateral hemisphere rather than the infarct volume. Because infarcted tissue is fragile 14 days after injury, accurate assessment of the tissue was not precise. Figure 4 shows the volume of non-ischemic tissue reported in mm^3. NIR-treated animals had significantly more non-infarcted tissue on the ipsilateral hemisphere than untreated controls (237.4 mm^3, SD 29.95 vs. 200 mm^3,

SD 17.44; p=0.042).

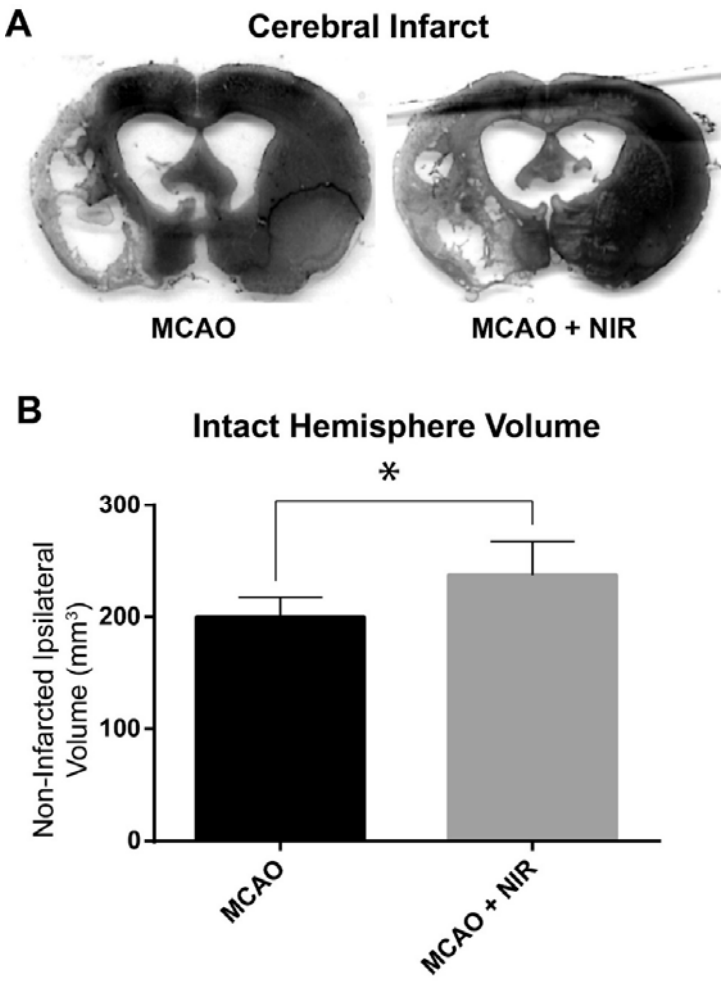

Figure 4. Histological analysis 14 days post-stroke. Volume of non-ischemic ipsilateral hemisphere tissue calculated from H&E stained tissue slices. NIR-treated animals had significantly more non-ischemic tissue in the ipsilateral hemisphere than untreated controls.

Apomorphine-Induced Rotation Test for Functional Recovery

We next looked at whether NIR treated animals showed evidence of functional recovery in addition to having smaller infarct volumes both acutely and chronically (Figure 5). No significant difference was seen between control and treated animals (control: 119, SD 49.74; NIR treated: 83.14, SD 56.05; p=0.28).

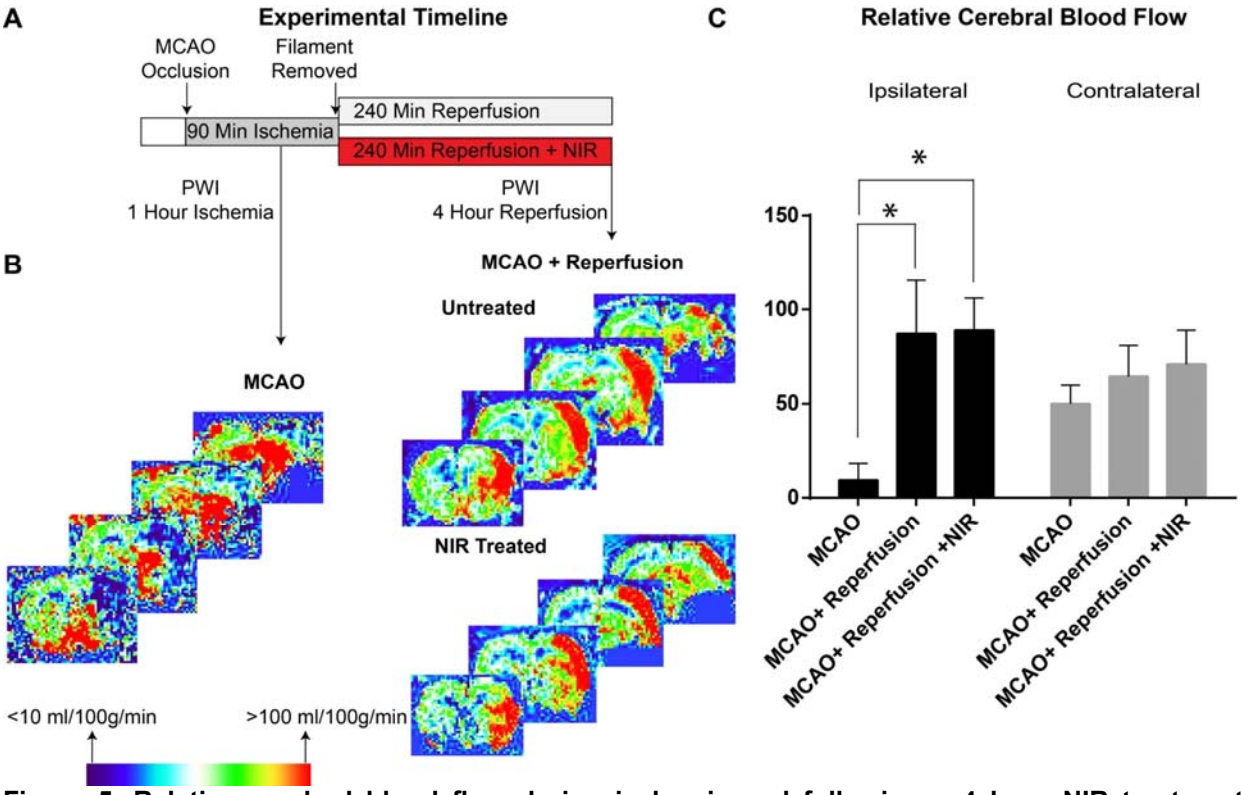

Figure 5. Relative cerebral blood flow during ischemia and following a 4 hour NIR treatment. Averaged regional relative cerebral blood flow in the ipsilateral and contralateral MCA territories during ischemia and following 4 hours of reperfusion. The untreated ischemic hemispheres showed average flow rates of 10.94 mL/100 g/min while the contralateral hemisphere had flow rates of 50.78 mL/100 g/min. Those animals that would receive NIR treatment had ipsilateral MCA territory flow rates 12.125 mL/100g/min during ischemia while the contralateral hemisphere had 53.8 mL/100 g/min. Following reperfusion, ipsilateral hemispheres of untreated animals had an average flow rate of 85.92 mL/100 g/min while the contralateral side had 62.04 mL/100 g/min. The ipsilateral hemispheres of the NIR treated animals had flow rates of 86.03 mL/100 g/min following 4 hours of reperfusion while the contralateral hemisphere had 63.8 mL/100 g/min.

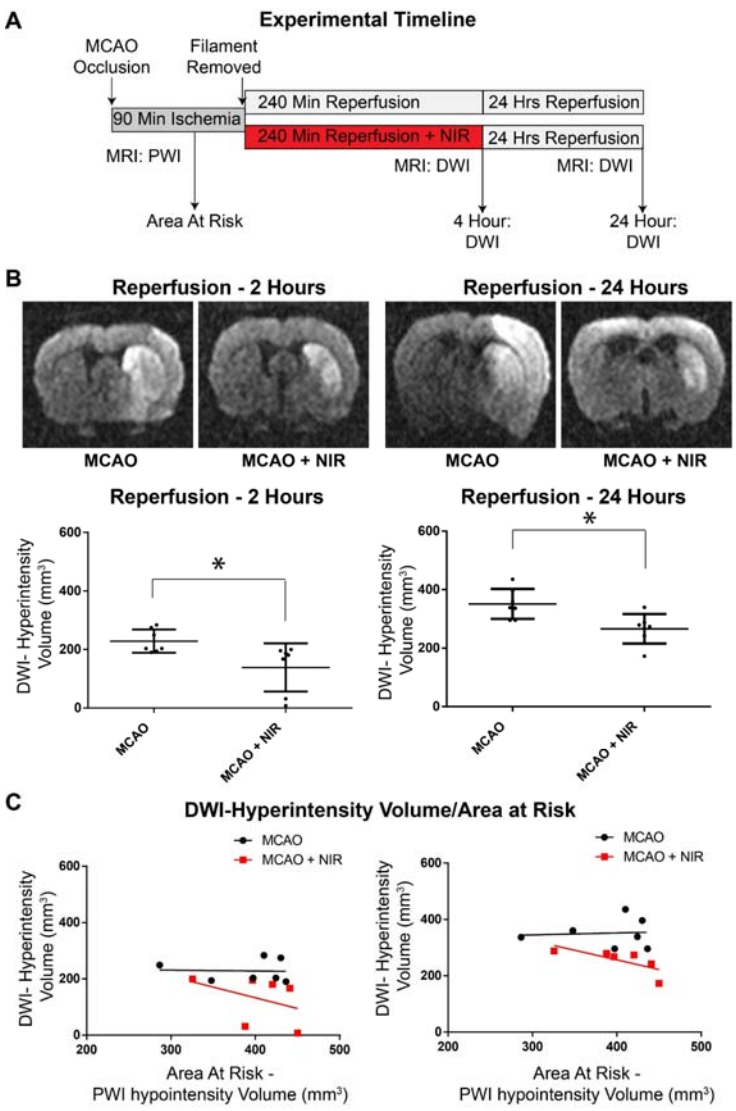

Figure 6. A. Infarct volumes in the acute phase of stroke in MCAO rats treated for 4 hours. Diffusion weighted imaging data was acquired 4 hours following reperfusion. Results are reported as infarct volume in mm^3 and were based on DWI hyperintensities. A significant difference was seen between control animals (228.4 mm^3, SD 39.79) and NIR-treated animals (138.4, SD 82.23), p=0.023. B. DWI-based infarct volumes 24-hours following reperfusion. A significant difference between control animals (351.3 mm^3, SD 51.25) and NIR-treated animals (266.3 mm^3, SD 50.62) was observed in the acute phase of stroke, p=0.0088. Perfusion/Diffusion mismatch. C, at-risk area during ischemia vs area of infarction at 4 hours following reperfusion plotted against area of infarction. The slopes of the two lines are non-significantly different (p=0.41); the intercepts of the lines are significantly different (p=0.031). D. At risk area vs infarction 24 hours following reperfusion. Slopes of the lines are not significantly different (p=0.23); intercepts are significantly different (p=0.0061)

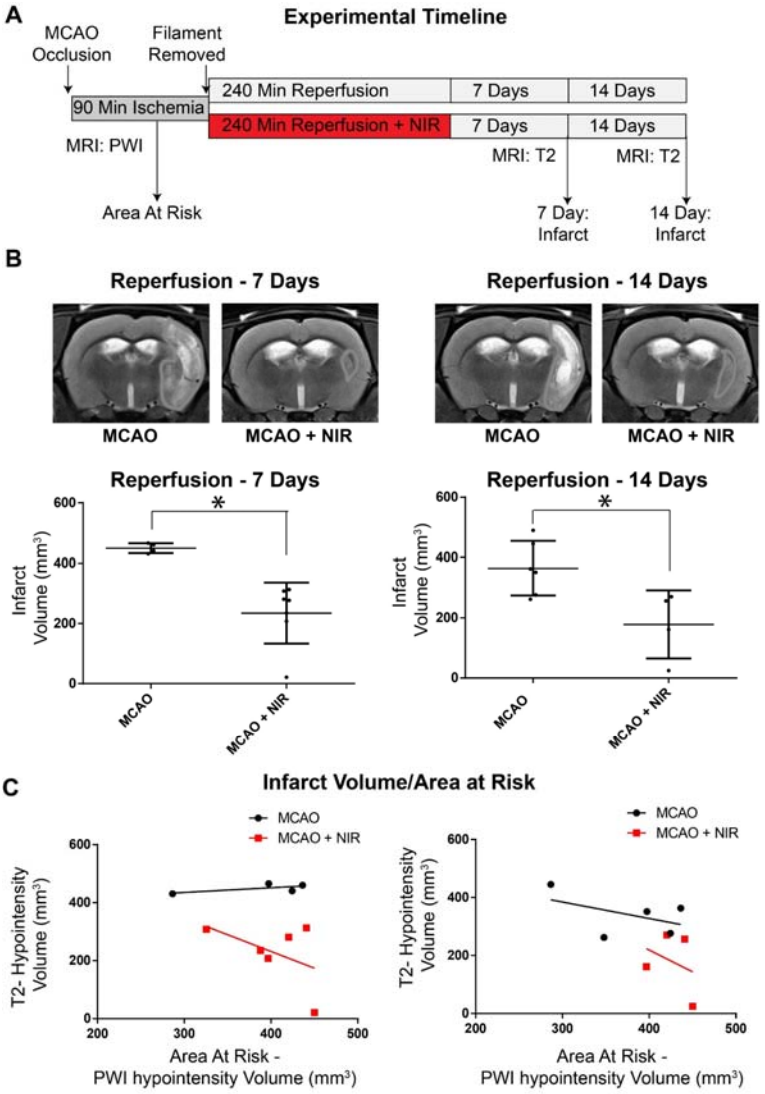

Figure 7. T2 Weighted imaging infarct volumes during the chronic phase of stroke in MCAO rats. A. Seven days following reperfusion, NIR treated animals showed a significant difference in infarct volume when compared with untreated controls (control: 449.3 mm^3, SD 16.4; NIR treated: 234.8 mm^3, SD 111.2). B. Fourteen days following reperfusion, the significant difference seen at 7 days persisted (control: 339.9 mm^3, SD 73.92; NIR treated: 178.4 mm^3, SD 113.3). C. At risk area vs area of infarction 7 days post reperfusion. Slope of the lines is not significantly different (p=0.34); intercepts show significant difference (p=0.018). D. At risk vs infarction 14 days following reperfusion.

Figure 8. Apomorphine induced rotation behavioral test data. NIR treated animals trended towards fewer clockwise rotations when given apomorphine than untreated controls (control: 199, SD 49.74; NIR treated: 84.17, SD 61.33; p= 0.28).

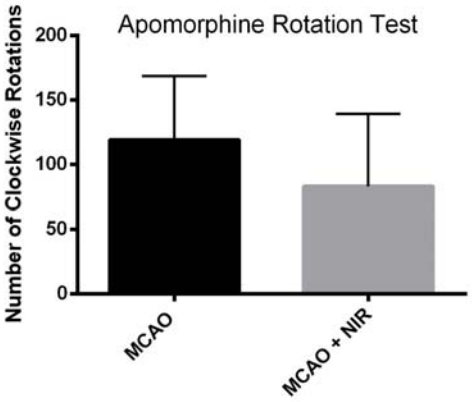

CHAPTER 5 - DISCUSSION: APPLICATIONS AND FUTURE DIRECTIONS

Discussion

Ischemic stroke accounts for about 9% of deaths globally and is the second leading cause of death following heart disease. Those who survive this debilitating disease often face a lifetime of neurological deficits and hence a drastic reduction in quality of life. Unlike other diseases, neurological pathologies such as stroke can affect all aspects of a person's life – cognitive, emotional and functional – and in many ways hinder his or her ability to live fully. Stroke treatment has come a long way in the last several decades though there is still much work to be done. What once was palliative and supportive care has burgeoned into nuanced and individualized paradigms tailored to each patient's disease and prognosis.

The gold standard for stroke treatment is rapid restoration of blood flow in order to reverse neuronal injury and cell death, though this can perpetuate brain injury through the production of ROS during early reperfusion, though this is not the only detrimental effect of reperfusion. Oxidative stress is a common pathological mechanism in many disease states which arises from an imbalance between ROS production and ROS scavenging. Once produced, ROS damage cells either directly, or through diverse and complex cell signaling cascades damage DNA, proteins and lipids.(Zimmerman 1995) In chapter 1 of this work we laid out a theoretical framework in which we argued that ROS production is exponentially related to mitochondrial membrane potential. Membrane potential, in turn, is subject to fluctuations in both substrate availability, and, in higher organisms, post-translational modifications such as changes in the phosphorylation states of ETC enzymes. We argued that enzymatic dephosphorylation during ischemia led to priming for hyperactivation which, upon reperfusion, resulted in large increases in membrane

potential and bursts of ROS. It has thus become a critical objective of both stroke clinicians and stroke researchers to target reperfusion injury at its source and therefore to save neurons. Pharmacologic agents targeting ROS have been shown to be ineffective and thus an adjuvant therapy to tPA or thrombectomy is critically needed to target reperfusion injury.

In this study we sought to show the effectiveness of targeting ROS at their source: directly in the mitochondrial electron transport chain during the early period of blood flow restoration using infrared light therapy. Building on our previous work, we reasoned that this therapy is noninvasive, can be applied immediately at the onset of reperfusion and has shown to have sufficient penetrating depth to target brain tissue during reperfusion. We hypothesized that irradiation of the brain with combination dual wavelength NIR immediately upon reperfusion would reduce infarct size both acutely and chronically in stroke. Since this therapy targets the penumbra rather than the stroke core, we first needed to demonstrate that the MCA territory was sufficiently hypoperfused. Our data indicate that cerebral blood flow which was averaged across three slices of perfusion weighted MRI is significantly reduced below ischemic thresholds in the ipsilateral hemisphere and returns to normal levels following reperfusion. Interestingly, infarct volumes were not different between treated and control animals immediately following treatment when animals were treated for 120 minutes but animals treated for 240 minutes showed significant reductions in infarct volume when compared to untreated controls. Importantly, these significant reductions in infarct volume persisted in both treatment-duration groups when 24 hour DWI scans were taken. This suggests that NIR targets ROS-mediated pathways in the delayed neuronal death cascade that extends beyond the initial 120 minutes of reperfusion. While this suggests that neurons in the penumbra were

being salvaged by NIR therapy, we needed to confirm this by examining whether a significant mismatch existed between perfusion and diffusion weighted imaging. In chapter 3 of this dissertation we outlined a long-standing argument in neuroimaging that any difference between at-risk tissue and infarcted tissue as measured by perfusion and diffusion MRI modalities respectively could be considered a measure of hypoperfused areas that have not yet died and thus could be potentially salvaged. When we plotted at-risk area against area of infarction in both the 120 minute and 240 minute treated groups, we saw non-significant slopes but statistically significant intercepts. A non-significant slope indicates that the rate of change between the two variables in both groups is the same – the lines are parallel. This suggests that the relationship between area at risk and area of infarction is linear, i.e., the area of infarction is proportional to the area at risk and this holds true for both treated and untreated groups. The elevation of the two lines, however, is significantly different indicating to us a mismatch between at-risk and infarction in treated animals. This finding allows us to conclude that in both the 120 minute and 240 minute NIR treated animals, neurons in the penumbra are being salvaged by our approach which results in significantly smaller infarct volumes overall at both 4 hours (in the 240 minute treated group) and 24 hours (in both groups).

We next asked whether the benefit of NIR could be extended into the chronic phase of stroke. Our data show that infarct volumes as measured by T2WI remained significantly smaller at 7 and 14 days post stroke in both 120 and 240 minute NIR treated animals. Moreover, PWI/DWI mismatches had intercepts that remained significantly smaller in both groups when compared to untreated controls. The animals treated for 240 minutes had significant reductions in infarct volumes of about 50% at 7 and 14 days indicating to us that extending treatment duration significantly improves neurological

outcome as measured by clinically translatable imaging modalities. Additional targeting of late-stage ROS production caused by excitotoxicity, inhibition of inflammatory cell conversion through ROS signaling in the immune cell as well as longer than predicted window of mitochondrial stress and other, unknown mechanisms can all potentially explain how the longer treatment duration had such profound reductions in infarct volume during the chronic phase of stroke.

Finally, in the animals treated for 240 minutes we employed an apomorphine-induced rotational test to see whether changes in infarct volume correlated to observable functional improvements in neurological function. Apomorphine is a non-selective dopamine agonist which exerts its action on D_2-like and D_1-like receptors. Unilateral striatal lesions lead to increased rotation in one direction when striatal dopaminergic neurons are agonized. Our data indicate that while on average 4-hour NIR treated animals had fewer rotations than untreated controls, these results were not statistically different. This data is promising and likely due to the large amount of variability seen in behavioral tests and the need for large sample sizes that are not feasible in such a study.(Rewell et al. 2017)

Conclusions

In conclusion, this is the first study of its kind demonstrating in the rat MCAO model that immediate, reversible, non-invasive inhibition of photoreceptive mitochondrial CcO by dual-wavelength NIR in vivo during reperfusion following focal stroke can have profound and sustained reductions in tissue death. Furthermore, these reductions in infarct volume were measured by clinically relevant MRI modalities, which allowed assessment of stroke evolution over time to be monitored in vivo and in real time as is done in the clinic. Thus, based on our previous work demonstrating that NIR treatment

limits mitochondrial ROS production when applied during reperfusion after global brain ischemia, we here demonstrate that such treatment reduces the progression of reperfusion injury following focal brain ischemia and thereby minimized brain damage caused by stroke. Furthermore, this work has shown that NIR can target more than the initial burst of ROS following reperfusion. Extending treatment duration to 240 minutes had profound effects on infarct volume that were sustained during the chronic phase of the stroke. It is likely that this is due to NIR affecting the immune response. As a result, this project has shifted the paradigm on the role that NIR can play at longer stages of the reperfusion injury process. Future studies ought to examine the effect of NIR on immune responses, and other potential long-duration targets of NIR in other brain ischemia/reperfusion pathologies

APPENDIX

IACUC Protocol Approval Letter

WAYNE STATE UNIVERSITY

Institutional Animal Care
And Use Committee
87 East Canfield, Second Floor
Detroit, Michigan 48201
Phone: (313) 577-1629

ANIMAL WELFARE ASSURANCE # A3310-01

TO: Thomas Sanderson
Emergency Medicine

FROM: Institutional Animal Care and Use Committee

DATE: September 30, 2015

SUBJECT: Approval of Protocol 15-08-002

TITLE: Therapeutic modulation of mitochondrial function to minimize brain injury from stroke

Protocol Effective Period: September 30, 2015 - September 22, 2018

Your animal research protocol has been approved by the Wayne State University Institutional Animal Care and Use Committee (IACUC).

Be advised that this protocol must be reviewed by the IACUC on an annual basis to remain active. Any changes (e.g. procedures, lab personnel, strains, additional numbers of animals) must be submitted as amendments and require prior approval by the IACUC. Any animal work on this research protocol beyond the expiration date will require the submission of a new IACUC protocol application for committee review and approval.

The *Guide for the Care and Use of Laboratory Animals* (the Guide, NRC 2011) is the primary reference used for standards of animal care at Wayne State University. The University has submitted an appropriate assurance statement to the Office for Laboratory Animal Welfare (OLAW) of the National Institutes of Health. The animal care program at Wayne State University is accredited by the Association for Assessment and Accreditation of Laboratory Animal Care International (AAALAC).

REFERENCES

1. Acin-Perez, R. et al. 2003. 'An intragenic suppressor in the cytochrome c oxidase I gene of mouse mitochondrial DNA.', *Human molecular genetics*, 12: 329-39.
2. Adam-Vizi, V., and C. Chinopoulos. 2006. 'Bioenergetics and the formation of mitochondrial reactive oxygen species', *Trends Pharmacol Sci*, 27: 639-45.
3. Al-Macki, N., et al. 2009. 'The spectrum of abnormal neurologic outcomes subsequent to term intrapartum asphyxia', *Pediatr Neurol*, 41: 399-405.
4. Allisy-Roberts, Penelope, and Jerry Williams. 2008. 'Chapter 10 - Magnetic resonance imaging.' in Penelope Allisy-Roberts and Jerry Williams (eds.), *Farr's Physics for Medical Imaging (Second Edition)* (W.B. Saunders).
5. Alsop, D. C., and J. A. Detre. 1995. 'Reduced transit-time sensitivity in noninvasive magnetic resonance imaging of human cerebral blood flow', *J Cereb Blood Flow Metab* , 16: 1236-49.
6. Alsop DC and Detre JA. 1998. 'Multisection cerebral blood flow MR imaging with continuous arterial spin labeling', *Radiology*, 208: 410-6.
7. Arnold, S., and B. Kadenbach. 1999. 'The intramitochondrial ATP/ADP-ratio controls cytochrome c oxidase activity allosterically', *FEBS Letters*, 443: 105-8.
8. Astrup J Fau - Symon, L., N. M. Symon L Fau - Branston, N. A. Branston Nm Fau - Lassen, and N. A. Lassen. 1977. 'Cortical evoked potential and extracellular K+ and H+ at critical levels of brain ischemia', *Stroke*, 8: 51-7.
9. Astrup, J., B. K. Siesjö, and L. Symon. 1981. 'Thresholds in cerebral ischemia - the ischemic penumbra', *Stroke*, 12: 723.
10. Attwell, D., and S. B. Laughlin. 2001. 'An energy budget for signaling in the grey matter of the brain', *J Cereb Blood Flow Metab*, 21: 1133-45.

11. Back, T., M. Hoehn-Berlage, K. Kohno, and K. A. Hossmann. 1994. 'Diffusion nuclear magnetic resonance imaging in experimental stroke. Correlation with cerebral metabolites', *Stroke*, 25: 494.

12. Badaut, Jérôme, Lorenz Hirt, Cristina Granziera, Julien Bogousslavsky, Pierre J. Magistretti, and Luca Regli. 2001. 'Astrocyte-Specific Expression of Aquaporin-9 in Mouse Brain is Increased after Transient Focal Cerebral Ischemia', *Journal of Cerebral Blood Flow & Metabolism*, 21: 477-82.

13. Badaut, Jérôme, François Lasbennes, Pierre J. Magistretti, and Luca Regli. 2002. 'Aquaporins in Brain: Distribution, Physiology, and Pathophysiology', *Journal of Cerebral Blood Flow & Metabolism*, 22: 367-78.

14. Bae, C.S., et al. 2004. 'Effect of Ga-as laser on the regeneration of injured sciatic nerves in the rat', *In Vivo*, 18: 489-95.

15. Baird, A. E., and S. Warach. 1988. 'Magnetic resonance imaging of acute stroke', *J Cereb Blood Flow Metab*, 18: 583-609.

16. Barber, P. A., D. G. Darby, P. M. Desmond, Q. Yang, R. P. Gerraty, D. Jolley, G. A. Donnan, B. M. Tress, and S. M. Davis. 1998. 'Prediction of stroke outcome with echoplanar perfusion- and diffusion-weighted MRI', *Neurology*, 51: 418.

17. Barbier, E. L., M. Lamalle L Fau - Decorps, and M. Decorps. 2001. 'Methodology of brain perfusion imaging', *J Magn Reson Imaging*, 13: 496-520.

18. Barja, G. 1999. 'Mitochondrial oxygen radical generation and leak: sites of production in states 4 and 3, organ specificity, and relation to aging and longevity', *J Bioenerg Biomembr*, 31: 347-66.

19. Barja, G., and A. Herrero. 1998. 'Localization at complex I and mechanism of the higher free radical production of brain nonsynaptic mitochondria in the short-lived

rat than in the longevous pigeon', *J Bioenerg Biomembr*, 30: 235-43.

20. Barron, J. T., J. E. Gu L Fau - Parrillo, and J. E. Parrillo. 1998. 'Malate-aspartate shuttle, cytoplasmic NADH redox potential, and energetics in vascular smooth muscle', *J Mol Cell Cardiol*, 30: 1571-9.
21. Barros, L. F., Carla X. Castro J Fau - Bittner, and C. X. Bittner. 2002. 'Ion movements in cell death: from protection to execution', *Biol Res*, 35: 209-14.
22. Barros, L. F., J. Hermosilla T Fau - Castro, and J. Castro. 2001. 'Necrotic volume increase and the early physiology of necrosis', *Comp Biochem Physiol A Mol Integr Physiol*, 130: 401-9.
23. Beaulieu, C. 2002. 'The basis of anisotropic water diffusion in the nervous system - a technical review', *NMR Biomed*, 15: 435-55.
24. Benjamin, E. J., M. J. Blaha, S. E. Chiuve, M. Cushman, S. R. Das, R. Deo, S. D. de Ferranti, J. Floyd, M. Fornage, C. Gillespie, C. R. Isasi, M. C. Jimenez, L. C. Jordan, S. E. Judd, D. Lackland, J. H. Lichtman, L. Lisabeth, S. Liu, C. T. Longenecker, R. H. Mackey, K. Matsushita, D. Mozaffarian, M. E. Mussolino, K. Nasir, R. W. Neumar, L. Palaniappan, D. K. Pandey, R. R. Thiagarajan, M. J. Reeves, M. Ritchey, C. J. Rodriguez, G. A. Roth, W. D. Rosamond, C. Sasson, A. Towfighi, C. W. Tsao, M. B. Turner, S. S. Virani, J. H. Voeks, J. Z. Willey, J. T. Wilkins, J. H. Wu, H. M. Alger, S. S. Wong, P. Muntner, Committee American Heart Association Statistics, and Subcommittee Stroke Statistics. 2017. 'Heart Disease and Stroke Statistics-2017 Update: A Report From the American Heart Association', *Circulation*, 135: e146-e603.
25. Benson Dw Fau - Williams, G. R., Jr., F. C. Williams Gr Jr Fau - Spencer, A. J. Spencer Fc Fau - Yates, and A. J. Yates. 1959. 'The use of hypothermia after

cardiac arrest', *Anesth Analg*, 38: 423-8.

26. Bernard, S. A., Michael D. Gray Tw Fau - Buist, Bruce M. Buist Md Fau - Jones, William Jones Bm Fau - Silvester, Geoff Silvester W Fau - Gutteridge, Karen Gutteridge G Fau - Smith, and K. Smith. 2002. 'Treatment of comatose survivors of out-of-hospital cardiac arrest with induced hypothermia', *N Engl J Med*, 346: 557-63.

27. Bivard, A., Christopher R. Spratt N Fau - Levi, Mark W. Levi Cr Fau - Parsons, and M. W. Parsons. 2011. 'Acute stroke thrombolysis: time to dispense with the clock and move to tissue-based decision making?', *Expert Rev Cardiovasc Ther*, 9: 451-61.

28. Bourdillon Pd Fau - Poole-Wilson, P. A., and P. A. Poole-Wilson. 1981. 'Effects of ischaemia and reperfusion on calcium exchange and mechanical function in isolated rabbit myocardium', *Cardiovasc Res*, 15: 121-30.

29. Brennan, J. P., Rodolfo A. Southworth R Fau - Medina, Sean M. Medina Ra Fau - Davidson, Michael R. Davidson Sm Fau - Duchen, Michael J. Duchen Mr Fau - Shattock, and M. J. Shattock. 2006. 'Mitochondrial uncoupling, with low concentration FCCP, induces ROS-dependent cardioprotection independent of KATP channel activation', *Cardiovasc Res*, 72: 313-21.

30. Burdette, J. H., A. D. Durden Dd Fau - Elster, Y. F. Elster Ad Fau - Yen, and Y. F. Yen. 2001. 'High b-value diffusion-weighted MRI of normal brain', *J Comput Assist Tomogr*, 25: 515-9.

31. Buxton, R. B., E. C. Frank Lr Fau - Wong, B. Wong Ec Fau - Siewert, S. Siewert B Fau - Warach, R. R. Warach S Fau - Edelman, and R. R. Edelman. 1998. 'A general kinetic model for quantitative perfusion imaging with arterial spin labeling',

Magn Reson Med, 40: 383-96.

32. Cadenas E Fau - Boveris, A., C. I. Boveris A Fau - Ragan, A. O. Ragan Ci Fau - Stoppani, and A. O. Stoppani. 1977. 'Production of superoxide radicals and hydrogen peroxide by NADH-ubiquinone reductase and ubiquinol-cytochrome c reductase from beef-heart mitochondria', *Archives of Biochemistry and Biophysics*, 180: 248-57.

33. Canevari, L., E. A. Console A Fau - Tendi, J. B. Tendi Ea Fau - Clark, T. E. Clark Jb Fau - Bates, and T. E. Bates. 1999. 'Effect of postischaemic hypothermia on the mitochondrial damage induced by ischaemia and reperfusion in the gerbil', *Brain Res*, 817: 241-5.

34. Cao, G., Xiao Xing J Fau - Xiao, Anthony K. F. Xiao X Fau - Liou, Yanqin Liou Ak Fau - Gao, Xiao-Ming Gao Y Fau - Yin, Robert S. B. Yin Xm Fau - Clark, Steven H. Clark Rs Fau - Graham, Jun Graham Sh Fau - Chen, and J. Chen. 2007. 'Critical role of calpain I in mitochondrial release of apoptosis-inducing factor in ischemic neuronal injury', *J Neurosci*, 27: 9278-93.

35. Carden, D. L., and D. N. Granger. 2000. 'Pathophysiology of ischaemia-reperfusion injury', *J Pathol*, 190: 255-66.

36. Chance B Fau - Williams, G. R., and G. R. Williams. 1955. 'Respiratory enzymes in oxidative phosphorylation. I. Kinetics of oxygen utilization', *J Biol Chem*, 217: 383-93.

37. Chance, B. and Hollunger, G. 1961. 'The interaction of energy and electron transfer reactions in mitochondria. I. General properties and nature of the products of succinate-linked reduction of pyridine nucleotide', *J. Biol. Chem.*, 236: 1534-43.

38. Cheng, E. H., S. Wei Mc Fau - Weiler, R. A. Weiler S Fau - Flavell, T. W. Flavell

Ra Fau - Mak, T. Mak Tw Fau - Lindsten, S. J. Lindsten T Fau - Korsmeyer, and S. J. Korsmeyer. 2001. 'BCL-2, BCL-X(L) sequester BH3 domain-only molecules preventing BAX- and BAK-mediated mitochondrial apoptosis', *Mol Cell*, 8: 705-11.

39. Chobot, S.E., Zhang, H., Moser, C.C, & Dutton, P.L. 2008. 'Breaking the Q cycle: finding new ways to study Qo through thermodynamic manipulations', *Journal of bioenergetics and biomembranes*, 40.

40. Choi, K., Gyung W. Kim J Fau - Kim, Chulhee Kim Gw Fau - Choi, and C. Choi. 2009. 'Oxidative stress-induced necrotic cell death via mitochondira-dependent burst of reactive oxygen species', *Curr Neurovasc Res*, 6: 213-22.

41. Chouchani, E. T., V. R. Pell, E. Gaude, D. Aksentijevic, S. Y. Sundier, E. L. Robb, A. Logan, S. M. Nadtochiy, E. N. J. Ord, A. C. Smith, F. Eyassu, R. Shirley, C. H. Hu, A. J. Dare, A. M. James, S. Rogatti, R. C. Hartley, S. Eaton, A. S. H. Costa, P. S. Brookes, S. M. Davidson, M. R. Duchen, K. Saeb-Parsy, M. J. Shattock, A. J. Robinson, L. M. Work, C. Frezza, T. Krieg, and M. P. Murphy. 2014. 'Ischaemic accumulation of succinate controls reperfusion injury through mitochondrial ROS', *Nature*, 515: 431-35.

42. Chung J-W Fau - Chung, Jong-Won, Su Hyun Park Sh Fau - Park, Nayoung Kim N Fau - Kim, Wook-Joo Kim W-J Fau - Kim, Jung Hyun Park Jh Fau - Park, Youngchai Ko Y Fau - Ko, Mi Hwa Yang Mh Fau - Yang, Myung Suk Jang Ms Fau - Jang, Moon-Ku Han M-K Fau - Han, Cheolkyu Jung C Fau - Jung, Jae Hyoung Kim Jh Fau - Kim, Chang Wan Oh Cw Fau - Oh, and Hee-Joon Bae H-J Fau - Bae. 2014. 'Trial of ORG 10172 in Acute Stroke Treatment (TOAST) Classification and Vascular Territory of Ischemic Stroke Lesions Diagnosed by Diffusion-Weighted

Imaging', *J Am Heart Assoc*, 3.

43. Coifman, R. R., S. Lafon, A. B. Lee, M. Maggioni, B. Nadler, F. Warner, and S. W. Zucker. 2005. 'Geometric diffusions as a tool for harmonic analysis and structure definition of data: Diffusion maps', *Proceedings of the National Academy of Sciences of the United States of America*, 102: 7426.

44. Coifman, Ronald R., and Stéphane Lafon. 2006. 'Diffusion maps', *Applied and Computational Harmonic Analysis*, 21: 5-30.

45. Colbourne, F., A. M. Li H Fau - Buchan, J. A. Buchan Am Fau - Clemens, and J. A. Clemens. 1999. 'Continuing postischemic neuronal death in CA1: influence of ischemia duration and cytoprotective doses of NBQX and SNX-111 in rats', *Stroke*, 30: 662-8.

46. Colbourne, F., R. N. Sutherland Gr Fau - Auer, and R. N. Auer. 1999. 'Electron microscopic evidence against apoptosis as the mechanism of neuronal death in global ischemia', *J Neurosci*, 19: 4200-10.

47. Crofts, A.R. 2004. 'The cytochrome bc1 complex: function in context of structure', *Annual Reviews of Physiology*, 66: 689-733.

48. Crofts, A.R., Berry, E.A. 1998. 'Structure and function of the cytochrome bc1 complex of mitochondria and photosynthetic bacteria', *Current Opinion in Structural Biology*, 8: 501-09.

49. Dalmonte, M. E. et al. 2009. 'Control of respiration by cytochrome c oxidase in intact cells: role of the membrane potential. ', *The Journal of biological chemistry*, 284: 32331-35.

50. Darby, D. G., R. P. Barber Pa Fau - Gerraty, P. M. Gerraty Rp Fau - Desmond, Q. Desmond Pm Fau - Yang, M. Yang Q Fau - Parsons, T. Parsons M Fau - Li, B. M.

Li T Fau - Tress, S. M. Tress Bm Fau - Davis, and S. M. Davis. 1999. 'Pathophysiological topography of acute ischemia by combined diffusion-weighted and perfusion MRI', *Stroke*, 30: 2043-52.

51. De Georgia, M. A., A. Krieger Dw Fau - Abou-Chebl, T. G. Abou-Chebl A Fau - Devlin, M. Devlin Tg Fau - Jauss, S. M. Jauss M Fau - Davis, W. J. Davis Sm Fau - Koroshetz, G. Koroshetz Wj Fau - Rordorf, S. Rordorf G Fau - Warach, and S. Warach. 2004. 'Cooling for Acute Ischemic Brain Damage (COOL AID): a feasibility trial of endovascular cooling', *Neurology*, 63: 312-7.
52. DeGracia, Donald J., Doaa Taha, Fika Tri Anggraini, and Zhifeng Huang. 2017. 'Neuroprotection Is Technology, Not Science.' in Paul A. Lapchak and John H. Zhang (eds.), *Neuroprotective Therapy for Stroke and Ischemic Disease* (Springer International Publishing: Cham).
53. DeLellis, S.L., D.H. Carnegie, and T.J. Burke. 2005. 'Improved sensitivity in patients with peripheral neuropathy: effects of monochromatic infrared photo energy', *J Am Podiatr Med Assoc*, 95: 143-7.
54. Deshpande, J., T. Bergstedt K Fau - Linden, H. Linden T Fau - Kalimo, T. Kalimo H Fau - Wieloch, and T. Wieloch. 1992. 'Ultrastructural changes in the hippocampal CA1 region following transient cerebral ischemia: evidence against programmed cell death', *Exp Brain Res*, 88: 91-105.
55. Detaboada, L. et al. 2006. 'Transcranial application of low-energy laser irradiation improves neurological deficits in rats following acute stroke', *Lasers Surg Med*, 38: 70-3.
56. Detre, J. A., D. S. Leigh Js Fau - Williams, A. P. Williams Ds Fau - Koretsky, and A. P. Koretsky. 1992. 'Perfusion imaging', *Magn Reson Med*, 23: 37-45.

57. Detre, J. A., D. A. Zhang W Fau - Roberts, A. C. Roberts Da Fau - Silva, D. S. Silva Ac Fau - Williams, D. J. Williams Ds Fau - Grandis, A. P. Grandis Dj Fau - Koretsky, J. S. Koretsky Ap Fau - Leigh, and J. S. Leigh. 1994. 'Tissue specific perfusion imaging using arterial spin labeling', *NMR Biomed*, 7: 75-82.

58. Dirnagl U, MA Iadecola C Fau-Moskowitz, and MA Moskowitz. 1999. 'Pathobiology of ischaemic stroke: an integrated view', *Trends Neurosci*, 22: 391-7.

59. Easlon, E., Craig Tsang F Fau - Skinner, Chen Skinner C Fau - Wang, Su-Ju Wang C Fau - Lin, and S. J. Lin. 2008. 'The malate-aspartate NADH shuttle components are novel metabolic longevity regulators required for calorie restriction-mediated life span extension in yeast', *Genes Dev*, 22: 931-44.

60. Edelman, R. R., D. G. Siewert B Fau - Darby, V. Darby Dg Fau - Thangaraj, A. C. Thangaraj V Fau - Nobre, M. M. Nobre Ac Fau - Mesulam, S. Mesulam Mm Fau - Warach, and S. Warach. 1994. 'Qualitative mapping of cerebral blood flow and functional localization with echo-planar MR imaging and signal targeting with alternating radio frequency', *Radiology*, 192: 513-20.

61. Eells, J.T. et al. 2003. 'Therapeutic photobiomodulation for methanol-induced retinal toxicity', *Proceedings of the National Academy of Sciences*, 100: 3439-44.

62. Eells JT1, Wong-Riley MT, VerHoeve J, Henry M, Buchman EV, Kane MP, Gould LJ, Das R, Jett M, Hodgson BD, Margolis D, Whelan HT.. 2004. 'Mitochondrial signal transduction in accelerated would and retinal healing by near-infrared light therapy', *Mitochondrion*, 4: 559-67.

63. Einstein, A. 1905. 'INVESTIGATIONS ON THE THEORY OF THE BROWNIAN MOVEMENT', *Ann. der Physik*.

64. Erecinska, M., Ian A. Thoresen M Fau - Silver, and I. A. Silver. 2003. 'Effects of

hypothermia on energy metabolism in Mammalian central nervous system', *J Cereb Blood Flow Metab*, 23: 513-30.

65. Fabian, R. H., T. A. DeWitt Ds Fau - Kent, and T. A. Kent. 1995. 'In vivo detection of superoxide anion production by the brain using a cytochrome c electrode', *J Cereb Blood Flow Metab*, 15: 242-7.

66. Fang, Ji-Kang, Subbuswamy K. Prabu, Naresh B. Sepuri, Haider Raza, Hindupur K. Anandatheerthavarada, Domenico Galati, Joseph Spear, and Narayan G. Avadhani. 2007. 'Site Specific Phosphorylation of Cytochrome c Oxidase Subunits I, IVi1 and Vb in Rabbit Hearts Subjected to Ischemia/Reperfusion', *FEBS Letters*, 581: 1302-10.

67. Feigin, V. L., B. Norrving, and G. A. Mensah. 2017. 'Global Burden of Stroke', *Circ Res*, 120: 439-48.

68. Ferré, J. C., E. Bannier, H. Raoult, G. Mineur, B. Carsin-Nicol, and J. Y. Gauvrit. 2013. 'Arterial spin labeling (ASL) perfusion: Techniques and clinical use', *Diagnostic and Interventional Imaging*, 94: 1211-23.

69. Fiskum, G. 2000. 'Mitochondrial participation in ischemic and traumatic neural cell death', *J Neurotrauma*, 17: 843-55.

70. Fiskum, G., M. F. Murphy An Fau - Beal, and M. F. Beal. 1999. 'Mitochondria in neurodegeneration: acute ischemia and chronic neurodegenerative diseases', *J Cereb Blood Flow Metab*, 19: 351-69.

71. Friberg, H., A. P. Connern C Fau - Halestrap, T. Halestrap Ap Fau - Wieloch, and T. Wieloch. 1999. 'Differences in the activation of the mitochondrial permeability transition among brain regions in the rat correlate with selective vulnerability', *J Neurochem*, 72: 2488-97.

72. Fujimura, M., K. Morita-Fujimura Y Fau - Murakami, M. Murakami K Fau - Kawase, P. H. Kawase M Fau - Chan, and P. H. Chan. 1998. 'Cytosolic redistribution of cytochrome c after transient focal cerebral ischemia in rats', *J Cereb Blood Flow Metab*, 18: 1239-47.

73. Gladstone, D. J., Antoine M. Black Se Fau - Hakim, and A. M. Hakim. 2002. 'Toward wisdom from failure: lessons from neuroprotective stroke trials and new therapeutic directions', *Stroke*, 33: 2123-36.

74. Golay, X., Tchoyoson C. C. Hendrikse J Fau - Lim, and T. C. Lim. 2004. 'Perfusion imaging using arterial spin labeling', *Top Magn Reson Imaging*, 15: 10-27.

75. Gong, P., Rong Li Cs Fau - Hua, Hong Hua R Fau - Zhao, Zi-Ren Zhao H Fau - Tang, Xue Tang Zr Fau - Mei, Ming-Yue Mei X Fau - Zhang, Juan Zhang My Fau - Cui, and J. Cui. 2012. 'Mild hypothermia attenuates mitochondrial oxidative stress by protecting respiratory enzymes and upregulating MnSOD in a pig model of cardiac arrest', *PLoS One*, 7.

76. Granger, D. N., and P. R. Kvietys. 2015. 'Reperfusion injury and reactive oxygen species: The evolution of a concept', *Redox Biol*, 6: 524-51.

77. Green, D. R., and J. C. Reed. 1998. 'Mitochondria and apoptosis', *Science*, 28: 1309-12.

78. Griffiths DE, Wharton DC. 1961. 'Studies of the electron transport system. XXXV. Purification and properties of cytochrome oxidase', *J Biol Chem*, 236: 1850-56.

79. Guo, D., Mourad Nguyen T Fau - Ogbi, Huda Ogbi M Fau - Tawfik, Guochun Tawfik H Fau - Ma, Qilin Ma G Fau - Yu, Robert W. Yu Q Fau - Caldwell, John A. Caldwell Rw Fau - Johnson, and J. A. Johnson. 2007. 'Protein kinase C-epsilon coimmunoprecipitates with cytochrome oxidase subunit IV and is associated with

improved cytochrome-c oxidase activity and cardioprotection', *Am J Physiol Heart Circ Physiol*, 293.

80. Hacke, W. 2015. 'Interventional thrombectomy for major stroke--a step in the right direction', *N Engl J Med*, 372: 76-7.

81. Hazeki O, Tamura M. 1988. 'Quantitative analysis of hemoglobin oxygenation state of rat brain in situ by near-infrared spectrophotometry', *J Appl Physiol*, 64: 796-802.

82. Hetz, C., Agnes Vitte Pa Fau - Bombrun, Tatiana K. Bombrun A Fau - Rostovtseva, Sylvie Rostovtseva Tk Fau - Montessuit, Agnes Montessuit S Fau - Hiver, Matthias K. Hiver A Fau - Schwarz, Dennis J. Schwarz Mk Fau - Church, Stanley J. Church Dj Fau - Korsmeyer, Jean-Claude Korsmeyer Sj Fau - Martinou, Bruno Martinou Jc Fau - Antonsson, and B. Antonsson. 2005. 'Bax channel inhibitors prevent mitochondrion-mediated apoptosis and protect neurons in a model of global brain ischemia', *J Biol Chem*, 280: 42960-70.

83. Hirsch, T., I. Susin Sa Fau - Marzo, P. Marzo I Fau - Marchetti, N. Marchetti P Fau - Zamzami, G. Zamzami N Fau - Kroemer, and G. Kroemer. 2005. 'Mitochondrial permeability transition in apoptosis and necrosis', *Cell Death And Differentiation*, 12: 1478-80.

84. Hirst, J., Ian M. Carroll J Fau - Fearnley, Richard J. Fearnley Im Fau - Shannon, John E. Shannon Rj Fau - Walker, and J. E. Walker. 2003. 'The nuclear encoded subunits of complex I from bovine heart mitochondria', *Biochem Biophys Acta*, 1604: 135-50.

85. Hirst, J., Kenneth R. King Ms Fau - Pryde, and K. R. Pryde. 2008. 'The production of reactive oxygen species by complex I', *Biochem Soc Trans*, 36: 976-80.

86. Hochachka Pw Fau - Storey, K. B., and K. B. Storey. 1975. 'Metabolic consequences of diving in animals and man', *Science*, 187: 613-21.

87. Hossmann, K. A. 2009. 'Pathophysiological basis of translational stroke research', *Folia Neuropathol*, 47: 213-27.

88. Hossmann Ka Fau - Sakaki, S., V. Sakaki S Fau - Zimmerman, and V. Zimmerman. 1977. 'Cation activities in reversible ischemia of the cat brain', *Stroke*, 8: 77-81.

89. Huh, P. W., W. Belayev L Fau - Zhao, S. Zhao W Fau - Koch, R. Koch S Fau - Busto, M. D. Busto R Fau - Ginsberg, and M. D. Ginsberg. 2009. 'Comparative neuroprotective efficacy of prolonged moderate intraischemic and postischemic hypothermia in focal cerebral ischemia', *J Neurosurg*, 92: 91-9.

90. Huttemann, Maik, Icksoo Lee, Alena Pecinova, Petr Pecina, Karin Przyklenk, and Jeffrey W. Doan. 2008. 'Regulation of oxidative phosphorylation, the mitochondrial membrane potential, and their role in human disease', *Journal of bioenergetics and biomembranes*, 40: 445-56.

91. Iijima, T., Kimio Mishima T Fau - Akagawa, Yasuhide Akagawa K Fau - Iwao, and Y. Iwao. 2006. 'Neuroprotective effect of propofol on necrosis and apoptosis following oxygen-glucose deprivation--relationship between mitochondrial membrane potential and mode of death', *Brain Res*, 1099: 25-32.

92. Ishimaru, M. J., T. I. Ikonomidou C Fau - Tenkova, T. C. Tenkova Ti Fau - Der, K. Der Tc Fau - Dikranian, M. A. Dikranian K Fau - Sesma, J. W. Sesma Ma Fau - Olney, and J. W. Olney. 1999. 'Distinguishing excitotoxic from apoptotic neurodegeneration in the developing rat brain', *J Comp Neurol*, 408: 461-76.

93. Jansen O Fau - Schellinger, P., J. Schellinger P Fau - Fiebach, W. Fiebach J Fau - Hacke, K. Hacke W Fau - Sartor, and K. Sartor. 1999. 'Early recanalisation in

acute ischaemic stroke saves tissue at risk defined by MRI', *Lancet (London, England)*, 353: 2036-7.

94. Kadenbach, B., Li Ramzan R Fau - Wen, Sebastian Wen L Fau - Vogt, and S. Vogt. 2010. 'New extension of the Mitchell Theory for oxidative phosphorylation in mitochondria of living organisms', *Biochem Biophys Acta*, 1800: 205-12.

95. Karu, T. 1999. 'Primary and secondary mechanisms of action of visible to near-IR radiation on cells', *Journal of photochemistry and photobiology. B, Biology*, 49: 1-17.

96. Karu, T. I., and N. I. Afanas'eva. 1995. '[Cytochrome c oxidase as the primary photoacceptor upon laser exposure of cultured cells to visible and near IR-range light]', *Doklady Akademii nauk*, 342: 693-95.

97. Kim, S. G. 1995. 'Quantification of relative cerebral blood flow change by flow-sensitive alternating inversion recovery (FAIR) technique: application to functional mapping', *Magn Reson Med*, 34: 293-301.

98. Kimelberg, H. K. 2004. 'Water homeostasis in the brain: basic concepts', *Neuroscience*, 129: 851-60.

99. Kingsley, P. B., and W. G. Monahan. 2004. 'Selection of the optimum b factor for diffusion-weighted magnetic resonance imaging assessment of ischemic stroke', *Magn Reson Med*, 51: 996-1001.

100. Knauth, M., O. von Kummer R Fau - Jansen, S. Jansen O Fau - Hahnel, A. Hahnel S Fau - Dorfler, K. Dorfler A Fau - Sartor, and K. Sartor. 1997. 'Potential of CT angiography in acute ischemic stroke', *AJNR Am J Neuroradiol*, 18: 1001-10.

101. Koroshetz Wj Fau - Gonzalez, G., and G. Gonzalez. 1997. 'Diffusion-weighted MRI: an ECG for "brain attack"?', *Ann Neurol*, 41: 565-6.

102. Korshunov, S. S., A. A. Skulachev Vp Fau - Starkov, and A. A. Starkov. 1997. 'High protonic potential actuates a mechanism of production of reactive oxygen species in mitochondria', *FEBS Letters*, 416: 15-18.

103. Krebs, H. A., A. Ruffo, Monica Johnson, L. V. Eggleston, and R. Hems. 1953. 'Oxidative phosphorylation', *Biochemical Journal*, 54: 107-16.

104. Kuboyama, K., A. Safar P Fau - Radovsky, S. A. Radovsky A Fau - Tisherman, S. W. Tisherman Sa Fau - Stezoski, H. Stezoski Sw Fau - Alexander, and H. Alexander. 1993. 'Delay in cooling negates the beneficial effect of mild resuscitative cerebral hypothermia after cardiac arrest in dogs: a prospective, randomized study', *Crit Care Med*, 21: 1348-58.

105. Kudin, A. P., Stefan Bimpong-Buta Ny Fau - Vielhaber, Christian E. Vielhaber S Fau - Elger, Wolfram S. Elger Ce Fau - Kunz, and W. S. Kunz. 2004. 'Characterization of superoxide-producing sites in isolated brain mitochondria', *J Biol Chem*, 279: 4127-35.

106. Kudin, A. P., Wolfram S. Malinska D Fau - Kunz, and W. S. Kunz. 2008. 'Sites of generation of reactive oxygen species in homogenates of brain tissue determined with the use of respiratory substrates and inhibitors', *Biochem Biophys Acta*, 1777: 689-95.

107. Kunimatsu, T., Anzu Kobayashi K Fau - Yamashita, Toshiharu Yamashita A Fau - Yamamoto, Masaichi-Chang-il Yamamoto T Fau - Lee, and M. C. Lee. 2011. 'Cerebral reactive oxygen species assessed by electron spin resonance spectroscopy in the initial stage of ischemia-reperfusion are not associated with hypothermic neuroprotection', *J Clin Neurosci*, 18: 545-8.

108. Kunz, W. S. et al. 2000. 'Flux control of cytochrome c oxidase in human skeletal

muscle', *J Biol Chem*, 275: 27741-45.

109. Kussmaul, L., and J. Hirst. 2006. 'The mechanism of superoxide production by NADH:ubiquinone oxidoreductase (complex I) from bovine heart mitochondria', *Proceedings of the National Academy of Sciences*, 103: 7607-12.

110. Kuwana, T., and D. D. Newmeyer. 2003. 'Bcl-2-family proteins and the role of mitochondria in apoptosis', *Curr Opin Cell Biol*, 15: 691-9.

111. Lambert, A. J. and Brand, M. D. 2004. 'Superoxide production by NADH:ubiquinone oxidoreductase (complex I) depends on the pH gradient across the mitochondrial inner membrane.', *Biochem. J.*, 382: 511-17.

112. Lapchak, P. A., Linda J. Zhang Jh Fau - Noble-Haeusslein, and L. J. Noble-Haeusslein. 2013. 'RIGOR guidelines: escalating STAIR and STEPS for effective translational research', *Transl Stroke Res*, 4: 279-85.

113. Lapchak, P.A. et al. . 2007. 'Transcranial near-infrared light therapy improves motor function following embolic strokes in rabbits: an extended therapeutic window study using continuous and pulse frequency delivery modes', *Neuroscience*, 148: 907-14.

114. Lapchak, P.A., J Wei, and J.A. Zivin. 2004. 'Transcranial infrared laser therapy improves clinical rating scores after embolic strokes in rabbits', *Stroke*, 35: 198508.

115. Lauterbur, P. C. 1973. 'Image Formation by Induced Local Interactions: Examples Employing Nuclear Magnetic Resonance', *Nature*, 242: 190.

116. Lee, I., Scott Salomon Ar Fau - Ficarro, Isabella Ficarro S Fau - Mathes, Friedrich Mathes I Fau - Lottspeich, Lawrence I. Lottspeich F Fau - Grossman, Maik Grossman Li Fau - Huttemann, and M. Huttemann. 2005. 'cAMP-dependent tyrosine phosphorylation of subunit I inhibits cytochrome c oxidase activity', *J Biol*

Chem, 280: 6094-100.

117. Lee, I., Kebing Salomon Ar Fau - Yu, Jeffrey W. Yu K Fau - Doan, Lawrence I. Doan Jw Fau - Grossman, Maik Grossman Li Fau - Huttemann, and M. Huttemann. 2006. 'New prospects for an old enzyme: mammalian cytochrome c is tyrosine-phosphorylated in vivo', *Biochemistry*, 45: 9121-8.

118. Lee, Jin-Moo, Gregory J. Zipfel, and Dennis W. Choi. 1999. 'The changing landscape of ischaemic brain injury mechanisms', *Nature*, 399: A7.

119. Lees, K. R., Peter D. Bath Pm Fau - Schellinger, Daniel M. Schellinger Pd Fau - Kerr, Rachael Kerr Dm Fau - Fulton, Werner Fulton R Fau - Hacke, David Hacke W Fau - Matchar, Ruchir Matchar D Fau - Sehra, Danilo Sehra R Fau - Toni, and D. Toni. 2012. 'Contemporary outcome measures in acute stroke research: choice of primary outcome measure', *Stroke*, 43: 1163-70.

120. Lees, Kennedy R., Justin A. Zivin, Tim Ashwood, Antonio Davalos, Stephen M. Davis, Hans-Christoph Diener, James Grotta, Patrick Lyden, Ashfaq Shuaib, Hans-Göran Hårdemark, and Warren W. Wasiewski. 2006. 'NXY-059 for Acute Ischemic Stroke', *New England Journal of Medicine*, 354: 588-600.

121. Lenaz, Giorgio, Romana Fato, Maria Luisa Genova, Christian Bergamini, Cristina Bianchi, and Annalisa Biondi. 2006. 'Mitochondrial Complex I: Structural and functional aspects', *Biochimica et Biophysica Acta (BBA) - Bioenergetics*, 1757: 1406-20.

122. Leonard, DR., M.H. Farooqui, and S Myers. 2004. 'Restoration of sensation, reduced pain, and improved balance in subjects with diabetic peripheral neuropathy: a double-blind, randomized, placebo-controlled study with monochromatic near infrared light treatement', *Diabetes Care*, 27: 168-72.

123. Leonov, Y., P. Sterz F Fau - Safar, A. Safar P Fau - Radovsky, K. Radovsky A Fau - Oku, S. Oku K Fau - Tisherman, S. W. Tisherman S Fau - Stezoski, and S. W. Stezoski. 1990. 'Mild cerebral hypothermia during and after cardiac arrest improves neurologic outcome in dogs', *J Cereb Blood Flow Metab*, 10: 57-70.

124. Leonov, Y., P. Sterz F Fau - Safar, A. Safar P Fau - Radovsky, and A. Radovsky. 1990. 'Moderate hypothermia after cardiac arrest of 17 minutes in dogs. Effect on cerebral and cardiac outcome', *Stroke*, 21: 1600-6.

125. Liang, Danny, Sergei Bhatta, Volodymyr Gerzanich, and J. Marc Simard. 2007. 'Cytotoxic edema: mechanisms of pathological cell swelling', *Neurosurgical focus*, 22: E2-E2.

126. Liebeskind, D. S. 2003. 'Collateral circulation', *Stroke*, 34: 2279-84.

127. Lim, J et al. . 2009. 'Effects of low-level light herapy on hepatic antioxidant defense in acute and chronic diabetic rats', *J Biochem Mol Toxicol*, 23: 1-8.

128. Lipton, P. 1999. 'Ischemic cell death in brain neurons', *Physiol Rev*, 79: 1431-568.

129. Liu, S. S. 1997. 'Generating, partitioning, targeting and functioning of superoxide in mitochondria.', *Biosc. Rep*, 17: 259-72.

130. Liu SS. 1999. 'Cooperation of a "reactive oxygen cycle" with the Q cycle and the proton cycle in the respiratory chain--superoxide generating and cycling mechanisms in mitochondria', *J Bioenerg Biomembr*, 31: 367-76.

131. Liu SS. 2010. 'Mitochondrial Q cycle-derived superoxide and chemiosmotic bioenergetics', *Ann NY Acad Sci*, 1201: 84-95.

132. Liu, T. T., and G. G. Brown. 2007. 'Measurement of cerebral perfusion with arterial spin labeling: Part 1. Methods', *J Int Neuropsychol Soc*, 13: 517-25.

133. Liu, Y., David Fiskum G Fau - Schubert, and D. Schubert. 2002. 'Generation of

reactive oxygen species by the mitochondrial electron transport chain', *J Neurochem*, 80: 780-7.

134. Lutsep, H. L., G. W. Albers, A. Decrespigny, G. N. Kamat, M. P. Marks, and M. E. Moseley. 2004. 'Clinical utility of diffusion-weighted magnetic resonance imaging in the assessment of ischemic stroke', *Annals of neurology*, 41: 574-80.

135. MacIntosh, B. J., Michael A. Filippini N Fau - Chappell, Mark W. Chappell Ma Fau - Woolrich, Clare E. Woolrich Mw Fau - Mackay, Peter Mackay Ce Fau - Jezzard, and P. Jezzard. 2010. 'Assessment of arterial arrival times derived from multiple inversion time pulsed arterial spin labeling MRI', *Magn Reson Med*, 63: 641-7.

136. MacManus, J. P., and M. D. Linnik. 1997. 'Gene expression induced by cerebral ischemia: an apoptotic perspective', *J Cereb Blood Flow Metab*, 17: 815-32.

137. MacManus, John P., and Alastair M. Buchan. 2000. 'Apoptosis After Experimental Stroke: Fact or Fashion?', *Journal of Neurotrauma*, 17: 899-914.

138. Maier, C. M., D. Sun Gh Fau - Kunis, M. A. Kunis D Fau - Yenari, G. K. Yenari Ma Fau - Steinberg, and G. K. Steinberg. 2001. 'Delayed induction and long-term effects of mild hypothermia in a focal model of transient cerebral ischemia: neurological outcome and infarct size', *J Neurosurg*, 94: 90-6.

139. Majno, G., and I. Joris. 1995. 'Apoptosis, oncosis, and necrosis. An overview of cell death', *Am J Pathol*, 146: 3-15.

140. Marks, M. P., D. de Crespigny A Fau - Lentz, D. R. Lentz D Fau - Enzmann, G. W. Enzmann Dr Fau - Albers, M. E. Albers Gw Fau - Moseley, and M. E. Moseley. 1996. 'Acute and chronic stroke: navigated spin-echo diffusion-weighted MR imaging', *Radiology*, 199: 403-8.

141. Martin, L. J., A. M. Al-Abdulla Na Fau - Brambrink, J. R. Brambrink Am Fau -

Kirsch, F. E. Kirsch Jr Fau - Sieber, C. Sieber Fe Fau - Portera-Cailliau, and C. Portera-Cailliau. 1998. 'Neurodegeneration in excitotoxicity, global cerebral ischemia, and target deprivation: A perspective on the contributions of apoptosis and necrosis', *Brain Res Bull*, 46: 281-309.

142. Mason, MG., Nicholls, P., Cooper, CE. 2014. 'Re-evaluation of the near infrared spectra of mitochondrial cytochrome c oxidase: Implications for non-invasive in vivo monitoring of tissues', *Biochem Biophys Acta*, 1837: 1882-91.

143. Mergenthaler, P., and A. Meisel. 2012. 'Do stroke models model stroke?', *Dis Model Merch*, 5: 718-25.

144. Merten, C. L., J. Knitelius Ho Fau - Assheuer, B. Assheuer J Fau - Bergmann-Kurz, J. P. Bergmann-Kurz B Fau - Hedde, H. Hedde Jp Fau - Bewermeyer, and H. Bewermeyer. 1999. 'MRI of acute cerebral infarcts, increased contrast enhancement with continuous infusion of gadolinium', *Neuroradiology*, 41: 242-8.

145. Michalet, Xavier. 2010. 'Mean Square Displacement Analysis of Single-Particle Trajectories with Localization Error: Brownian Motion in Isotropic Medium', *Physical review. E, Statistical, nonlinear, and soft matter physics*, 82: 041914-14.

146. Mies, G., S. Ishimaru, Y. Xie, K. Seo, and K. A. Hossmann. 1991. 'Ischemic thresholds of cerebral protein synthesis and energy state following middle cerebral artery occlusion in rat', *Journal of cerebral blood flow and metabolism : official journal of the International Society of Cerebral Blood Flow and Metabolism*, 11: 753-61.

147. Hypothermia after Cardiac Arrest Study Group. 'Mild therapeutic hypothermia to improve the neurologic outcome after cardiac arrest'. 2002. *New England Journal of Medicine*: 549-56.

148. Mitchell Dg Fau - Burk, D. L., Jr., S. Burk Dl Jr Fau - Vinitski, M. D. Vinitski S Fau - Rifkin, and M. D. Rifkin. 1987. 'The biophysical basis of tissue contrast in extracranial MR imaging', *AJR Am J Roentgenol*, 149: 831-7.

149. Mitchell, P. 1975a. 'The protonmotive Q cycle: a general formulation', *FEBS Letters*, 59: 137-39.

150. Mitchell P. 1975b. 'Protonmotive redox mechanism b-c1 complex in the respiratory chain: protonmotive ubiquinone cycle', *FEBS Letters*, 56: 1-6.

151. Mitchell, Peter, and Jennifer Moyle. 1967. 'Chemiosmotic Hypothesis of Oxidative Phosphorylation', *Nature*, 213: 137.

152. Modo, M., R. P. Stroemer, E. Tang, T. Veizovic, P. Sowniski, and H. Hodges. 2000. 'Neurological sequelae and long-term behavioural assessment of rats with transient middle cerebral artery occlusion', *Journal of Neuroscience Methods*, 104: 99-109.

153. Mohr, J. P., S. K. Biller J Fau - Hilal, W. T. Hilal Sk Fau - Yuh, T. K. Yuh Wt Fau - Tatemichi, S. Tatemichi Tk Fau - Hedges, E. Hedges S Fau - Tali, H. Tali E Fau - Nguyen, I. Nguyen H Fau - Mun, H. P. Mun I Fau - Adams, Jr., H. P. Adams, Jr., and et al. 1995. 'Magnetic resonance versus computed tomographic imaging in acute stroke', *Stroke*, 26: 807-12.

154. Moseley, M. E., J. Cohen Y Fau - Mintorovitch, L. Mintorovitch J Fau - Chileuitt, H. Chileuitt L Fau - Shimizu, J. Shimizu H Fau - Kucharczyk, M. F. Kucharczyk J Fau - Wendland, P. R. Wendland Mf Fau - Weinstein, and P. R. Weinstein. 1990. 'Early detection of regional cerebral ischemia in cats: comparison of diffusion- and T2-weighted MRI and spectroscopy', *Magn Reson Med*, 14: 330-46.

155. Moseley, M. E., J. Kucharczyk J Fau - Mintorovitch, Y. Mintorovitch J Fau - Cohen,

J. Cohen Y Fau - Kurhanewicz, N. Kurhanewicz J Fau - Derugin, H. Derugin N Fau - Asgari, D. Asgari H Fau - Norman, and D. Norman. 1990. 'Diffusion-weighted MR imaging of acute stroke: correlation with T2-weighted and magnetic susceptibility-enhanced MR imaging in cats', *AJNR Am J Neuroradiol*, 11: 423-9.

156. Murphy, M. P. 2009. 'How mitochondria produce reactive oxygen species', *Biochem J*, 417: 1-13.

157. Niatsetskaya, Z. V., Dzmitry Sosunov Sa Fau - Matsiukevich, Irina V. Matsiukevich D Fau - Utkina-Sosunova, Veniamin I. Utkina-Sosunova Iv Fau - Ratner, Anatoly A. Ratner Vi Fau - Starkov, Vadim S. Starkov Aa Fau - Ten, and V. S. Ten. 2012. 'The oxygen free radicals originating from mitochondrial complex I contribute to oxidative brain injury following hypoxia-ischemia in neonatal mice', *J Neurosci*, 32: 3235-44.

158. Northington, F. J., E. M. Ferriero Dm Fau - Graham, R. J. Graham Em Fau - Traystman, L. J. Traystman Rj Fau - Martin, and L. J. Martin. 2001. 'Early Neurodegeneration after Hypoxia-Ischemia in Neonatal Rat Is Necrosis while Delayed Neuronal Death Is Apoptosis', *Neurobiol Dis*, 8: 207-19.

159. Ogbi, M., Jan Chew Cs Fau - Pohl, Olga Pohl J Fau - Stuchlik, Safia Stuchlik O Fau - Ogbi, John A. Ogbi S Fau - Johnson, and J. A. Johnson. 2004. 'Cytochrome c oxidase subunit IV as a marker of protein kinase Cepsilon function in neonatal cardiac myocytes: implications for cytochrome c oxidase activity', *Biochem J*, 382: 923-32.

160. Ogbi, M., and J. A. Johnson. 2006. 'Protein kinase Cepsilon interacts with cytochrome c oxidase subunit IV and enhances cytochrome c oxidase activity in neonatal cardiac myocyte preconditioning', *Biochem J*, 393: 191-9.

161. Oron, A., et al., . 2006. 'Low-level laser therapy applied transcranially to rats after induction of stroke significantly reduces long-term neurological deficits', *Stroke*, 37: 2620-4.

162. Osyczka, A., Moser, C.C. & Dutton, P.L. 2005. 'Fixing the Q cycle', *Trends in Biochemical Sciences*, 30: 176-82.

163. Ouyang, Y. B., M. Tan Y Fau - Comb, C. L. Comb M Fau - Liu, M. E. Liu Cl Fau - Martone, B. K. Martone Me Fau - Siesjo, B. R. Siesjo Bk Fau - Hu, and B. R. Hu. 1999. 'Survival- and death-promoting events after transient cerebral ischemia: phosphorylation of Akt, release of cytochrome C and Activation of caspase-like proteases', *J Cereb Blood Flow Metab*, 19: 1126-35.

164. Pandya JD1, Pauly JR, Sullivan PG. 2009. 'The optimal dosage and window of opportunity to maintain mitochondrial homeostasis following traumatic brain injury using the uncoupler FCCP', *Exp Neurol*, 218: 381-9.

165. Parsons, M. W., Jonathon Barber Pa Fau - Chalk, David G. Chalk J Fau - Darby, Stephen Darby Dg Fau - Rose, Patricia M. Rose S Fau - Desmond, Richard P. Desmond Pm Fau - Gerraty, Brian M. Gerraty Rp Fau - Tress, Peter M. Tress Bm Fau - Wright, Geoffrey A. Wright Pm Fau - Donnan, Stephen M. Donnan Ga Fau - Davis, and S. M. Davis. 2002. 'Diffusion- and perfusion-weighted MRI response to thrombolysis in stroke', *Ann Neurol*, 51: 28-37.

166. Parsons, M. W., Patrick Christensen S Fau - McElduff, Christopher R. McElduff P Fau - Levi, Ken S. Levi Cr Fau - Butcher, Deidre A. Butcher Ks Fau - De Silva, Martin De Silva Da Fau - Ebinger, P. Alan Ebinger M Fau - Barber, Christopher Barber Pa Fau - Bladin, Geoffrey A. Bladin C Fau - Donnan, Stephen M. Donnan Ga Fau - Davis, and S. M. Davis. 2010. 'Pretreatment diffusion- and perfusion-MR

lesion volumes have a crucial influence on clinical response to stroke thrombolysis', *J Cereb Blood Flow Metab*, 30: 1214-25.

167. Pastore, D., M. Greco, and S. Passarella. 2000. 'Specific helium-neon laser sensitivity of the purified cytochrome c oxidase', *International journal of radiation biology*, 76: 863-70.

168. Perez-Trepichio, Alejandro D., Min Xue, Thian C. Ng, Anthony W. Majors, Anthony J. Furlan, Issam A. Awad, and Stephen C. Jones. 1995. 'Sensitivity of Magnetic Resonance Diffusion-Weighted Imaging and Regional Relationship Between the Apparent Diffusion Coefficient and Cerebral Blood Flow in Rat Focal Cerebral Ischemia', *Stroke*, 26: 667.

169. Petersen, E. T., Y. C. L. Zimine I Fau - Ho, X. Ho Yc Fau - Golay, and X. Golay. 2006. 'Non-invasive measurement of perfusion: a critical review of arterial spin labelling techniques', *Br J Radiol*, 79: 688-701.

170. Piantadosi, C. A., and J. Zhang. 1996. 'Mitochondrial generation of reactive oxygen species after brain ischemia in the rat', *Stroke*, 27: 327-31.

171. Piccoli, C., Scrima, R., Boffoli, D. & Capitanio, N. 2006. 'Control by cytochrome c oxidase of the cellular oxidative phosphorylation system depends on the mitochondrial energy state.', *Biochem J*, 396: 573-83.

172. Polderman, K. H. 2009. 'Mechanisms of action, physiological effects, and complications of hypothermia', *Crit Care Med*, 37: S186-202.

173. Powers, William J., Alejandro A. Rabinstein, Teri Ackerson, Opeolu M. Adeoye, Nicholas C. Bambakidis, Kyra Becker, José Biller, Michael Brown, Bart M. Demaerschalk, Brian Hoh, Edward C. Jauch, Chelsea S. Kidwell, Thabele M. Leslie-Mazwi, Bruce Ovbiagele, Phillip A. Scott, Kevin N. Sheth, Andrew M.

Southerland, Deborah V. Summers, and David L. Tirschwell. 2018. '2018 Guidelines for the Early Management of Patients With Acute Ischemic Stroke: A Guideline for Healthcare Professionals From the American Heart Association/American Stroke Association', *Stroke*.

174. Prabu, S. K., Haider Anandatheerthavarada Hk Fau - Raza, Satish Raza H Fau - Srinivasan, Joseph F. Srinivasan S Fau - Spear, Narayan G. Spear Jf Fau - Avadhani, and N. G. Avadhani. 2006. 'Protein kinase A-mediated phosphorylation modulates cytochrome c oxidase function and augments hypoxia and myocardial ischemia-related injury', *J Biol Chem*, 281: 2061-70.
175. Proskuryakov, S. Y., Vladimir L. Konoplyannikov Ag Fau - Gabai, and V. L. Gabai. 2003. 'Necrosis: a specific form of programmed cell death?', *Exp Cell Res*, 283: 1-16.
176. Pryde, K. R., and J. Hirst. 2011. 'Superoxide is produced by the reduced flavin in mitochondrial complex I: a single, unified mechanism that applies during both forward and reverse electron transfer', *J Biol Chem*, 286: 18056-65.
177. Puka-Sundvall, M., M. Gajkowska B Fau - Cholewinski, K. Cholewinski M Fau - Blomgren, J. W. Blomgren K Fau - Lazarewicz, H. Lazarewicz Jw Fau - Hagberg, and H. Hagberg. 2000. 'Subcellular distribution of calcium and ultrastructural changes after cerebral hypoxia-ischemia in immature rats', *Brain Res Dev Brain Res*, 125: 31-41.
178. Rabi, I. I., J. R. Zacharias, S. Millman, and P. Kusch. 1938. 'A New Method of Measuring Nuclear Magnetic Moment', *Physical Review*, 53: 318-18.
179. Raedschelders, K., David D. Y. Ansley Dm Fau - Chen, and D. D. Chen. 2012. 'The cellular and molecular origin of reactive oxygen species generation during

myocardial ischemia and reperfusion', *Pharmacol Ther*, 133: 230-55.

180. Reith, W., Y. Hasegawa, L. L. Latour, B. J. Dardzinski, C. H. Sotak, and M. Fisher. 1995. 'Multislice diffusion mapping for 3-D evolution of cerebral ischemia in a rat stroke model', *Neurology*, 45: 172.

181. Rewell, S. S. Auid-Orcid http orcid org, L. Churilov, T. K. Sidon, E. Aleksoska, S. F. Cox, M. R. Macleod, and D. W. Howells. 2017. 'Evolution of ischemic damage and behavioural deficit over 6 months after MCAo in the rat: Selecting the optimal outcomes and statistical power for multi-centre preclinical trials', *PLoS One*, 12.

182. Reynolds, Christian A. 2015. 'Preclinical evaluation of infrared light therapy in a rat model of neonatal hypoxic-ischemic encephalopathy', Dissertation Wayne State University

183. Rosen, B. R., J. M. Belliveau Jw Fau - Vevea, T. J. Vevea Jm Fau - Brady, and T. J. Brady. 1990. 'Perfusion imaging with NMR contrast agents', *Magn Reson Med*, 14: 249-65.

184. Rungta, R. L., H. B. Choi, J. R. Tyson, A. Malik, L. Dissing-Olesen, P. J. C. Lin, S. M. Cain, P. R. Cullis, T. P. Snutch, and B. A. MacVicar. 2015. 'The cellular mechanisms of neuronal swelling underlying cytotoxic edema', *Cell*, 161: 610-21.

185. Safar, P., A. Xiao F Fau - Radovsky, K. Radovsky A Fau - Tanigawa, U. Tanigawa K Fau - Ebmeyer, N. Ebmeyer U Fau - Bircher, H. Bircher N Fau - Alexander, S. W. Alexander H Fau - Stezoski, and S. W. Stezoski. 1996. 'Improved cerebral resuscitation from cardiac arrest in dogs with mild hypothermia plus blood flow promotion', *Stroke*, 27: 105-13.

186. Sanderson, T. H., Jonathon M. Kumar R Fau - Sullivan, Gary S. Sullivan Jm Fau - Krause, and G. S. Krause. 2008. 'Insulin blocks cytochrome c release in the

reperfused brain through PI3-K signaling and by promoting Bax/Bcl-XL binding', *J Neurochem*, 106: 1248-58.

187. Sanderson, Thomas H., Christian A. Reynolds, Rita Kumar, Karin Przyklenk, and Maik Huttemann. 2013. 'Molecular mechanisms of ischemia-reperfusion injury in brain: pivotal role of the mitochondrial membrane potential in reactive oxygen species generation', *Molecular neurobiology*, 47: 9-23.

188. Sanderson, Thomas H., Joseph M. Wider, Icksoo Lee, Christian A. Reynolds, Jenney Liu, Bradley Lepore, Reneé Tousignant, Melissa J. Bukowski, Hollie Johnston, Alemu Fite, Sarita Raghunayakula, John Kamholz, Lawrence I. Grossman, Karin Przyklenk, and Maik Hüttemann. 2018. 'Inhibitory modulation of cytochrome c oxidase activity with specific near-infrared light wavelengths attenuates brain ischemia/reperfusion injury', *Scientific Reports*, 8: 3481-81.

189. Sazanov, L. A. 2007. 'Respiratory complex I: mechanistic and structural insights provided by the crystal structure of the hydrophilic domain', *Biochemistry*, 46: 2275-88.

190. Schellinger, P. D., Kennedy R. Bath Pm Fau - Lees, Natan M. Lees Kr Fau - Bornstein, Eitan Bornstein Nm Fau - Uriel, Wolfgang Uriel E Fau - Eisert, Didier Eisert W Fau - Leys, and D. Leys. 2012. 'Assessment of additional endpoints for trials in acute stroke - what, when, where, in who?', *Int J Stroke*, 7: 227-30.

191. Schellinger, P. D., O. Fiebach Jb Fau - Jansen, P. A. Jansen O Fau - Ringleb, A. Ringleb Pa Fau - Mohr, T. Mohr A Fau - Steiner, S. Steiner T Fau - Heiland, S. Heiland S Fau - Schwab, O. Schwab S Fau - Pohlers, H. Pohlers O Fau - Ryssel, B. Ryssel H Fau - Orakcioglu, K. Orakcioglu B Fau - Sartor, W. Sartor K Fau - Hacke, and W. Hacke. 2001. 'Stroke magnetic resonance imaging within 6 hours

after onset of hyperacute cerebral ischemia', *Ann Neurol*, 49: 460-9.

192. Schlaug, G., A. Siewert B Fau - Benfield, R. R. Benfield A Fau - Edelman, S. Edelman Rr Fau - Warach, and S. Warach. 1997. 'Time course of the apparent diffusion coefficient (ADC) abnormality in human stroke', *Neurology*, 49: 113-9.

193. Schulz, J. B., M. A. Weller M Fau - Moskowitz, and M. A. Moskowitz. 1999. 'Caspases as treatment targets in stroke and neurodegenerative diseases', *Ann Neurol*, 45: 421-9.

194. Sevick, R. J., J. Kanda F Fau - Mintorovitch, A. I. Mintorovitch J Fau - Arieff, J. Arieff Ai Fau - Kucharczyk, J. S. Kucharczyk J Fau - Tsuruda, D. Tsuruda Js Fau - Norman, M. E. Norman D Fau - Moseley, and M. E. Moseley. 1992. 'Cytotoxic brain edema: assessment with diffusion-weighted MR imaging', *Radiology*, 185: 687-90.

195. Shrier, D. A., Y. Tanaka H Fau - Numaguchi, S. Numaguchi Y Fau - Konno, U. Konno S Fau - Patel, D. Patel U Fau - Shibata, and D. Shibata. 1997. 'CT angiography in the evaluation of acute stroke', *AJNR Am J Neuroradiol*, 18: 1011-20.

196. Shuaib, Ashfaq, Kennedy R. Lees, Patrick Lyden, James Grotta, Antonio Davalos, Stephen M. Davis, Hans-Christoph Diener, Tim Ashwood, Warren W. Wasiewski, and Ugochi Emeribe. 2007. 'NXY-059 for the Treatment of Acute Ischemic Stroke', *New England Journal of Medicine*, 357: 562-71.

197. Singer, Michael B., June Chong, Dongfeng Lu, Wouter J. Schonewille, Stanley Tuhrim, and Scott W. Atlas. 1998. 'Diffusion-Weighted MRI in Acute Subcortical Infarction', *Stroke*, 29: 133.

198. Song, Y., and G. R. Buettner. 2010. 'Thermodynamic and kinetic considerations

for the reaction of semiquinone radicals to form superoxide and hydrogen peroxide', *Free Radic Biol Med*, 49: 919-62.

199. Sorensen, A. G., R. G. Buonanno Fs Fau - Gonzalez, L. H. Gonzalez Rg Fau - Schwamm, M. H. Schwamm Lh Fau - Lev, F. R. Lev Mh Fau - Huang-Hellinger, T. G. Huang-Hellinger Fr Fau - Reese, R. M. Reese Tg Fau - Weisskoff, T. L. Weisskoff Rm Fau - Davis, N. Davis Tl Fau - Suwanwela, U. Suwanwela N Fau - Can, J. A. Can U Fau - Moreira, W. A. Moreira Ja Fau - Copen, R. B. Copen Wa Fau - Look, S. P. Look Rb Fau - Finklestein, B. R. Finklestein Sp Fau - Rosen, W. J. Rosen Br Fau - Koroshetz, and W. J. Koroshetz. 1996. 'Hyperacute stroke: evaluation with combined multisection diffusion-weighted and hemodynamically weighted echo-planar MR imaging', *Radiology*, 199: 391-01.

200. Sridharan, V., Chuan-Yuan Guichard J Fau - Li, Robin Li Cy Fau - Muise-Helmericks, Craig Cano Muise-Helmericks R Fau - Beeson, Gary L. Beeson Cc Fau - Wright, and G. L. Wright. 2008. 'O(2)-sensing signal cascade: clamping of O(2) respiration, reduced ATP utilization, and inducible fumarate respiration', *Am J Physiol Cell Physiol*, 295: C29-C37.

201. St-Pierre, J., Stephen J. Buckingham Ja Fau - Roebuck, Martin D. Roebuck Sj Fau - Brand, and M. D. Brand. 2002. 'Topology of superoxide production from different sites in the mitochondrial electron transport chain', *J Biol Chem*, 277: 44784-90.

202. Starkov, A. A., and G. Fiskum. 2002. 'Regulation of brain mitochondrial H2O2 production by membrane potential and NAD(P)H redox state', *J Neurochem*, 86: 1101-7.

203. Steenaart NA, and GC Shore. 1997. 'Mitochondrial cytochrome c oxidase subunit IV is phosphorylated by an endogenous kinase', *FEBS Letters*, 415: 294-98.

204. Stejskal, E. O., and J. E. Tanner. 1965. 'Spin Diffusion Measurements: Spin Echoes in the Presence of a Time-Dependent Field Gradient', *The Journal of Chemical Physics*, 42: 288-92.

205. Sterz, F., S. Safar P Fau - Tisherman, A. Tisherman S Fau - Radovsky, K. Radovsky A Fau - Kuboyama, K. Kuboyama K Fau - Oku, and K. Oku. 1991. 'Mild hypothermic cardiopulmonary resuscitation improves outcome after prolonged cardiac arrest in dogs', *Crit Care Med*, 19: 379-89.

206. Streeter, J., De Taboada, U. Oron. 2004. 'Mechanism of action of light therapy for stroke and acute myocardial infarction', *Mitochondrion*, 4: 569-76.

207. Sugawara, T., Y. Fujimura M Fau - Morita-Fujimura, M. Morita-Fujimura Y Fau - Kawase, P. H. Kawase M Fau - Chan, and P. H. Chan. 1999. 'Mitochondrial release of cytochrome c corresponds to the selective vulnerability of hippocampal CA1 neurons in rats after transient global cerebral ischemia', *J Neurosci*, 19.

208. Suski, J. M., Massimo Lebiedzinska M Fau - Bonora, Paolo Bonora M Fau - Pinton, Jerzy Pinton P Fau - Duszynski, Mariusz R. Duszynski J Fau - Wieckowski, and M. R. Wieckowski. 2012. 'Relation between mitochondrial membrane potential and ROS formation', *Methods Mol Biol*, 810: 183-205.

209. Szabo, C. 2008. 'Mechanisms of cell necrosis', *Curr Mol Med*, 8: 207-20.

210. Taegtmeyer, H. 1978. 'Metabolic responses to cardiac hypoxia. Increased production of succinate by rabbit papillary muscles', *Circ Res*, 43: 808-15.

211. Taylor, D. L., Ernest B. Mehmet H Fau - Cady, A. David Cady Eb Fau - Edwards, and A. D. Edwards. 2002. 'Improved neuroprotection with hypothermia delayed by 6 hours following cerebral hypoxia-ischemia in the 14-day-old rat', *Pediatr Res*, 51: 13-9.

212. Tissier, R., Sandrine Chenoune M Fau - Pons, Roland Pons S Fau - Zini, Lys Zini R Fau - Darbera, Fanny Darbera L Fau - Lidouren, Bijan Lidouren F Fau - Ghaleh, Alain Ghaleh B Fau - Berdeaux, Didier Berdeaux A Fau - Morin, and D. Morin. 2013. 'Mild hypothermia reduces per-ischemic reactive oxygen species production and preserves mitochondrial respiratory complexes', *Resuscitation*, 84: 249-55.

213. The National Institute of Neurological Disorders and Stroke rt-PA Stroke Study Group 1995 'Tissue Plasminogen Activator for Acute Ischemic Stroke'. *New England Journal of Medicine*, 333: 1581-88.

214. Tong, D. C., M. A. Yenari, G. W. Albers, M. Brien, M. P. Marks, and M. E. Moseley. 1998. 'Correlation of perfusion- and diffusion-weighted MRI with NIHSS score in acute (<6.5 hour) ischemic stroke', *Neurology*, 50: 864.

215. Trumpower, B.I. 1976. 'Evidence for a protonmotive Q cycle mechanism of electron transfer through the cytochrome bc1 comples', *Biochemical and Biophysical Research Communications*, 70: 73-80.

216. Tsukihara, T., E. Aoyama H Fau - Yamashita, T. Yamashita E Fau - Tomizaki, H. Tomizaki T Fau - Yamaguchi, K. Yamaguchi H Fau - Shinzawa-Itoh, R. Shinzawa-Itoh K Fau - Nakashima, R. Nakashima R Fau - Yaono, S. Yaono R Fau - Yoshikawa, and S. Yoshikawa. 1996. 'The whole structure of the 13-subunit oxidized cytochrome c oxidase at 2.8 A', *Science*, 272: 1136-44.

217. Turrens, Julio F., Adolfo Alexandre, and Albert L. Lehninger. 1985. 'Ubisemiquinone is the electron donor for superoxide formation by complex III of heart mitochondria', *Archives of Biochemistry and Biophysics*, 237: 408-14.

218. Van Bruggen, N., M. D. Cullen Bm Fau - King, M. King Md Fau - Doran, S. R. Doran M Fau - Williams, D. G. Williams Sr Fau - Gadian, J. E. Gadian Dg Fau -

Cremer, and J. E. Cremer. 1992. 'T2- and diffusion-weighted magnetic resonance imaging of a focal ischemic lesion in rat brain', *Stroke*, 23: 576-82.

219. Van den Berghe, G., J. Vincent Mf Fau - Jaeken, and J. Jaeken. 1997. 'Inborn errors of the purine nucleotide cycle: adenylosuccinase deficiency', *J Inherit Metab Dis*, 20: 193-202.

220. Van Everdingen, K. J., J. van der Grond, L. J. Kappelle, L. M. P. Ramos, and W. P. T. M. Mali. 1998. 'Diffusion-Weighted Magnetic Resonance Imaging in Acute Stroke', *Stroke*, 29: 1783.

221. Van Lookeren Campagne, M., and R. Gill. 1996. 'Ultrastructural morphological changes are not characteristic of apoptotic cell death following focal cerebral ischaemia in the rat', *Neurosci Let*, 213: 111-4.

222. Villani, G. & Attardi, G. 1997. 'In vivo control of respiration by cytochrome c oxidase in wild-type and mitochondrial DNA mutation-carrying human cells.', *Proceedings of the National Academy of Sciences of the United States of America*, 94: 1166-71.

223. Votyakova, T. V. and Reynolds, I. J. 2001. 'Δψm-Dependent and -independent

224. production of reactive oxygen species by rat brain mitochondria', *J. Neurochem*, 79: 266-77.

225. Wang, J., Lin Alsop Dc Fau - Li, John Li L Fau - Listerud, Julio B. Listerud J Fau - Gonzalez-At, Mitchell D. Gonzalez-At Jb Fau - Schnall, John A. Schnall Md Fau - Detre, and J. A. Detre. 2002. 'Comparison of quantitative perfusion imaging using arterial spin labeling at 1.5 and 4.0 Tesla', *Magn Reson Med*, 48: 242-54.

226. Warach, S., R. R. Dashe Jf Fau - Edelman, and R. R. Edelman. 1996. 'Clinical outcome in ischemic stroke predicted by early diffusion-weighted and perfusion

magnetic resonance imaging: a preliminary analysis', *J Cereb Blood Flow Metab*, 16: 53-9.

227. Weerasinghe, P., and L. M. Buja. 2012. 'Oncosis: an important non-apoptotic mode of cell death', *Exp Mol Pathol*, 93: 302-8.

228. Weinrauch, V., S. Safar P Fau - Tisherman, K. Tisherman S Fau - Kuboyama, A. Kuboyama K Fau - Radovsky, and A. Radovsky. 1992. 'Beneficial effect of mild hypothermia and detrimental effect of deep hypothermia after cardiac arrest in dogs', *Stroke*, 23: 1454-62.

229. Wharton DC, Tzagoloff A. 1964. 'Studies on the Electron Transfer System. Lvii. The near Infrared Absorption Band of Cytochrome Oxidase', *J Biol Chem*, 239.

230. Whelan, Harry T. 2003. 'Effect of NASA light-emitting diode irradiation on molecular changes for wound healing in diabetic mice', *J Clin Laser Med Surg*, 21: 67-74.

231. White, Blaine C., Lawrence I. Grossman, Brian J. O'Neil, Donald J. DeGracia, Robert W. Neumar, José A. Rafols, and Gary S. Krause. 1996. 'Global Brain Ischemia and Reperfusion', *Annals of Emergency Medicine*, 27: 588-94.

232. Williams, D. S., J. A. Detre, J. S. Leigh, and A. P. Koretsky. 1992. 'Magnetic resonance imaging of perfusion using spin inversion of arterial water', *Proceedings of the National Academy of Sciences of the United States of America*, 89: 212-16.

233. Williams, George S. B., Liron Boyman, Aristide C. Chikando, Ramzi J. Khairallah, and W. J. Lederer. 2013. 'Mitochondrial calcium uptake', *Proceedings of the National Academy of Sciences of the United States of America*, 110: 10479-86.

234. Wolf, R. L., and J. A. Detre. 2007. 'Clinical neuroimaging using arterial spin-labeled perfusion magnetic resonance imaging', *Neurotherapeutics*, 4: 356-59.

235. Wong, E. C., Wen-Chau Cronin M Fau - Wu, Ben Wu Wc Fau - Inglis, Lawrence R. Inglis B Fau - Frank, Thomas T. Frank Lr Fau - Liu, and T. T. Liu. 2006. 'Velocity-selective arterial spin labeling', *Magn Reson Med*, 55: 1334-41.

236. Wong-Riley, Margaret T. T. 2001. 'Light-emitting diode treatment reverses the effect of TTX on cytochrome oxidase in neurons', *Neuroreport*, 12: 3033-7.

237. Wong-Riley, Margaret T. T., Huan Ling Liang, Janis T. Eells, Britton Chance, Michele M. Henry, Ellen Buchmann, Mary Kane, and Harry T. Whelan. 2005. 'Photobiomodulation directly benefits primary neurons functionally inactivated by toxins: role of cytochrome c oxidase', *The Journal of biological chemistry*, 280: 4761-71.

238. Wu, W. C., John A. Fernandez-Seara M Fau - Detre, Felix W. Detre Ja Fau - Wehrli, Jiongjiong Wehrli Fw Fau - Wang, and J. Wang. 2007. 'A theoretical and experimental investigation of the tagging efficiency of pseudocontinuous arterial spin labeling', *Magn Reson Med*, 58: 1020-7.

239. Yeager, R.L., et al., . 2005. 'Effects of 670-nm photothereapy on development', *Photomed Laser Surg*, 23: 268-72.

240. Yellen, G. Auid-Orcid http orcid org. 2018. 'Fueling thought: Management of glycolysis and oxidative phosphorylation in neuronal metabolism', *J Cell Biol*, 217: 2235-46.

241. Yu, H., Arthur R. Lee I Fau - Salomon, Kebing Salomon Ar Fau - Yu, Maik Yu K Fau - Huttemann, and M. Huttemann. 2008. 'Mammalian liver cytochrome c is tyrosine-48 phosphorylated in vivo, inhibiting mitochondrial respiration', *Biochem Biophys Acta*, 17777: 1066-71.

242. Yu, W., et al. 1997. 'Photomodulation of oxidative metabolism and electron chain

enzymes in rat liver mitochondria', *Photochem Photobiol*, 66: 866-71.

243. Zhang, W., D. S. Silva Ac Fau - Williams, A. P. Williams Ds Fau - Koretsky, and A. P. Koretsky. 1995. 'NMR measurement of perfusion using arterial spin labeling without saturation of macromolecular spins', *Magn Reson Med*, 33: 370-6.

244. Zimmerman, J. J. 1995. 'Defining the role of oxyradicals in the pathogenesis of sepsis', *Crit Care Med*, 23: 616-7.

ABSTRACT

NON-INVASIVE MITOCHONDRIAL MODULATION WITH NEAR-INFRARED LIGHT REDUCES BRAIN INJURY AFTER STROKE

by

CHRISTOS DIONISOS STRUBAKOS

December 2018

Advisors: Maik Huttemann, Ph.D. and Thomas Sanderson, Ph.D.

Major: Physiology

Degree: Doctor of Philosophy

Acute ischemic stroke is a debilitating disease that causes significant brain injury. While rapid restoration of blood flow is critical to salvage the ischemic brain, reperfusion of tissue can further drive brain damage by inducing generation of mitochondrial reactive oxygen species (Chouchani et al., 2014a). Recent studies by our group found that non-invasive mitochondrial modulation (NIMM) with near-infrared (NIR) light can limit the production of reactive oxygen species following global brain ischemia (T. H. Sanderson et al., 2018). NIR interacts with the rate limiting step of the mitochondrial electron transport chain (ETC), cytochrome c oxidase (COX), and modulates mitochondrial respiration. Under conditions of mitochondrial stress, such as reperfusion following ischemia, specific wavelengths of NIR can limit the production of ROS by transiently reducing COX activity, and thus limiting a critical force for ROS production, stress-induced mitochondrial membrane potential hyperpolarization. Here, we evaluated a specific combination of COX-inhibitory NIR (750nm and 950nm) as a potential therapy for acute ischemic stroke using a rat MCAO model. We found the NIMM at the onset of reperfusion resulted in a 20% reduction of infarct volume measured 24 hours post reperfusion. This

reduction in infarct was sustained through the chronic phase of stroke and the neuroprotective benefit increased to 50% infarct reduction when treatment duration was douple to 240 minutes. Our data suggest that NIMM by targeting COX with NIR irradiation at the onset of reperfusion can be a beneficial therapy to minimize reperfusion injury following acute ischemic stroke and that extending the treatment window beyond the initial ROS burst can target other long-term causes of neuronal death following stroke such as inflammation.

AUTOBIOGRAPHICAL STATEMENT

CHRISTOS DIONISOS STRUBAKOS

EDUCATION

September 2018 PhD in Physiology, Wayne State University, Michigan

June 2012 EMT-B Training, Boston EMS

May 2012 Holy Cross Greek Orthodox School of Theology, Master of Divinity Theology (*Summa Cum Laude)* Massachusetts

March 2012 BLS Certified, American Heart Association Boston EMS, Massachusetts

June 2010 University of Windsor Honors Bachelor of Arts (*Cum Laude)*.
Major: Classics and Psychology

SCIENTIFIC RESEARCH EXPERIENCE

Clinical

Henry Ford Hospital, Detroit, Michigan. Department of Neurology. Clinical research examining cardiac dysfunction following acute stroke using MRI and patient clinical data.
Dr. Panayiotis Mitsias, Advisor.
September 2012-Present

Basic Science

Wayne State University, Detroit, Michigan. Department of Physics and Astronomy.
Single Molecule Biophysics and Biomedical Physics
Project: *in vitro* actin bundling and polymerization visualized using TIRF microscopy
Dr. Takeshi Sakamoto, Advisor.
May 2013-August 2015

Wayne State University, Detroit, Michigan. Department of Emergency Medicine and Physiology.
Project: Translational research in focal ischemia using rat model
Drs. Maik Huttemann and Thomas Sanderson, Advisors
January 2015- Present

SCIENTIFIC MEETINGS

February 2015: International Stroke Conference, Nashville TN. Poster
Specific Infarct Locations Define Troponin Elevation in Acute Ischemic Stroke
Panayiotis D. Mitsias, MD, PhD, **Christos Strubakos**, Ahmed Dakka, Patricia Penstone, RN, Kourosh Jafari, PhD, Lonni Schultz, PhD, Hamid Soltanian-Zadeh, PhD